# Karyotyping and *in silico* characterisation of the chromosomes of *Diuraphis noxia* (Hemiptera: Aphididae)

By

**Louis Johannes Steyn**

***Magister Scientiae***

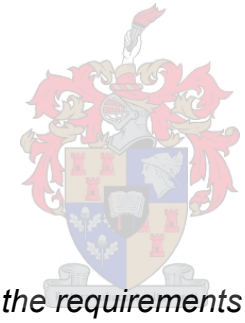

*Thesis presented in fulfilment of the requirements for the degree of Magister Scientiae in the Faculty of Natural Science at Stellenbosch University*

**Department of Genetics**
**Stellenbosch University**
**Private Bag X1**
**Matieland**
**7602**
**South Africa**

Supervisor: Professor Anna-Maria Oberholster

Co-supervisor: Doctor Anandi Bierman

**December 2016**

# Declaration

By submitting this thesis electronically, I declare that the entirety of the work contained therein is my own, original work, that I am the sole author thereof (save to the extent where explicitly otherwise stated), that reproduction and publication thereof by Stellenbosch University will not infringe any third party rights and that I have not previously in its entirety or in part submitted it for obtaining any qualification.

**Date:** . . . . . December 2016 . . . . . .

# Abstract

*Diuraphis noxia* Kurdjumov (Russian wheat aphid (RWA)), is an economically important agricultural pest that causes substantial losses in small grain production, particularly wheat and barley. Approaches that can be taken to manage this invasive pest include the cultivation of RWA resistant cultivars. The development of new RWA biotypes, virulent against previously classified resistant wheat cultivars presents, an additional problem to the goal of reducing crop losses. Therefore, studying the underlying molecular genetics of the RWA brings us closer to understanding wheat resistance to the RWA and ultimately battling this pest in small grain fields. The objectives of this study were: to study the sex (X) chromosome of the RWA by karyotyping and isolation using flow cytometry; to sequence the X chromosome; and then to map it against the reference genomes of the RWA and *Acyrthosiphon pisum* (pea aphid). Since aphids reproduce via parthenogenesis, mapping populations reliant on sexual recombination are not available, and therefore information about the locations of genes on chromosomes is completely lacking. To this end, reference mapping against the X chromosome of *Drosophila melanogaster* (fruit fly) was conducted to identify orthologous regions spanning the X chromosome of RWA. The results confirmed that the RWA karyotype consists of a diploid chromosome number of 10, with a large X chromosome pair and four autosomal chromosome pairs. Flow sorting yielded 2,047,296 X chromosomes and sequencing produced a total read count of 136,814,894 with a Q20 score of 96.32%. The X chromosome had a higher mapping percentage to the RWA genome (82.88%) compared to that of the pea aphid (51.3%). Interestingly, a high mapping coverage across the entire genome of both aphids was observed, suggesting that flow cytometry did not separate the X chromosome from the rest of the chromosomes of the RWA but allowed unintended chromosomes to contaminate the series. Mapping against the fruit fly X chromosome produced eight orthologous regions of which six was confirmed to be present in the RWA

karyotype through *in situ* hybridization, while a protein BLAST of the fruit fly X chromosome against the RWA genome aided in determining approximately 67.42% of the length of the RWA X chromosome.

# Uittreksel

*Diuraphis noxia* Kurdjumov, algemeen bekend as die Russiese koringluis (RWA), is ‘n ekonomiese belangrike landboupes wat ‘n groot afname in klein graangewas produksie, spesifiek koring en gars, veroorsaak. Metodes wat geiimplementeer kan word om hierdie indringer pes te beheer en gewas verliese te verhoed, sluit die kultivering van RWA weerstandbiedende kultivars in. Die ontwikkeling van RWA-biotipes, wat luis populasies is virulent teen voorheen weerstandbiedende koring kultivars, dra addisioneel tot die probleem by. Daarom is dit belangrik om die onderliggende molekulêre genetika van die RWA te verstaan, sodat ons ook koring weerstand tot RWA kan begryp om uiteindelik graangewasse teen die pes te beskerm. Die doel van hierdie studie is: om die seks (X-) chromosoom van die RWA te bestudeer deur kariotipering en te isoleer deur van vloeisitometrie gebruik te maak; die X-chromosoom se volgorde te bepaal; en om dit dan teen die verwysings genome van RWA en *Acyrthosiphon pisum* (ertjieluis) te vergelyk. Aangesien hierdie luise ongeslagtelik voortplant, bestaan daar nie karteringspopulasies vir RWA nie, en daarom ontbreek inligting oor die ligging van gene op die chromosome. Ten einde die studie doel te bereik, was verwysingkartering teen *Drosophila melanogaster* (vrugtevlieg) se X-chromosoom gedoen met die doel om ooreenstemmende areas oor die X-chromosoom te identifiseer. Die resultate het bewys dat die RWA-kariotipe uit ‘n diploïde chromosoomgetal van 10 bestaan, met ‘n groot X-chromosoompaar en vier outosomale chromosoompare. Vloeisortering het 2,047,296 X-chromosome opgelewer en volgordebepaling het ‘n totale leesraam-telling van 136,814,894 teen ‘n Q20-telling van 96.32% gelewer. Die X-chromosoom het ‘n hoër ooreenstemming teenoor die genoom van die RWA (82.88%), in vergelyking met die ertjieluis (51.3%) vertoon. Beide luise het n hoë karteringdekking oor hulle hele genoom gehad. Dit was onverwags en dui daarop dat vloeisitometrie nie spesifiek genoeg was vir net die X-chromosoom nie en het dus nie-geteikende chromosome deur gelaat wat die

monster gekontamineer het. Kartering teenoor die vrugtevlieg X-chromosoom het agt ooreenstemende streke geproduseer waarvan ses bewys was om voor te kom in die RWA kariotipe deur *in situ* hibridisering, terwyl ‘n proteïen BLAST van die vrugtevlieg X-chromosoom teenoor die RWA genoom bygedra het tot die bepaling van minstens 67.42% van die lengte van die RWA X-chromosoom.

# Acknowledgements

I would like to thank and express my heartfelt appreciation to the following people and organisations for their support, guidance, and patience during the period of this study.

Professor Anna-Maria Oberholster, whose vast knowledge and proficiency made this M.Sc. a reality. Thank you for growing my fascination with agriculture and the improvement thereof. I want to especially express my gratitude for your assistance in securing me with a National Research Foundation (NRF) grantholder bursary, as well as appointing me as your lab assistant to gain experience outside of my particular line of work.

Thank you so much Doctor Anandi Bierman for all the time and effort you put into guiding and helping me with this project, i.e., the writing of this thesis, with lab work, and the planning around presentations. No task is ever too small or big for you and your ability to pass on information reasonably is truly a gift.

Lize Engelbrecht and Rozanne Adams at the Central Analytical Facility (CAF) Fluoresent Microscopy Unit, Stellenbosch University, for their assistance and guidance during my fluorescent microscopy and flow cytometry training and experiments.

Colleagues in the Cereal Genomic Laboratory at the Department of Genetics, Stellenbosch University: Ilze Visser, Francois Burger, Nadia Fisher, Kelly Breeds, Marlon Le Roux, and Hendrik Swiegers.

Department of Genetics, Stellenbosch University, for providing me the education and infrastructure I needed to facilitate my studies.

To my inspirational parents, Lops and Hanlie Steyn, for their infinite love, support, and motivation during my education.

To my biggest enthusiast and fiancé, Louzel Lombard, for supporting me in accomplishing my dreams. I appreciate your continuous love and reassurance the last few years.

# Table of contents

## Chapter 3 – Research

## Chapter 4 – Summary

# List of figures

# List of tables

# List of abbreviations

°C – degrees Celsius

µg – microgram

µl – microliter

µm – micrometre

1C – haploid genome size

2C – diploid genome size

2N – diploid

A – adenine

a – area

ABI – Applied Biosystems

BLAST – Basic Local Alignment Search Tool

BLASTn – nucleotide BLAST

BLASTp – protein BLAST

bp – base pair

BSA – bovine serum albumin

BWA – Burrows-Wheeler aligner

BWT – Burrows-Wheeler transform

C – cytosine

CAF – Central Analytical Facility

CDS – coding sequence

Cy – cyanine

*Dn – Diuraphis noxia*

DNA – deoxyribonucleic acid

dNTP – deoxynucleotide triphosphate

dUTP – deoxyuridine triphosphate

FISH – fluorescent *in situ* hybridization

FunCat – Functional Catalogue

G – guanine

GO – Gene Ontology

H – height

h – hour

ha – hectare

IPRI – International Plant Resistance to Insects

kb – kilobase

kg/ha – kilogram per hectare

M – molar or mole/litre

m/v – mass/volume

mb – megabase

mg/ml – milligram/millilitre

mm – millimetre

N – normality

ng/µl – nanogram/microliter

NGS – next generation sequencing

nm – nanometre

NOR – nucleolus organiser region

nt – nucleotide

PALM – photo-activated localization microscopy

PBS – phosphate-buffered saline

PCR – polymerase chain reaction

pg – picogram

PGM – personal genome machine

PGS – protein coding gene

PI – propidium iodide

*PR – pathogenesis related*

PVC-U – unplasticized polyvinyl chloride

Q20 – quality score (20)

QTL – quantitative trait locus

R – rand

*R – resistance*

RAM – random access memory

RNA – ribonucleic acid

rpm – revolutions per minute

rRNA – ribosomal RNA

RT – room temperature

RWA – Russian wheat aphid

s – second

S – string

SA1 – South African biotype 1

SA2 – South African biotype 2

SA3 – South African biotype 3

SA4 – South African biotype 4

SAM – South African mutant biotype

SD – standard deviation

SNP – single nucleotide polymorphism

SSC – saline sodium citrate

ssc – side scatter

T – thiamine

Taq – thermus aquaticus polymerase

US – United States

v – version

v/v – volume/volume

w/v – weight/volume

x – times

X chromosome – sex chromosome

XX/XO or XX/XY – XO or XY sex-determination system

# Chapter 1

# Introduction

## 1.1 Introduction

*Diuraphis noxia* (Kurdjumov, Hemiptera, Aphididae), frequently referred to as the Russian wheat aphid (RWA), is a severe agricultural pest of many cereal crops, such as wheat (*Triticum aestivum* L.) and barley (*Hordeum vulgare* L.) and has had a significant economic impact worldwide especially on wheat. The RWA is characterised by its ability to develop virulent biotypes that are capable of feeding on former resistant wheat cultivars (Burd *et al*. 2006), thus counteracting the host's defensive responses. Therefore, it is crucial to research and understand the constant evolutionary struggle between the RWA and wheat (Botha 2013).

Cytogeneticists have been using aphids as a model group more frequently in the twentieth century, with numerous species within the Aphididae family that have already been karyotyped. The results show a big inconsistency in chromosome number and morphology between and even within the species (Novotná *et al.* 2011). Furthermore, most of the studies on chromosomes of aphids only mention the diploid chromosome numbers without providing further information on their karyotypes (Samkaria *et al*. 2010).

Aphids have holocentric chromosomes that lack centromeres and therefore display kinetic activity along most of the chromosome length (Blackman 1987). The absence of centromeres makes it almost impossible to distinguish between aphid chromosomes of similar size, mostly because in karyotype studies the centromere is an important identification feature (Novotná *et al.* 2011).

In the RWA, the karyotype differs between sexes, with females showing a diploid chromosome number of 2n = 10 and males 2n = 9. Furthermore, the chromosomes are classified by size into three groups: a pair of large chromosomes, three pairs of middle-sized chromosomes, and one pair of small chromosomes. The male RWA only has one copy of the X chromosome, whereas the female has two copies (Novotná *et al.* 2011).

The large size of the X chromosome in the RWA makes it an ideal candidate to isolate and characterise *in silico*. Flow cytometry sorting is a method that is successful in isolating chromosomes of interest, especially if it can be distinguished from other chromosomes in the karyotype. Sorting of chromosomes play a particularly important role in the analysis of nuclear genome structure and the study of specific and unusual chromosomes (Doležel *et al*. 2012).

Therefore, the aim of this study was to verify the karyotype of the South African RWA by investigating the chromosomal ultrastructure, where after we wanted to characterise the X chromosome of the RWA through the analysis of chromosomal properties and with high resolution mapping techniques. In order to reach these research goals the following objectives were set. Firstly, to construct the RWA karyotype through fluorescent microscopy using mitotic chromosomes obtained from whole RWA embryos. Secondly, to isolate the X chromosome of the RWA using a flow cytometry approach, thereby obtaining DNA from only the X chromosome, to sequence it. Thirdly, to map the sequenced reads obtained from the X chromosome against the genomes of the RWA (SAM_Contigs_Version 1.1; GCA_001465515.1; Botha *et al.* 2016 – *in press*) and *Acyrthosiphon pisum* (pea aphid) (Acyr_2.0; GCA_000142985.2; The International Aphid Genomics Consortium 2010). Fourthly, to align the well characterised X chromosome of *Drosophila melanogaster* (fruit fly) (BDGP6; Adams *et al.* 2000) against the RWA genome, in order to identify orthologous regions with high similarity. Lastly, to perform fluorescent *in situ* hybridization (FISH) with probes derived from the X chromosome of the fruit fly that is suspected to also hybridize to the X chromosome of the RWA.

## 1.2 Thesis outline

The thesis consist of four chapters. **Chapter 2** contains a brief summary of literature on the RWA, its relationship to wheat, virulent biotypes, the RWA karyotype, RWA reproduction, sequencing platforms and single-chromosome isolation techniques.

**Chapter 3** focuses on the research conducted in this study and consists of the constructed karyotype of the RWA, the isolation of the X chromosome of the RWA through flow cytometry, bioinformatic analysis of the RWA X chromosome through reference mapping against the RWA genome, pea aphid genome, and the X chromosome of the fruit fly, and then finally also FISH studies.

**Appendix A** contains tables and supplemental folders of flow cytometry gating strategies and results, raw data and mapping comparisons of the isolated X chromosome of the RWA against the RWA and pea aphid genomes, raw data of the alignments of the RWA genome against the X chromosome of the fruit fly, and also figures related to FISH.

**Chapter 4** contains a summary of the main findings of this study and the implications thereof.

## 1.3 Preface

The findings obtained and presented in this thesis are the results of a study undertaken between January 2014 and July 2016 in the Department of Genetics, Stellenbosch University, under the supervision of Professor Anna-Maria Oberholster.

## 1.4 Research outputs

The following outputs were achieved:

Steyn, L. J., A. Bierman, and A. M. Botha, 2016 Karyotyping and *in silico* characterisation of the chromosomes of *Diuraphis noxia* (Hemiptera: Aphididae). Biennial

International Plant Resistance to Insects (IPRI) conference. International oral presentation, Cape Town, South Africa – *award for first runner up in M.Sc. student's category.*

Steyn, L. J., A. Bierman, N. F. V. Burger, and A. M. Botha, 2016 Partial characterisation of the X chromosome of *Diuraphis noxia* (Hemiptera: Aphididae). Chromosome Research – *in preparation.*

Botha, A. M., N. F. V. Burger, W. Cloete, L. van Eck, K. Breeds, L. J. Steyn, *et al.*, 2016 Draft genome of female *Diuraphis noxia* (Hemiptera: Aphididae) reveals high levels of genetic diversity despite parthenogenecity and hypomethylation as a mean to enhance genomic plasticity. Genome Biology – *in press.*

## 1.5 List of references

Adams, M. D., S. E. Celniker, R. A. Holt, C. A. Evans, J. D. Cocayne, *et al.*, 2000 The genome sequence of *Drosophila melanogaster*. Science 287: 2185-2195.

Botha, A. M., 2013 A co-evolutionary conundrum: The arms race between *Diuraphis noxia* (Kurdmojov) a specialist pest and its host *Triticum aestivum* (L.). Arthropod Plant Interactions 7: 359-372.

Botha, A. M., N. F. V. Burger, W. Cloete, L. van Eck, K. Breeds, *et al.*, 2016 Draft genome of female *Diuraphis noxia* (Hemiptera: Aphididae) reveals high levels of genetic diversity despite parthenogenecity and hypomethylation as a mean to enhance genomic plasticity. Genome Biology – *in press.*

Blackman, R. L., 1987 Reproduction, cytogenetics and development. *In:* A. K. Minsk and P. Harrewijn (eds), Aphids: their biology, natural enemies and control 2: 163-195.

Burd, J. D., D. R. Porter, G. J. Puterka, S. D. Haley, and F. B. Peairs, 2006 Biotypic variation among North American Russian wheat aphid (Homoptera: Aphididae) populations. Journal of Economical Entomology 99: 1862-1866.

Doležel, J., J. Vrána, J. Šafář, J. Bartoš, M. Kubaláková, *et al.*, 2012 Chromosomes in the flow to simplify genome analysis. Functional and Integrative Genomics 12: 397-416.

Novotná, J., J. Havelka, P. Starý, P. Koutecký, and M. Vítková, 2011 Karyotype analysis of the Russian wheat aphid, *Diuraphis noxia* (Kurdjumov) (Hemiptera: Aphididae) reveals a large X chromosome with rRNA and histone gene families. Genetica 139: 281-289.

Samkaria, R., J. Bala, and D. C. Gautum, 2010 Karyotype studies on some commonly occurring aphid species. Nucleus 53: 55-59.

The International Aphid Genomics Consortium, 2010 Genome sequence of the pea aphid *Acyrthosiphon pisum*. PLoS Biology 8: e1000313.

# Chapter 2

# Literature review

## 2.1 Insect pests

An insect is characterised as a pest if it has an impact on human lifestyle, natural habitats, or ecosystems (Meyer 2007). One of the main problems associated with insect pests include the damaging effects on crops and subsequently a decrease in food production (Bailey *et al.* 2010). There are approximately 6 million species of insects, of which 50% are known to be herbivorous (Schoonhoven *et al.* 2005). Different insect pests use various approaches to salvage nutrients from plants. All known plant feeding (phytophagous) insects cause mechanical damage to plant tissues, but the degree of injury varies between different species of insect, mainly because of their contrasting strategies of feeding (Howe and Jander 2008).

The majority (60%) of herbivorous insect species have been identified as leaf-eating beetles (Coleoptera) or caterpillars (Lepidoptera) that mainly cause damage with their mouthparts which have evolved for chewing, snipping, or tearing (Schoonhoven *et al.* 2005). Other insects like thrips and spider mites, suck the liquid content from lacerated cells through tube-like structures, whereas leaf miners develop and feed on soft tissue between epidermal cell layers. Aphids, whiteflies, and other Hemiptera insert specialized stylets between cells to create a feeding site in the phloem (Howe and Jander 2008).

## 2.2 Insect-plant interactions

In the course of insect-plant interactions both partners send and receive chemical cues that influence the outcome of the interaction. Contact chemoreceptors on the insect mouthparts, antennae, and tarsi, measure the suitability of the host as a food source. In opposition, plant cells detect and respond to insect movement, wound trauma caused by feeding, and compounds in insect oral secretions (Howe and Jander 2008).

The choice of an insect to reject or accept a host plant is influenced by a number of chemical deterrents and attractants. A considerable amount of specialised plant

compound (secondary metabolites) diversity, is a result of the co-evolutionary struggle between insects and plants (Becerra 2007).

## 2.3 Aphids

The Aphididae family consists of approximately 4700 aphid species of which 450 have been identified as small grain pests. One hundred of these aphids have taken advantage of the monoculture environment of modern agriculture, resulting in extensive economic damage globally (Van Emden and Harrington 2007).

Aphids have small soft bodies and belong to the order Hemiptera (Sternorrhyncha) that also include whiteflies, mealybugs, and psyllids. The insects that belong to this order are all evolutionary adapted to consume phloem sap as a main or only food source. Aphids are further grouped into two subfamilies namely, the Aphididae that comprise of “true” aphids, as well as the Aphidinae that consist of several aphid pests of food crops (De Jager *et al.* 2014).

Aphids are dispersed worldwide and are specialised phloem feeders that cause severe damage to numerous cultivated plants (Tagu *et al.* 2008). The devastating impact of aphids is associated with their efficient colonization and settlement traits, because of several advantageous biological characteristics. Firstly, parthenogenesis allows a double intrinsic rate of increase and a shortened reproductive time. Secondly, the aphids can colonize new host plants through winged adults while the wingless adults invest more of their energy in reproduction. Thirdly, they cause a significant nutrient withdrawal from sieve tubes, because of high population densities and, lastly, they transmit numerous phytoviruses (Giordanengo *et al*. 2010).

The survival of aphids depend on their ability to access phloem bundles, disrupting and evading the plant defence responses, and their capability of keeping the phloem cells functioning while withdrawing their liquid diet. In contrast to grazing insects that remove

big sections of plant tissues, aphids only cause minor physical damage. Aphids insert long and flexible stylets that primarily move in the cell wall apoplasm, between cells, to access the sieve tubes (Tjallingii 2006).

The best studied aphids and their hosts include, *Schizaphis graminum* (greenbug) that feed on winter and spring grain (Kindler *et al.* 2002), *Acyrthosiphon pisum* (pea aphid) that feed on legume crops (Edwards 2001), and *Diuraphis noxia* Kurdjumov (Russian wheat aphid) that feed on wheat and barley (Botha *et al.* 2005). All of these host-specific aphids are considered as agricultural pests and are highly adapted to their specific environmental conditions.

## 2.4 Russian wheat aphid (RWA)

### 2.4.1 Host plant

Bread wheat (*Triticum aestivum* L.) was one of the first domesticated crops and is the most recent polyploid species among the agricultural crops. Wheat is classified as a major food source, as it is one of the world's leading crops and holds the record for the highest trade value amongst the cereal species (Gill *et al.* 2004). A total area of approximately 218.46 million ha of the world is occupied by wheat production with a grain yield of around 713.18 million tons and an average yield of 2,900 kg/ha (Khan *et al.* 2015). Wheat has a higher nutritive value than other grains, and together with other major crops like rice and maize, supplies almost two thirds of the world's daily calorie and protein intake. It is an important source of protein, vitamins, and minerals and serves as the staple food source of 30% of the human population. Wheat thrives in temperate regions unlike other similar cereal crops, rice and maize, that is best adapted for tropical environments (Gill *et al.* 2004).

Over 600 million tons of wheat is harvested annually, but the yield must rise exponentially (2% per annum on an area of land) over the next 50 years in order to meet the ever

increasing human demand. Food security is projected to become more critical as a result of population growth (Gill *et al*. 2004). Therefore a multidisciplinary, combined approach to crop enhancement is necessary to guarantee sustainability. To reach this objective, high-production irrigated regions will carry on to play a key role, but the total yield will mostly be affected by genetic potential, the level of diseases, and pests (Duveiller *et al.* 2007). Wheat is susceptible to many kinds of insects, but the few species with damaging effects on yields are especially presenting a challenge to farmers. It has been calculated that pest infestations on average cause 20-37% wheat yield loss worldwide. This calculation translates to approximately $70 billion a year (Dilbirligi *et al.* 2004).

## 2.4.2 RWA background

Russian wheat aphid (RWA) is an economically important agricultural pest that causes substantial losses in small grains, particularly wheat (Lapitan *et al.* 2007), but also damages barley, rye, oats, and other triticale crops (Webster *et al.* 1987). It is an elongated small insect, relatively 1.5 to 1.8 mm in length. This phloem-feeding pest is a lime-green colour and its body is spindle shaped. The RWA has short antennae and when it is viewed from the side, a characteristic double tail can be seen (Figure 2.1) (Stoetzel 1987).

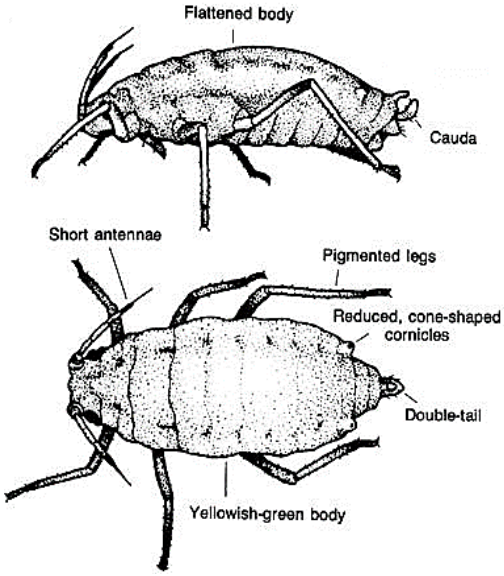


Figure 2.1: Physical characteristics of the RWA (Stoetzel 1987). Side and top view displaying the distinct morphological features of the RWA.

The RWA is native to southern Russia and central Asia, from where it dispersed to all cereal producing areas of the world, with the most severe cases occurring in South Africa, USA, Canada, and South America (Burd *et al.* 2006; Jankielsohn 2011). The RWA is characterised as an invasive species and was reported for the first time in South Africa in 1978 in an area around Bethlehem in the eastern Free State, from where it spread to the western Free State and parts of Lesotho. It was also present in small areas of Gauteng, the North West province, as well as Kwazulu-Natal (Walters *et al.* 1980), and more recently it has been reported in the Western Cape (Jankielsohn 2011).

Cilliers *et al.* (1992) predicted that the economic damage caused by the RWA in South Africa would amount to approximately R30 million in 1993, with almost half of that sum being spent on chemical control. The yield losses caused by the RWA are severe with recorded crop losses of 35-60% in South Africa for wheat alone (Robinson 1992). In the United States (US) damage has been estimated at $890 million from 1987-1993 (Morrison and Peairs 1998) with more recent research showing that in the US, the RWA can reduce wheat grain yield up to 82.9% and vegetative biomass up to 76.5% in Texas and the Oklahoma Panhandles (Mirik *et al.* 2009).

### 2.4.3 RWA feeding

The RWA feeds on phloem and maintains the interaction at a specific feeding site (Goggin 2007; Giordanengo *et al.* 2010). This must be done without killing the phloem cells, in addition to avoiding and disrupting plant defences (Powell *et al.* 2006). Before the RWA can establish a suitable relationship with its host, the aphid must firstly differentiate between host and non-host. The RWA inserts its stylet, comprised of two outer mandibules and two inner maxillae, into the host epidermal apoplasm, initiating shallow probes that last briefly (< 2 minutes), but result in host recognition by the aphid. This provokes the feeding response or host rejection that ultimately stimulates the flight

response. The flight response is a physiological reaction that occurs in response to a perceived harmful event, attack, or threat to survival (Tjallingii and Esch 1993; Will and Van Bel 2006).

As soon as the RWA have identified a suitable host, the adjustable stylets puncture further into the plant tissue, while proteinaceous gelling saliva is secreted. This forms a firming and lubricating sheath around the stylets (Tjallingii 2006). The RWA probe the internal chemistry of cells with the stylets throughout the transit to the phloem by briefly inserting and withdrawing the stylets into various cells (Tjallingii and Esch 1993; Giordanengo *et al.* 2010). This probing function is essential in locating the position of the phloem as well as to determine the progress of the stylets within the plant tissue (Giordanengo *et al.* 2010).

When the sieve tube elements are reached they are punctured and sap is ingested passively due to the high endogenous pressure in the cell (Will *et al.* 2009). Prior to feeding, the RWA injects the tubes with watery saliva that is known to mostly counteract the plant's defence mechanisms, causing the sap to flow uninterrupted (Will and Van Bel 2006). This factor allows the aphid to feed at a single site for many hours (Goggin 2007).

The phloem sap that is ingested by the aphid is full of nutrients such as sugars, but low in nitrogen in the form of free amino acids. The amino acids existing in the phloem sap are inadequate to meet the nutritional requirements of the aphid. Therefore, the RWA have acquired an endosymbiont, *Buchnera aphidicola* (coccoid y-proteobacterium), which utilizes the sucrose and aspartate present in the sap to biosynthesize essential amino acids (Miles 1999; Will *et al.* 2007). This symbiosis allows aphids to use a nutritionally imbalanced food source such as phloem on which other organisms cannot survive. *B. aphidicola* is maintained between generations within aphid produced cells called mycetocytes/bacteriocytes. Research suggests that *B. aphidicola* of different RWA

biotypes display small amounts of variation in sequence and have contrasting plasmid copy numbers (Swanevelder *et al.* 2010).

### 2.4.4 Symptoms of RWA infestation

While the RWA feeds it injects eliciting agents into the host plant, causing chloroplast and cellular membrane breakdown in the host plant and activating *pathogenesis-related* (*PR*) genes (Botha *et al.* 2005). The RWA feeds on the most recent plant growth and ultimately causes chlorophyll production standstill in those leaves (Botha *et al.* 2011). Damage symptoms of RWA infestations on susceptible wheat cultivars include stunted growth of the plant, chlorosis, leaf rolling, head trapping, and white, yellow, and in winter, purple longitudinal streaks on the upper side of the leaf surface (Figure 2.2)(Lapitan *et al.* 2007).


Figure 2.2: Symptoms of RWA infestation. A) Leaf rolling (http://californiaagriculture.ucanr.org). B) Chlorotic streaking (http://entomology.k-state.edu). C) Head trapping (http://www.fao.org).

The occurrence of chlorotic streaking inhibits normal growth of the host plant, which can result in death in the case of extreme infestations. There are two different types of leaf rolling in host plants that can be induced by the RWA (Goggin 2007). One is where the edges of fully expanded and mature leaves curl inward around the RWA colony, protecting it against natural enemies, climate, and insecticides. Another, is where the RWA decreases the size of newly formed leaves that are then prevented from unfolding. This action can result in stunted growth of the entire plant. Head trapping usually occurs later in the season, where infested leaves trap the emerging crop heads, preventing good

grain fill and ultimately affecting the yield production of the crops (Botha *et al.* 2005; Jyoti *et al.* 2006).

Approaches that can be taken to manage this pest to reduce crop losses include a mixture of contact and systemic insecticide, the cultivation of RWA resistant cultivars as well as the introduction of natural biological control agents such as predators, parasitoids, and pathogens which are also used to control aphid numbers when they are protected in the leaf sheath (Carver 2009; Webster et al. 1987).

### 2.4.5 RWA-wheat interaction

The RWA affects wheat throughout the growth season and infestations would usually commence from the appearance of the crop in autumn straight through to crop maturity (Shea *et al.* 2000). RWA infestations can result in 100% reductions in wheat yield or cause death of the plant, especially if the pest is abundant (Elliot *et al.* 2007). Therefore, early detection and timely controls are very important especially during the winter and spring growing seasons (Pike *et al.* 1989).

Host plants react to RWA infestations according to three categories. These can be defined as: (1) tolerance, i.e. the host withstands conditions of infestations which will severely harm susceptible plants; (2) antibiosis, i.e. the capability of the host plant to fatally change the biology of the pest; and (3) antixenosis, i.e. the disfavour or non-preference of plants for insect oviposition, shelter, or food (Painter 1958).

Wheat resistance to RWA can occur through one or a combination of factors. Firstly, the pest may not recognise the plant as a suitable host, because it is less attractive or distasteful, which is expressed as reduced feeding and oviposition. Preformed barriers and defence molecules may prevent attack and plants may initiate defence responses against the pest once it has been recognised. That negatively impacts the pest

performance, which is expressed as longer larval development time, mortality, and reduced larval mass (Hammon-Kosack and Jones 1996).

*Resistance* (*R*-) genes also confer resistance to the RWA in wheat (Dogimont *et al.* 2010). The genetic employment of *R*-genes in wheat is an efficient, economical, and well-tested method in controlling insect pests (Dilbirligi *et al.* 2004). Presently, 14 *R*-genes conferring RWA resistance have been identified in wheat and its relatives, and are titled as *Dn (Diuraphis noxia)* genes. These *Dn* genes are designated as follows: *Dn1* and *Dn2* (Du Toit 1987; 1988; 1989), *dn3* (Nkongolo *et al.* 1991a), *Dn4* (Nkongolo *et al.* 1991b), *Dn5* (Marais and Du Toit 1993), *Dn6* (Saidi and Quick 1996), *Dn7* (Marais and Du Toit 1993), *Dn8* and *Dn9* (Liu *et al.* 2001), *Dnx* (Harvey and Martin 1990), *Dny* (Smith *et al.* 2004), *Dn2414* (Peng *et al.* 2007), *Dn626580* (Valdez 2012), and *DnCI2401* (Fazel-Najafabadi 2015). Each *R*-gene may provide resistance to a single or to multiple biotypes, which is the case in wheat containing the *Dn7* resistance gene, the only recorded germplasm line resistant to all South African RWA biotypes (Dogimont *et al.* 2010; Jankielsohn 2011). The mode of response of these genes has been determined as well as the location for some of these genes on wheat chromosomes. The majority of these genes are located on either chromosome 1B or 7D in hexaploid wheat (Botha *et al.* 2005; Dogimont *et al.* 2010).

### 2.4.6 RWA biotypes

A RWA biotype is a population of aphids that can damage a wheat cultivar that was previously reported resistant to other biotypes of RWA (Burd *et al*. 2006). There is an arms race between plant resistance and aphid virulence. RWA adaptation results in new biotypes that are morphologically alike to the original biotypes, but different in their behavioural performance, such as their preference for different host genotypes (Lapitan *et al.* 2007). New RWA biotypes are likely due to the diversification theory – two

subpopulations live in different environments that select for different alleles at a particular locus – however, new aphid biotypes still show little nuclear and mitochondrial sequence variation. RWA biotypes are not differentiated on morphology, but on their potential to overcome resistance, their fecundity, and the destruction they cause to a plant differential (Swanevelder *et al.* 2010).

The observation of newly emerging RWA biotypes is a growing concern amongst farmers, especially in areas where resistant wheat cultivars are now put at risk because of new biotypes (Botha *et al.* 2005). The appearance of new RWA biotypes implies either new introductions or adaptations and diversification of existing populations. It is very important to research new sources of resistance that can be implemented immediately for more durable resistance (Haley *et al.* 2004). Biotypes can be differentiated from one another according to two types of existing classification systems. In the two-category system the aphids are categorized as virulent or avirulent, whereas in the three-category system the aphids are classified as virulent, intermediate, or avirulent. Classification of these systems is exclusively based on the phenotypic response of the host as a direct result of aphid feeding (Burd *et al.* 2006; Puterka *et al.* 2012).

A RWA biotype virulent to cultivars carrying the *Dn4* resistance gene was discovered in 2003 in south-eastern Colorado in the US (Haley *et al.* 2004). In South Africa four new RWA biotypes have been reported since 2005. The first resistance-breaking biotype against cultivars containing the *Dn1* resistance gene was reported in 2005 in the eastern Free State (Figure 2.3) and is known as SA2 (South African biotype 2) (Tolmay *et al.* 2007). Shortly thereafter, in 2009, a second resistance breaking biotype emerged that exhibited virulence to the same resistance sources as SA2 (*Dn1, Dn2, Dn3,* and *Dn9*) as well as virulence against *Dn4*, known as SA3 (South African biotype 3) (Jankielsohn 2011). During 2011, SA4 (South African biotype 4), relatively unaffected by the *Dn5* resistant gene, was discovered (Jankielsohn 2014). The SA2, SA3, and SA4 RWA

biotypes are highly virulent when compared to the original South African biotype, SA1 (Jankielsohn 2016). SA1 infestations do not cause damage to resistant wheat cultivars, except in the germplasm containing the *dn3* gene.

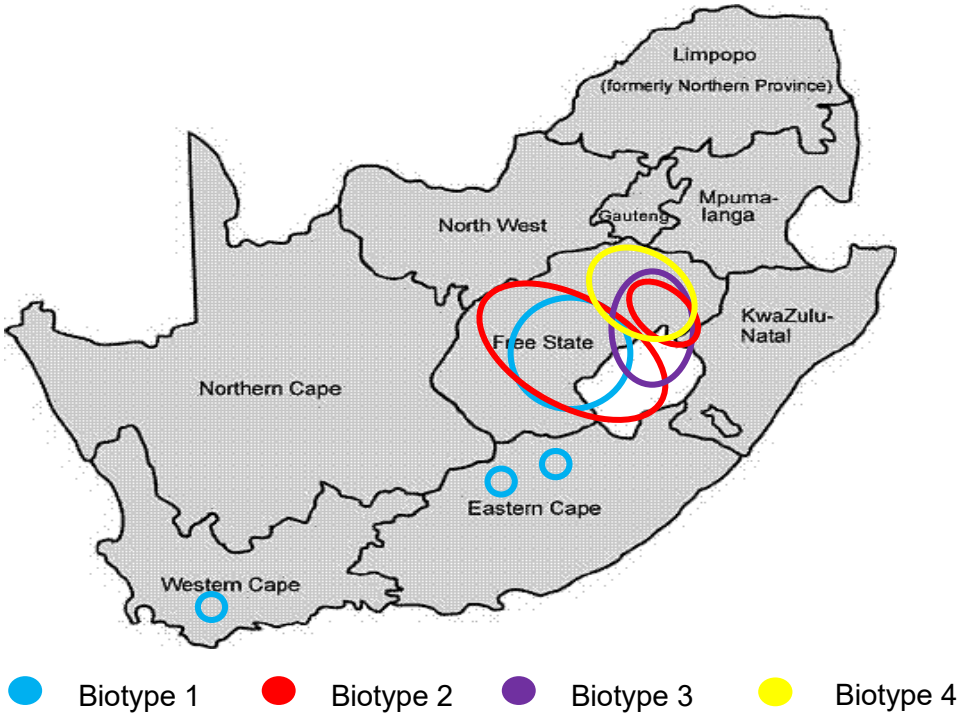


Figure 2.3: A general distribution map of the four RWA biotypes found in South Africa (Jankielsohn 2016).

The South African mutant biotype, SAM, was developed from SA1 after laboratory induced selective pressure on *Dn* resistant cultivars (Swanevelder *et al.* 2010). SAM causes symptoms in all known resistant wheat cultivars including those containing *Dn7*.

## 2.4.7 RWA karyotype

Cytogenetic research was restricted in aphids in the past and confined to counting and size-sorting of the chromosomes. However, presently aphids are a popular model group among cytogeneticists (Novotná *et al.* 2011). The interaction between histones and non-histone proteins leads to the formation of chromosomes (Margueron and Reinberg 2010; Zhou *et al.* 2011). Even though there is no noticeable connection between genome size and the amount of chromosomes (Heslop-Harrison and Schwarzacher 2011), Schubert *et al.* (2001) believed that large genomes must be spread into a number of smaller

chromosomes, ultimately because chromosome size has an upper boundary. The karyotype of aphids has been shown to vary in chromosome number and morphology between and even within the species (Novotná *et al.* 2011).

The female karyotype of the RWA (2*n* = 10) consists of 4 autosomal chromosome pairs as well as a pair of large X (sex) chromosomes (Figure 2.4). The male karyotype of the RWA (2*n* = 9) consists of 4 autosomal pairs, but only a single large X chromosome. The 4 autosomal chromosome pairs present in both sexes of the RWA can be classified according to size into 2 classes: 3 pairs of middle-sized chromosomes, and 1 pair of small chromosomes. The X chromosome/chromosomes are classified as the largest component of the karyotype (Novotná *et al.* 2011).

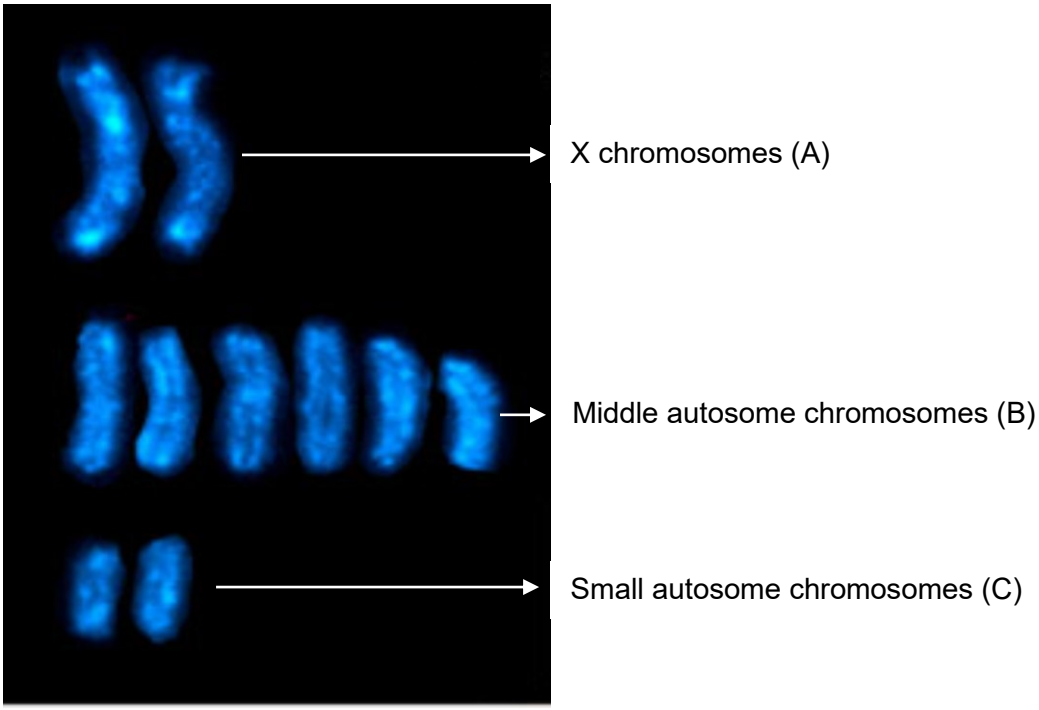


Figure 2.4: Female RWA karyotype. A) Two large X (sex) chromosomes. B) and C) four autosome chromosome pairs (Novotná *et al.* 2011).

The estimated genome sizes of the female and male RWA is 2C = 0.86 pg and 2C = 0.70 pg, respectively. The differences, with regard to the DNA content, of the two genders proposes that the X chromosomes occupies approximately 35% (1C = 0.43 pg) of the female haploid genome. The X chromosome in the RWA is one of the largest sex

chromosomes in the animal kingdom, measuring approximately 10 µm (Novotná *et al.* 2011).

Large X chromosomes are described in several aphid species. The *Neuquenaphis* (Neuquenaphidinae) have X chromosome sizes ranging from 11 to 15% of the total genome (Blackman *et al.* 2003), and for the related *Myzus persicae*, the X chromosome reaches almost 27% of the genome size (Blackman and Takada 1976). Several papers have presented data on large heterochromatin blocks and highly repetitive sequences in the X chromosomes of some aphid species (Mandrioli *et al.* 1999).

Karyotype variation is likely due to the holocentric chromosomes of the RWA. Holocentric chromosomes lack primary constrictions (centromeres) and thus have multiple sites of attachment to the spindle (Figure 2.5). Therefore, these holocentric chromosomes have kinetic activity spanning across most of the chromosome axis (Monti *et al.* 2012).

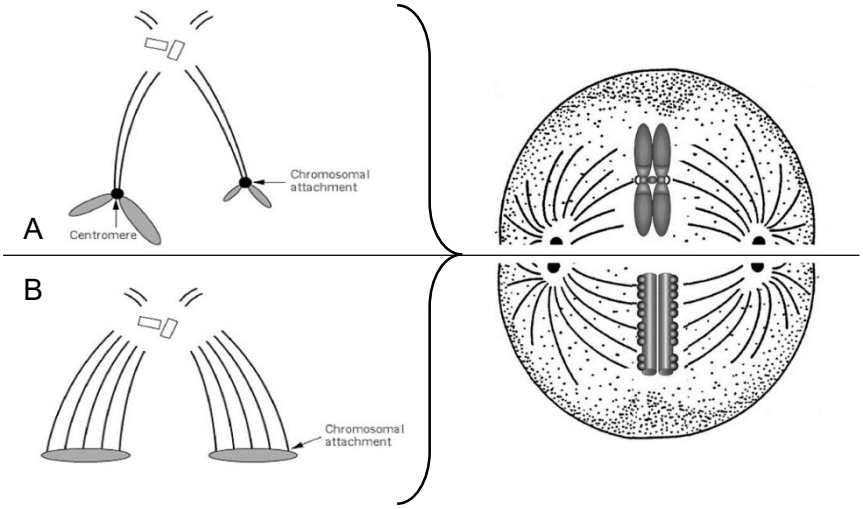


Figure 2.5: Monocentric (A) and holocentric (B) chromosomes. A) Single site of chromosomal attachment to the centromere. B) Multiple sites of chromosomal attachment.

In the course of mitotic anaphase, these chromosomes' sister chromatids disconnect in parallel and display a 'holokinetic' movement (Pérez *et al.* 1997). The kinetic activity along the chromosome causes chromosomal fragments to bind to the microtubules which causes them to move into the daughter cells during cell division (Blackman 1987). In

contrast, these chromosomal fragments may be lost during mitosis and meiosis in monocentric chromosomes (Figure 2.5), because chromosomes attach to microtubules at a certain region (the centromere) and move in the direction of the pole during anaphase with the centromere in front (Monti *et al.* 2012).

The position of the centromere in organisms with monocentric chromosomes is a valuable descriptive factor. The fact that the aphid chromosome lacks a centromere makes chromosomes of similar size almost indistinguishable within the species (Novotná *et al.* 2011).

### 2.4.8 RWA reproduction

In places where the RWA is indigenous, right before winter, males and females will mate and lay eggs. These eggs will stay as eggs for the whole winter, and then hatch in the spring. However, male RWA rarely develop and only exist in colder climates (Hodgson and Karren 2008).

There are no male RWA present in South Africa (Webster *et al.* 1987) and colonies are established by apterous virginopara (wingless parthenogenetic females) (Jyoti *et al.* 2006). Various reproductive and dispersal strategies are used by the RWA that finally result in their abundance (Goggin 2007). Parthenogenesis and vivipary, which are the primary modes of RWA reproduction, impart a highly efficient colonisation habit of new hosts to these aphids. Parthenogenesis is reproduction through development of unfertilised eggs. These unfertilised eggs will usually only give rise to females. Vivipary is the ability of each female RWA to give birth to live daughters (Goggin 2007; Giordanengo *et al.* 2010), and these daughters are already pregnant with embryonic granddaughters (Michaud and Sloderbeck 2005). These abilities of the RWA shortens the time between generations, allowing nymphs to reach maturity and reproduce at a rapid rate – a factor implicated for their large economic impact (Giordanengo *et al.* 2010).

Another effective method the RWA uses to colonize is through the winged dimorphism, which enable winged adults to colonize new, distant hosts during unfavourable seasons or in situations of high population densities, while the wingless adults redirect the energy required for producing flying organs into their reproductive cycles (Goggin 2007).

### 2.4.9 RWA sex chromosome system

The sex chromosome system for RWA has been identified as XX/XO, as seen in a number of different aphid species. This system never possesses a Y chromosome and is essential for parthenogenesis. Crucial biological processes like sex determination, imprinting, speciation, and genomic conflicts are all influenced by the sex chromosomes. Sex chromosomes display many unusual characteristics like inheritance patterns, reduced recombination, and hemizygosity, which all play a big role in their response to evolutionary factors (Jaquiéry *et al.* 2012).

The RWA male that has the sex-chromosome constitution XO can only be produced through modified mitosis by parthenogenetic XX females. During this process one of the X chromosomes is discarded to create eggs that consist of a single X chromosome as well as two autosomal sets. Thereafter while the autosomes divide or disconnect independently, the two X chromosomes are linked with one another at a single end, unlike normal mitosis which forms a C-shaped structure. Thereafter one of the X chromosomes is discarded from the complement and the sister chromatids of the other X chromosome move to the daughter cells (Orlando 1974; Blackman and Hales 1986).

One of the most prominent distinctions between RWA and other XX/XO organisms such as nematodes, insects, or molluscs is their unusual pattern of inheritance of the X chromosome during a life cycle where asexual and sexual reproduction is combined. Figure 2.6 displays the life cycle of the RWA and shows that it consists of numerous events of apomictic parthenogenesis, proceeding with a single round of sexual

reproduction in autumn. After 10-20 generations of apomictic parthenogenesis, asexual reproduction finally leads to the production of sexual RWA individuals, where the male aphids randomly inherit only one of the X chromosomes of the asexual female (Wilson *et al.* 1997; Caillaud *et al.* 2002).

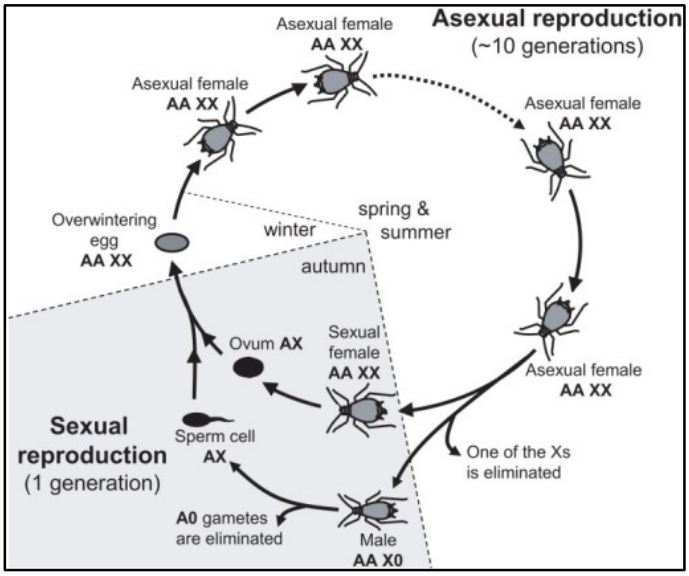


Figure 2.6: The yearly life cycle of the aphid and ploidy levels for autosomes (A) and sexual chromosomes (X) (Jaquiéry *et al.* 2013).

The male RWA produces gametes that are haploid for the X as well as autosome chromosomes. Therefore, when the male and female gametes fuse the diploidy of the X and autosome chromosomes are restored to generate an asexual female. This means that after sexual reproduction the asexual progeny inherited half of the autosomes and X chromosomes from the mother and the other half from the father (Figure 2.7).

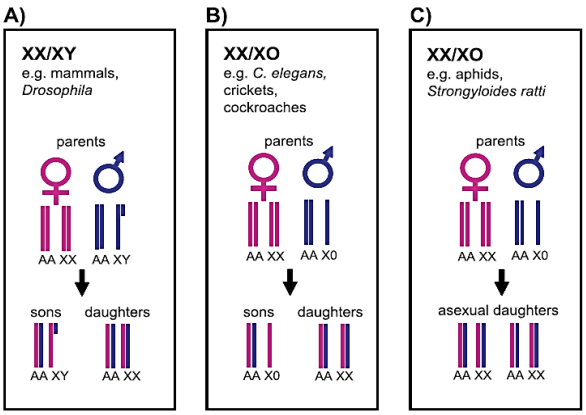


Figure 2.7: Inheritance of the X chromosome in XX/XY, standard XX/X0, and aphid-like XX/X0 sex-determining systems. In aphid-like XX/X0 systems the male transfer its X chromosome to 100% of its progeny, giving rise to only asexual daughters (Jaquiéry *et al.* 2012).

The RWA pattern of X chromosome inheritance is different from standard XX/XO or XX/XY systems where the female offspring inherits one X chromosome from each parent (mother and father), but where males only receive a copy of the X chromosome from the mother. As explained previously, during RWA sexual reproduction male aphids transmit their X chromosome to 100% of their progeny, ultimately only producing asexual daughters (Figure 2.7) (Jaquiéry *et al.* 2012).

## 2.5 Insect genomes

Over the last few years of declining DNA sequencing cost as well as more accessible sequencing services in primary laboratories and companies, it has become more economical for many entomologists to make use of *de novo* genome sequencing and assembly methods for insect species. However, in order to produce a high quality reference genome, sequence generation alone is not enough, and in various cases, extremely fragmented genome assemblies prevent high quality gene annotation and other sought after analysis of sequencing data (Richardson and Murali 2015).

The *de novo* assembly of insect genomes is often hampered by high polymorphism, the lack of ability to breed for genome homozygosity, and finally the small physical size of insects that ultimately limits the amount of DNA to be extracted from a single individual. Modern improvements in sequencing technology and assembly strategies allows insect genomes to be studied more effectively (Richardson and Murali 2015).

Arthropod genome sizes exhibit considerable diversity, with the largest reported to date being that of the grasshopper (Orthotera: *Neoconocephalus triops* L.) (1C = 7 125 Mb (male)/7 752 Mb (female); 7.93 pg) and the smallest being the two spotted spider mite (Trombidiformes: *Tetranychus urticae*) (1C = 90.7 Mb; 0.09 pg) (Hanraham and Johnston 2001; Johnston *et al.* 2007).

*Drosophila melanogaster* (fruit fly) was the first arthropod high quality, complete genome to be sequenced using shot-gun sequencing (BDGP6; Adams *et al.* 2000), and presently the model dataset for whole genome assembly amongst insects (Myers *et al.* 2000). The genome of the fruit fly has been determined to be 180 Mb in size, of which a third consists of centric heterochromatin. The 120 Mb of euchromatin is located on the sex chromosome and two large autosomal chromosomes, whereas the fourth small chromosome only comprises of 1 Mb of euchromatin. The heterochromatin mainly includes short, simple sequence elements repeated for many bases, which is occasionally interrupted by inserted transposable elements, and tandem arrays of ribosomal RNA genes (Adams *et al*. 2000).

The first aphid genome to be sequenced belonged to the pea aphid, *Acyrthosiphon pisum* (Acyr_2.0; GCA_000142985.2; The International Aphid Genomics Consortium 2010). It was also the first published whole genome sequence of a basal hemi-metabolous insect, in contrast to the numerous published genomes of homo-metabolous insects. The pea aphid that is commonly used in laboratory research is a pest of legume crops (*Fabaceae*) and is very closely related to many significant crop pests, such as the RWA as well as the green peach aphid (*Myzus persicae*) (Von Dohlen *et al.* 2006). The 464 Mb draft genome assembly of the pea aphid, together with the genomes of its dependant bacterial symbionts (Shigenobu *et al.* 2000; Degnan *et al.* 2009; 2010), offers important information that will enable researchers to discover the genetic basis of co-evolved symbiotic associations, of host plant specialization, of insect-plant interactions, and of the developmental causes of extreme phenotypic plasticity.

The International Aphid Genomics Consortium (2010) discovered that there was a major gene duplication in the pea aphid genome that seemed to come from the time around the origin of aphids. They also revealed that the pea aphid genome has more coding genes than any previously sequenced insects, with the high gene number being an indication of

both extensive duplication as well as the presence of genes with no orthologs in other insects. There are more than 2,000 gene families (for example chromatin modification, miRNA synthesis, and sugar transport) expanded in the aphid lineage, relative to other published genomes (The International Aphid Genomics Consortium 2010).

Recently, the genome sequence of the RWA (GCA_001186385.1) was published for the first time by Nickolson *et al*. (2015). The assembled genomic scaffolds cover 393 Mb, which is equal to 93% of its estimated 421 Mb genome and contained 19,097 genes. The authors determined that the RWA has the most AT-rich insect genome that have been sequenced to date, reaching 70.9%, with a bimodal CpG distribution and a whole set of methylation related genes. Nickolson *et al*. (2015) determined that the genome of the RWA has a prevalent, general reduction in the number of genes per ortholog group, which include defensive, detoxification, chemosensory, and sugar transporter groups when compared to the pea aphid genome, as well as a 65% decrease in chemoreceptor genes. Thirty of 34 known RWA salivary genes were found in the genome assembly that exhibited less homology with the salivary genes commonly expressed in insect saliva, including glucose dehydrogenase and trehalase. However, greater conservation was displayed among genes that are expressed in RWA saliva, but which is not detected in the saliva of other insects. Genes that are involved in insecticide activity and endosymbiont-derived genes were also discovered in the assembly, along with genes involved in virus transmission, even though RWA is not a viral vector (Nickolson *et al*. 2015).

The mitochondrial genomes of insects are closed, double stranded, and circular. Their sizes range between 13-20 kb, while their gene content is well conserved and they have a low rearrangement rate. These features make mitochondrial genomes of insects a very valuable tool to study deep divergences and molecular evolution (Hu *et al*. 2009). The insect mitochondrial genome characteristically encodes 37 genes that include 13 protein-

coding genes, 2 ribosomal RNA, and 22 transfer RNA. The whole insect mitochondrial genome is compactly arranged with very limited intergenic nucleotides, overlapping neighboring genes, and no introns (Chai *et al*. 2012). Furthermore, the gene order of mitochondria in aphids, psylids, and many whiteflies is known to resemble the projected Insecta ancestral gene order, with a mitochondrial sequence divergence of only 13.1% for aphids which is significantly less than that of psylids and whiteflies (Baumann *et al*. 2004).

Nucleotide diversity in aphid mitochondrial genomes has been extensively studied, even though only three genomes are currently available which includes the RWA. The complete RWA mitochondrial genome is 15,721 bp long and is comprised of 38 genes which is characteristic within most insects. These 38 genes consist of 20 different transfer RNA genes, 13 protein-coding genes, and 2 ribosomal genes (De Jager *et al.* 2014). The mitochondrial genome size of the RWA falls in the range of animal mitochondrial genomes (~16,000 bp) and corresponds to that of the ancestral aphid species (Crozier and Crozier 1993).

## 2.6 Single-chromosome analysis

Genomes may be large and complex, because of a high content of repetitive and duplicated sequences or as a result of ploidy. Even though it is not a problem to fingerprint the large numbers of clones necessary to create a physical map (Luo *et al.* 2003), and to sequence billions of DNA bases (Metzker 2010), the problem is to assemble the large number of fingerprints and short reads into an unambiguous order that correctly represents the genome (Wei *et al.* 2009; Alkan *et al.* 2011; Treangen and Salzberg 2012). These factors hinder the construction of clone-based physical maps, positional gene cloning, and *de novo* genome sequencing. One solution is to reduce the sample complexity by dissecting the genomes to single chromosomes. Another area which will

benefit from the analysis at single-chromosome level is the assembly of haplotype-resolved genome sequences (Yang *et al.* 2011).

Most of the cells in an organism contain chromosomes that are at interphase. Their nuclei consist of decondensed chromosomes that make it impossible to separate from one another. Separation is only possible when chromosomes are more condensed during the metaphase stage of cell devision (Doležel *et al.* 2012).

The utility of isolated, separated chromosome fractions is determined by their purity and quality of DNA. Purity depends on the degree to which the chromosome of interest can be resolved from other chromosomes, chromosome clumps, chromatids, and chromosome fragments in the sample (Doležel et al. 2012). Currently different methods of chromosome isolation exist, which include the following: micromanipulation, gradient centrifugation, magnetic chromosome separation, flow cytometry, etc.

### 2.6.1 Micromanipulation/Microdissection

Initial isolations of single chromosomes from spreads of metaphase chromosomes of dividing cells made use of a micromanipulator (Chambers and Sands 1923; Barigozzi 1939; Scalenghe *et al.* 1981; Schondelmaier *et al.* 1993). This device is used to physically interact with a sample under a microscope, where a level of precision of movement is required that simply cannot be achieved by the unaided human hand. Originally, the process of microdissection involved isolating the chromosome by using glass microneedles, which was a technically challenging task (Scalenghe *et al.* 1981). The introduction of laser microbeams in microdissection (Monajembashi *et al.* 1986) improved the isolation procedure, however it still involved the use of the glass microneedles to collect the chromosome isolated via the laser (Zhou and Hu 2007). More recently, the PALM® Robot-Microbeam system was introduced, that uses a laser to cut chromosomes from microscope slides as well as to catapult fragments into a collection tube (Olofsson

*et al.* 2012). This resulted in the negation of the glass needles and improvement of accuracy. One of the most prominent advantages of this technique is that the individual operating the micromanipulator can clearly identify the chromosomes to be isolated. A disadvantage is that only a few chromosomes can be collected or isolated at a time (Hobza and Vyskot 2007) which affects the quality of the chromosomal DNA making it only suitable for basic types of analysis (Ma *et al.* 2010). Ultimately, microdissection cannot meet the requirements for sequencing complete chromosomes because of low coverage. The latest developments in the area of isolating chromosomes through micromanipulation include the atomic force microscope nanolithography that makes the dissection/extraction of fragments as small as 0.4 µm possible (Di Bucchianico *et al.* 2011).

### 2.6.2 Gradient centrifugation

Another method that is presented to isolate chromosomes in large numbers is by making use of relative density by gradient centrifugation. Chromosomes are obtained from populations of dividing cells in an aqueous suspension. This method however only allows the large and small chromosomes to be separated from one another and is therefore not a viable option to isolate selected chromosomes within these fractions (Stubblefield and Oro 1982).

### 2.6.3 Magnetic chromosome separation

Magnetic sorting is a method that is used to separate cells, cell organelles, and microorganisms (Molday *et al.* 1977; Owen 1983). The process of magnetic sorting entails an affinity couple, usually an antibody that is covalently bound or physically absorbed to magnetic microspheres. Ugelstad *et al.* (1988) designed polysterene magnetic microspheres or beads for this purpose. Magnetic beads contain iron oxide ($Fe_3O_4$) (Lea *et al.* 1985; Howell *et al.* 1988), and by binding the chromosome of interest to these beads

trough an antigen-antibody approach and using a simple permanent magnet (Figure 2.8), enables large amounts of the chromosome to be sorted in a short time (Dudin *et al.* 1988). It is recommended to isolate and extract chromosomes from an unperturbed system or cell line (Vitharana and Wilson 2006).

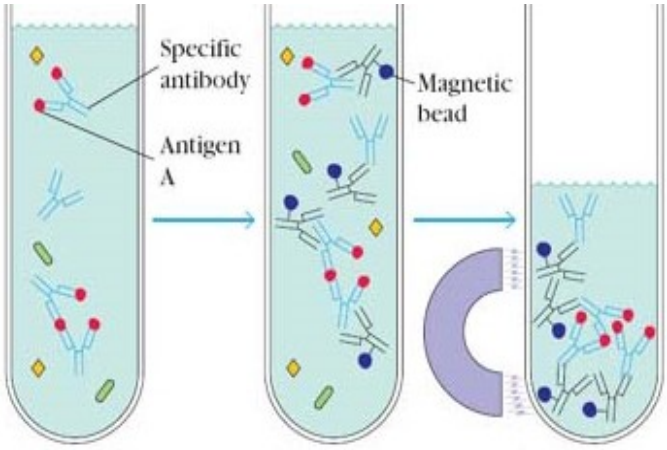


Figure 2.8: Process of magnetic sorting. The particle of interest is covalently bound with magnetic beads and sorted using a simple magnet.

The positive aspect of using magnetic beads is that it makes use of a probe that is specific to the chromosome of interest, eliminating the non-specific methods used to identify certain chromosomes through fluorescent dyes – DNA binding or intercalating (Vitharana and Wilson 2006). However, a disadvantage of this approach is that it suffers from lower purities in isolated fractions and target sequences must be available (Doležel *et al.* 2012).

## 2.6.4 Flow cytometry

Presently, the most effective and universally common method for separating chromosomes on a large scale is flow cytometry, which is an approach that studies and analysis the optical parameters of miniscule particles while they pass through a narrow stream of liquid. Flow cytometry analysis cells and cell organelles at rates of $10^2$–$10^4$/s. If a chromosome of interest can be identified from other chromosomes based on its optical properties (light scatter, fluorescence), it can be purified in large quantities (Doležel *et al.* 2012).

This method of chromosome isolation is normally used with mitotic preparations, because using suspensions of meiotic chromosomes is not practical (Bartholdi 1990). The tissues and cell cultures used to prepare the samples must be utilized in such a manner to produce the highest proportion of cells in metaphase. It has been determined that roughly 95% of animal cells can be accumulated in metaphase (Carrano *et al.* 1976, 1979), whereas in plants the value of metaphase cells decrease to round about 50% (Vrána *et al.* 2000; Vláčilová *et al.* 2002). The chromosomes are released into an appropriate isolation buffer from the enhanced metaphase cell population, where after the chromosomal DNA is stained with a DNA-specific fluorochrome, allowing the chromosomes to be identified according to their level of fluorescence intensity (DNA content) (Doležel *et al.* 2012).

The flow cytometer is fitted with a single laser that is used as a light source (Figure 2.9 A). During flow cytometry the chromosome of interest is labelled with a biotin- or fluorochrome-labeled chromosome-specific probe (Dudin *et al.* 1988; Vitharana and Wilson 2006) by initially staining the suspension of intact chromosomes with a DNA-specific dye. The sample is then introduced to the flow chamber of the instrument from where the chromosomes will be transported in a narrow stream of liquid (Figure 2.9 B). The chromosomes are individually measured and quantified by the laser beam, scattered light, and emitted fluorescence. During sorting the liquid stream containing the chromosome of interest is broken into droplets and electrically charged. The chromosome droplets are then sorted by electrostatically charged deflection plates and collected in suitable containers (Figure 2.9 D) (Meksem and Kahl 2005). Fundamentally, when the chromosomes have been analysed, the flow karyotype is generated (Figure 2.10). The flow karyotype consists of a histogram of fluorescence intensity, forming peaks for each chromosome relative to its DNA content (Meksem and Kahl 2005). Flow cytometry allows for the investigation of large populations of organelles in brief periods of time and

represents the output data in flow karyotypes (Figure 2.10). Flow karyotypes illustrate the distributions of chromosomal DNA content where each chromosome is represented by a distinctive peak. The peak/chromosome location is relative to fluorescence intensity and the volume indicates the rate of occurrence of that specific chromosome. It is possible that some chromosome peaks may overlap due to their similar sizes and total DNA content, making it very difficult to resolve the chromosomes from one another (Doležel et al. 2012).

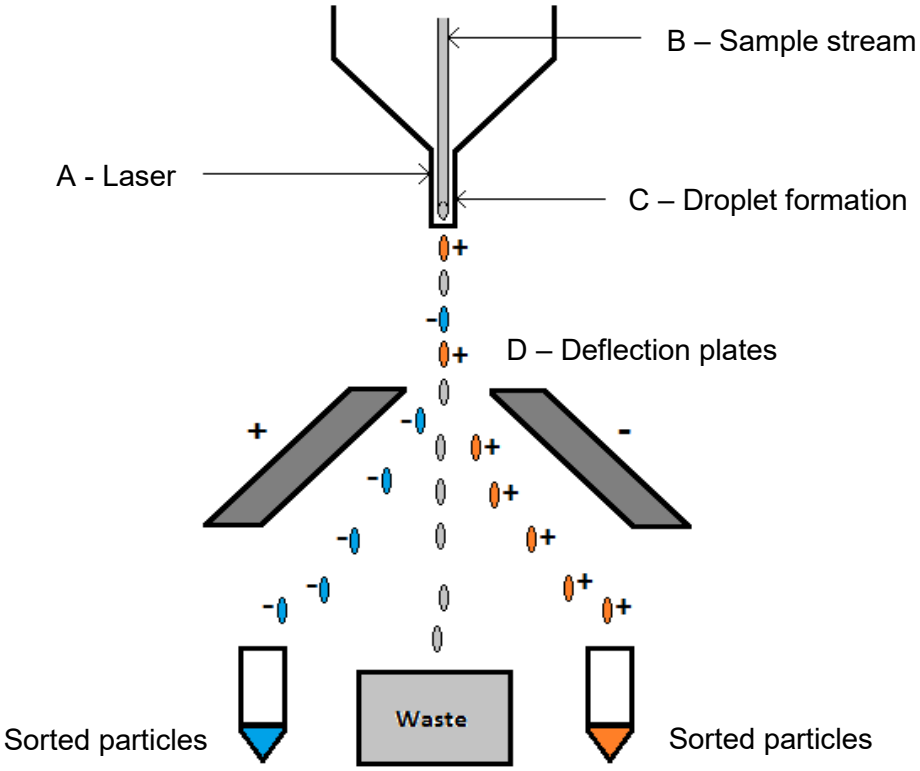


Figure 2.9: Schematic view of the components used by the flow cytometer during sorting of particles. The particles move through the sample stream (B) where a charge is pulsed at the break-off point, the precise area where the selected particle is formed into a droplet (C). Two charged deflection plates (D) situated below the break-off point deflect the charged droplets containing the particles of interest towards a collection tube, and the uncharged droplets are collected into a waste tube.

Flow cytometry software allows for gating strategies to sort particles of interest. Gating allows for the selection of single chromosomes through graphic depictions by identifying doublets (which are two chromosomes stuck together), clumps (which are more than two chromosomes stuck together), as well as debris that contaminate the series. Doublet and

clump discrimination are very important to prevent any chromosomes that are not of interest from passing through to sample collection (Kron and Husband 2015).

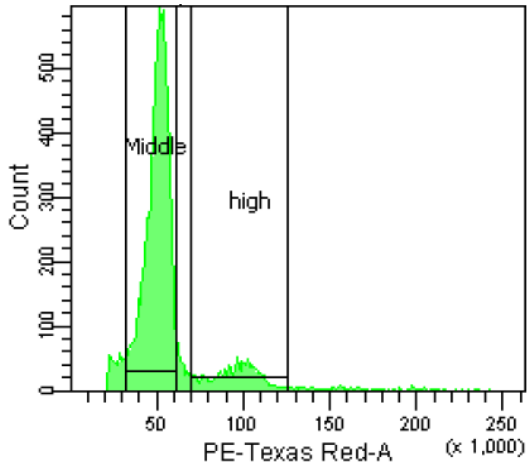


Figure 2.10: Example of a flow karyotype generated during flow sorting. The peaks represent the positive datasets. In this case the chromosomes of interest.

## 2.7 Sequencing

### 2.7.1 Sequencing platforms

Frederick Sanger and his associates developed the first method of determining the exact sequence of single stranded DNA molecules in 1977. The method became known as Sanger sequencing and is based on the selective incorporation of chain terminating labelled dideoxynucleotides by DNA polymerase during *in vitro* amplification (Sanger *et al*. 1977). In 2005, next generation sequencing (NGS) technologies were introduced and have since transformed genomic research. The development of NGS technologies were catalysed by the great demand for revolutionary methods that deliver rapid, low-cost, and accurate genome information. The inexpensive production of large volumes of sequence data - in some cases in excess of one billion short reads per instrument run - is the primary advantage over conventional methods (Metzker 2010). NGS methods overcome the limited scalability of traditional Sanger sequencing by either creating micro-reactors and/or attaching the DNA molecules to be sequenced to solid surfaces or beads, allowing for millions of sequencing reactions to happen in parallel (Reis-Filho 2009).

There is a wide selection of different major NGS technologies, such as Roche's 454 pyrosequencing, Illumina's MiSeq/HiSeq/NextSeq, Applied Biosystems' SOLiD, Ion Torrent's PGM, and the PacBio system (Table 2.1). These NGS platforms are different in many ways, including read length and the number of DNA molecules they sequence in parallel. Traditional Sanger sequencing machines analyse terminally labelled DNA strands and can read about 800 bases of 100 DNA molecules at the same time. The NGS platforms however, read numerous DNAs in parallel but have smaller read lengths. For instance, 454's machine reads 400,000 DNAs that are each about 250 bases in length; Illumina's MiSeq can produce paired-end reads that are 300 bases in length each while the platform with the greatest output overall is the HiSeq 2500, generating 4 billion fragments in a paired-end approach with 125 bases for each read in a single run. Illumina has also developed the HiSeq X Ten, which is an array of 10 HiSeq machines sold as a unit, for higher throughput than ever achieved in the past (Hodkinson and Grace 2015). NGS platforms also differ in cost per base: the 454 machine sequences are about ten times cheaper than traditional Sanger technology, and Illumina and ABI are 100 times cheaper (Von Bubnoff 2008). All of these technologies have different advantages and disadvantages (Table 2.1)

Chen *et al.* (2008; 2010) suggested that NGS of chromosomes provide a well-designed approach toward identifying the chromosome composition as well as to map chromosomal breakpoints with an error margin of less than 1,000 bp. Sudbery *et al*. (2009) determined with studies on mice that sequencing entire chromosomes permits the generation of condensed maps of genetic variation between diverse genotypes. They also confirmed that it is a powerful tactic to discover single nucleotide polymorphisms (SNPs) to derive high resolution images of quantitative trait locus (QTL) regions.

Table 2.1: Advantages and disadvantages of various NGS platforms (Van Dijk *et al.* 2014).

| NGS Platform | Advantages | Disadvantages |
|---|---|---|
| **Roche's 454** | The long reads (1 kb maximum) are easier to map to a reference genome, and are an advantage for *de novo* genome assemblies or for metagenomics applications.<br>Run times are relatively fast (23h). | Relatively low throughput (about 1 million reads, 700 Mb sequence data) and high reagent cost.<br>High error rates in homo-polymer repeats.<br>Roche announced that it will discontinue 454 and stop supporting the platform in 2016. |
| **Illumina's MiSeq/HiSeq** | Most library preparation protocols are compatible with the Illumina system.<br>Illumina offers the highest throughput of all platforms and the lowest per-base cost.<br>Read lengths of up to 300 bp, compatible with almost all types of application. | Overloading results in overlapping clusters and poor sequence quality.<br>Sequence complexity - low-complexity samples such as 16S metagenomics libraries must be diluted or mixed with a reference PhiX library to generate diversity.<br>Sample loading is technically challenging. |
| **ABI's SOLiD** | Second (after Illumina) highest throughput system on the market.<br>The SOLiD system is widely claimed to have lower error rates, 99.94% accuracy, than most other systems owing to the fact that each base is read twice. | Shortest reads (75 nt maximum) of all platforms, and relatively long run times.<br>Less-well-suited for *de novo* genome assembly.<br>The SOLiD system is much less widely used than the Illumina system and the panel of sample preparation kits and services is less developed. |
| **Ion Torrent's PGM** | Semi-conductor technology, no requirement for optical scanning and fluorescent nucleotides.<br>Fast run times and a broad range of applications. | This technology suffers from the same issue as 454 with high error rates in homopolymers. |
| **PacBio system** | Extremely long reads of 20 kb and even longer make this technology an ideal tool to finish genome assemblies or to improve existing draft genomes.<br>Run times are fast (typically a few hours). | High cost, $2–17 per Mb, high overall error rates (14%).<br>Lowest throughput of all platforms (maximum 500 Mb).<br>Limited range of applications. |

### 2.7.2 Next generation sequencing (NGS) analysis

Sequencing the chromosomes of organisms with available reference genomes is a fast approach to study variation at DNA level. Single chromosome sequencing not only decreases cost, but it also simplifies data analysis compared to whole genome sequencing (Doležel *et al*. 2012).

The advent of NGS technologies is accompanied by the development of many whole-genome sequence assembly methods and software, especially for *de novo* fragment assembly. Selecting a suitable assembler becomes a tough task as computational time, access to maximum random access memory (RAM), assembly accuracy, and integrity should be considered (Zhang *et al*. 2011).

Pevzner and Tang (2001) as well as Pevzner *et al*. (2001) pioneered short read assembly that is based on de Bruijn graphs (Table 2.2). Other methods beside the de Bruijn graph-based method include prefix tree-based approaches (Warren *et al*. 2007) plus overlap-layout-consensus approaches (Hernandez *et al*. 2008). The genome size as well as the sequencing error rate both have an impact on the speed at which these programs function (Li and Durbin 2009).

Alignment-based methods were often used as a substitute when data volume produced by larger eukaryotic genomes became an obstructing factor. Therefore, Simpson *et al*. (2009) developed assemblers that ran the task in parallel, which increased the memory for assembly and consequently permitted the use of much larger data sets. An alternative method to construct functional sequence scaffolds from shorter reads is to make use of alignment-based approaches and comparisons to known reference genomes. The Burrows-Wheeler transform (BWT) algorithms (Table 2.2) have demonstrated to be very effective by means of collapsing exact reads together and not aligning reads against simpler copies (Li and Durbin 2009).

The *k-mer* is a very important parameter in sequence data analysis. The *k-mer* is defined as a short DNA sequence consisting of a fixed number (*K*) of bases. In other words it refers to all the possible substrings of length *k* that are contained in a string (S). Detemining *k-mer* occurrence in numbers, is known as *k-mer* counting. *K-mer* counting is essential, because various genome assemblers use this parameter to identify overlaps in sequence and a genome size estimation can be made with the *k-mer* count statistics (Marçais and Kingsford 2011). The likelihood of sequencing errors are assessed by using *k-mer* frequencies (Kelley *et al*. 2010). These frequencies are also used to identify candidate regions in *de novo* repeat annotation (Campagna *et al*. 2004; Healy *et al*. 2003). KmerGenie (Chikhi and Medvedev 2014) and Jellyfish (Marçais and Kingsford 2011) are two of the more popular *k-mer* counting algorithms.

Several strategies are available to estimate the genes present in a sequencing data set. Genes have long been regarded as discrete entities located linearly along chromosomes, but recent investigations have demonstrated extensive transcriptional overlap between different genes (Denoeud *et al*. 2007). An experimental approach is described by Vossen *et al*. (2013) in which degenerate primers are designed for specific motifs associated with, for instance, resistance genes. This method of profiling permits gene candidates to be amplified as well as either analysed on a gel, cut out, and sequenced. Alternatively, NGS platforms can be used to directly sequence the polymerase chain reaction (PCR) products. Another approach allows protein coding genes (PGS) to be explored using software packages like FunCat (Functional Catalogue) that classify proteins from whole genome data (Ruepp *et al*. 2004) or Gene Ontology (GO) (Ashburner *et al*. 2000). The vast majority of the biology of a newly sequenced genome is inferred from the set of encoded proteins. Predicting the gene set is therefore invariably the first step that is taken after the genome sequence has been determined (Harrow *et al*. 2009).

There are also numerous sequencing studies that prefer to use manual data mining implementing BLAST algorithms to compare genome sequence data to known genes in databases such as Ensembl (http://ensemblgenomes.org/; Thole *et al*. 2012), SwissProt (Vitulo *et al*. 2011), and GenBank UniGene (Vitulo *et al*. 2011).

Table 2.2: Methods for alignment, assembly, and annotation.

| **Objective** | **Approach** | **Software** | **Reference** |
|---|---|---|---|
| *de novo* contig assembly | de Bruijn graphs | SOAPdenovo | Luo *et al.* 2012 |
| | | Velvet | Zerbino and Berney 2008 |
| Similarity searches and assigning gene ontology | Local alignment geno ontology | BLAST | Altschul *et al.* 1997 |
| | | FASTA | Pearson and Lipman 1988 |
| Alignment of larger scale sequence comparisons | Burrows-Wheeler transform (BWT) | BWA | Li and Durbin 2009 |
| | | Bowtie | Langmead *et al.* 2009 |

In the present study, the following NGS platform and software will be used to assemble and characterise the X chromosome of the RWA: Illumina® HiSeq™ platform as well as BWA -, KmerGenie -, SOAPdenovo -, and BLAST software.

## 2.8 List of references

Adams, M. D., S. E. Celniker, R. A. Holt, C. A. Evans, J. D. Gocayne, *et al.*, 2000 The genome sequence of *Drosophila melanogaster*. Science 287: 2185-2195.

Alkan, C., S. Sajjadian, and E. E. Eichler, 2011 Limitations of next generation genome sequence assembly. Nature Methods 8: 61-65.

Altschul, S. F., T. L. Madden, A. A. Schäffer, J. Zhang, Z. Zhang, *et al.*, 1997 Gapped BLAST and PSI-BLAST: a new generation of protein database search programs. Nucleic Acids Research 25: 3389-3402.

Ashburner, M., C. A. Ball, J. A. Blake, D. Botstein, H. Butler, *et al.*, 2000 Gene ontology: tool for the unification of biology. Nature Genetics 25: 25-29.

Bailey, A., D. Chandler, W. P. Grant, J. Greaves, G. Prince, *et al.,* 2010 Pests of crops. Biopesticides: pest management and regulation 19-70.

Barigozzi, C., 1939 Experiments with microdissection of the chromosome of the salivary glands of *Chironomus* sp. Archiv Exp Zellforsch 22: 190-194.

Bartholdi, M. F., J. D. Parson, K. A. Albright, and L. S. Cram, 1990 System for flow sorting chromosomes on the basis of pulse shape. Cytometry 11: 165-172.

Baumann, P., L. Baumann, and M. L. Thao, 2004 Organization of the mitochondrial genomes of whiteflies, aphids and psylids (Hemiptera, Sternorrhyncha). BMS Evolutionary Biology 4: 25.

Becerra, J. X., 2007 The impact of herbivore-plant coevolution on plant community structure. Proceedings of the National Academy of Sciences 104: 7483-7488.

Blackman, R. L., and H. Takada, 1976 Naturally occurring chromosomal translocation in *Myzus persicae* (Sulzer). Journal of Entomology 50: 147-156.

Blackman, R. L., and D. F. Hales, 1986 Behaviour of the X chromosomes during growth and maturation of parthenogenetic eggs of *Amphorophora tuberculata* (Homoptera, Aphididae), in relation to sex determination. Chromosoma 94: 59-64.

Blackman, R. L., 1987 Reproduction, cytogenetics and development. *In:* A. K. Minsk and P. Harrewijn (eds), Aphids: their biology, natural enemies and control 2: 163-195.

Blackman, R. L., P. A. Brown, C. C. Ramfrez, and H. M. Niemeyer, 2003 Karyotype variation in the South American aphid genus *Neuquenaphis* (Hemiptera, Aphididae, Neuquenaphidinae). Hereditas 138: 6-10.

Botha, A. M., Y. Li, and N. L. V. Lapitan, 2005 Cereal host interactions with Russian wheat aphid: A review. Journal of Plant Interactions 1: 211-222.

Botha, A. M., L. van Eck, C. S. Jackson, N. F. V. Burger, and T. Schultz, 2011 Phloem feeding insect stress and photosynthetic gene expression. Applied Photosynthesis. Online at http://www.intechopen.com/books/applied-photosynthesis/phloem-feeding-insect-stress-and-photosynthetic-gene-expression.

Hodkinson, B. P., and E. A. Grace, 2015 Next-Generation Sequencing: A review of technologies and tools for wound microbiome research. Advances in Wound Care 4: 50-58.

Burd, J. D., D. R. Porter, G. J. Puterka, S. D. Haley, and F. B. Pears, 2006 Biotypic variation among North American Russian wheat aphid (Homoptera: Aphididae) populations. Journal of Economic Entomology 99: 1862-1866.

Caillaud, M. C., M. Boutin, C. Braendle, and J. C. Simon, 2002 A sex-linked locus controls wing polymorphism in males of the pea aphid, *Acyrthosiphon pisum* (Harris). Heredity 89: 346-352.

Campagna, D., C. Romualdi, N. Vitulo, M. Del Favero, M. Lexa, *et al.*, 2004 RAP: a new computer program for *de novo* identification of repeated sequences in whole genomes. Bioinformatics 21: 582-588.

Carrano, A. V., J. W. Gray, D. H. Moore, J. L. Minkler , B. H. Mayall, *et al.*, 1976 Purification of the chromosomes of the Indian muntjac by flow sorting. Journal of Histochemistry and Cytochemistry 24: 348-354.

Carrano, A. V., J. W. Gray, R. G. Langlios, K. J. Burkhart-Schultz, and M. A. van Dilla, 1979 Measurement and purification of human chromosomes by flow cytometry and sorting. Proceedings of the National Academy of Sciences 76: 1382-1384.

Carver, B. F., 2009 Wheat: science and trade. The Journal of Agricultural Science 148: 736-737.

Chai, H. N., Y. Z. Du, and B. P. Zhai, 2012 Characterisation of the complete mitochondrial genome of *Cnaphalocrocis medinalis* and *Chilo suppressalis* (Lepidoptera: Pyralidae). International Journal of Biological Sciences 8: 561-579.

Chambers, R., and C. Sands, 1923 A dissection of the chromosomes in the pollen mother cells of *Tradescantia virginiana*. The Journal of General Physiology 5: 815-821.

Chen, W., V. Kalscheuer, A. Tzschach, C. Menzel, R. Ullmann, *et al.*, 2008 Mapping translocation breakpoints by next generation sequencing. Genome Research 18: 1143-1149.

Chen, W., R. Ullmann, C. Langnick, C. Menzel, Z. Wotschofsky, *et al.*, 2010 Breakpoint analysis of balanced chromosome rearrangements by next generation paired-end sequencing. European Journal of Human Genetics 18: 539-543.

Chikhi, R., and P. Medvedev, 2014 Informed and automated *k-mer* size selection for genome assembly. Bioinformatics 30: 31-37.

Cilliers, P. R., V. L. Tolmay, and H. A. van Niekerk, 1992 Kleingraansentrum stuur Russiese luis planke (Afrikaans). Wheat Focus 10: 7.

Crozier, R. H., and Y. C. Crozier, 1993 The mitochondrial genome of the honeybee *Apis mellifera*: Complete sequence and genome organization. Genetics 133: 97-117.

Degnan, P. H., Y. Yu, N. Sisneros, R. A. Wing, and N. A. Moran, 2009 *Hamiltonella defensa*, genome evolution of a protective bacterial endosymbiont from pathogenic ancestors. Proceedings of the National Academy of Sciences 106: 9063-9068.

Degnan, P. H., T. E. Leonardo, B. Cass, B. Hurwitz, S. Richards, *et al*., 2010 Dynamics of genome evolution in faculatitve symbionts of aphids. Environmental Microbiology 12: 2060-2069.

De Jager, L., N. F. V. Burger, and A. M. Botha, 2014 Complete mitochondrial genome of *Diuraphis noxia* (Hemiptera: Aphididae) from nine populations, SNP variation between populations, and comparison with other Aphididae species. African Entomology 22: 847-862.

Denoeud, F., P. Kapranov, C. Ucla, A. Frankish, R. Castelo, *et al.,* 2007 Prominent use of distal 5' transcription start sites and discovery of a large number of additional exons in ENCODE regions. Genome Research 17: 746-759.

Di Bucchianico, S., A. M. Poma, M. F. Giardi, L. Di Leandro, F. Valle, *et al*., 2011 Atomic force microscope nanolithography on chromosomes to generate single-cell genetic probes. Journal of Nanobiotechnology 9: 27-33.

Dilbirligi, M., M. Erayman, D. Sandhu, D. Sidhu, and K. S. Gill, 2004 Identification of wheat chromosomal regions containing expressed resistance genes. Genetics 166: 461-481.

Dogimont, C., A. Bendahmane, V. Chovelon, and N. Boissot, 2010 Host plant resistance to aphids in cultivated crops: genetic and molecular bases, and interaction with aphid populations. Comptes Rendus Biologies 333: 566-573.

Doležel, J., J. Vrána, J. Šafář, J. Bartoš, M. Kubaláková, *et al.*, 2012 Chromosomes in the flow to simplify genome analysis. Functional and Integrative Genomics 12: 397-416.

Dudin, G., E. W. Steegmayer, P. Vogt, H. Schnitzer, E. Diaz, *et al.*, 1988 Sorting of chromosomes by magnetic separation. Human Genetics 80: 111-116.

Du Toit, F., 1987 Resistance in wheat (*Triticum aestivum*) to *Diuraphis noxia* (Homoptera: Aphididae). Cereal Research Communications 15: 175-179.

Du Toit, F., 1988 Another source of Russian wheat aphid (*Diuraphis noxia*) resistance in *Triticum aestivum*. Cereal Research Communications 16: 105-106.

Du Toit, F., 1989 Components of resistance in three bread wheat lines to Russian wheat aphid (Homoptera: Aphididae) in South Africa. Journal of Economic Entomology 82: 1779-1781.

Duveiller, E., R. P. Singh, and J. M. Nicol, 2007 The challenges of maintaining wheat productivity: pests, diseases, and potential epidemics. Euphytica 157: 417-430.

Edwards, O. R., 2001 Interspecific and intraspecific variation in the performance of three pest aphid species on five grain legume hosts. Entomologia Experimentalis et Applicata 100: 21-30.

Elliott, N., M. Mirik, Z. Yang, T. Dvorak, M. Rao, *et al.*, 2007 Airborne multi-spectral remote sensing of Russian wheat aphid injury to wheat. Southwestern Entomologist 32: 213-219.

Fazel-Najafabadi, M., J. Peng, F. B. Peairs, H. Simkova, A. Killian, *et al.*, 2015 Genetic mapping of resistance to *Diuraphis noxia* (Kurdjumov) biotype 2 in wheat (*Triticum aestivum* L.) accession CI2401. Euphytica 203: 607-614.

Gill, B. S., R. Appels, A. M. Botha-Oberholster, C. R. Buell, J. L. Bennetzen, *et al.*, 2004 A workshop report on wheat genome sequencing; International Genome Research on Wheat Consortium. Genetics 168: 1087-1096.

Giordanengo, P., L. Brunissen, C. Rusterucci, C. Vincent, A. Van Bel, *et al.*, 2010 Compatible plant-aphid interaction: how aphids manipulate plant responses. Comptes Rendus Biologies 333: 516-523.

Goggin, F. L., 2007 Plant-aphid interactions: molecular and ecological perspectives. Current Opinion in Plant Biology 10: 399-408.

Haley, S. D., F. B. Peairs, C. B. Walker, J. B. Rudolph, and T. L. Randolph, 2004 Occurrence of a new Russian wheat aphid biotype in Colorado. Crop Science 44: 1589-1592.

Hammon-Kosack, K. E., and J. D. G. Jones, 1996 Resistance gene-dependent plant defence responses. American Society of Plant Physiologists 8: 1773-1791.

Hanrahan, S. J., and J. S. Johnston, 2001 New genome size estimates of 134 species of arthropods. Chromosome Research 19: 809-823.

Harrow, J., A. Nagy, A. Reymond, T. Aliota, L. Patthy, *et al.,* 2009 Identifying protein-coding genes in genomic sequences. Genome Biology 10: 201.

Harvey, T. L., and T. J. Martin, 1990 Resistance to Russian wheat aphid *Diuraphis noxia*, in wheat (*Triticum aestivum*). Cereal Research Communications 18: 127- 129.

Healy, J., E. E. Thomas, J. T. Schwartz, and M. Wigler, 2003 Annotating large genomes with exact word matches. Genome Research 13: 2306-2315.

Hernandez, D., P. Francois, L. Farinelli, M. Osteras, and J. Schrenzel, 2008 *De novo* bacterial genome sequencing: millions of very short reads assembled on a desktop computer. Genome Research 18: 802-809.

Heslop-Harrison, J. S., and T. Schwarzacher, 2011 Organisation of the plant genome in chromosomes. Plant Journal 66: 18-33.

Hobza, R., and B. Vyskot, 2007 Laser microdissection-based analysis of plant sex chromosomes. Methods in Cell Biology 82: 433-453.

Hodgson, E., and J. Karren, 2008 Russian Wheat Aphid. Online at http://extension.usu.edu/files/publications/factsheet/russian-wheat-aphids08.pdf.

Howe, G. A., and G. Jander, 2008 Plant immunity to insect herbivores. Annual Review of Plant Biology 59: 41-66.

Howell, K. E., J. Gruenberg, A. Ito, and G. E. Palade, 1988 Immuno-isolation of subcellular components. Progress in Clinical Biological Research 270: 77-90.

Hu, Li., G. Jianyu, L. Hayiyu, and C. Wanzhi, 2009 Progress in researches on insect mitochondrial genome and analysis of gene order. Reviews: Science Foundation in China 17: 39-45.

Jankielsohn, A., 2011 Distribution and diversity of Russian wheat aphid (Hemiptera: Aphididae) biotypes in South Africa and Lesotho. Journal of Economic Entomology 104: 1736-1741.

Jankielsohn, A., 2014 The Russian wheat aphid. Farmer Weekly 17: 22-23.

Jankielsohn, A., 2016 Changes in the Russian wheat aphid (Hemiptera: Aphididae) biotype complex in South Africa. Journal of Economic Entomology 109: 907-912.

Jaquiéry, J., S. Stoeckel, C. Rispe, L. Mieuzet, F. Legeai, *et al.*, 2012 Accelerated evolution of sex chromosomes in aphids, an XO system. Molecular Biology and Evolution 29: 837-847.

Jaquiéry, J., C. Rispe, D. Roze, F. Legeai, G. Le Trionnaire, *et al.*, 2013 Masculinization of the X chromosome in the pea aphid. Plos Genetics 9: e1003690.

Johnston, J. S., K. S. Yoon, J. P. Strycharz, B. R. Pittendrigh, and J. M. Clark, 2007 Body lice and head lice (Anoplura: Pediculidae) have the smallest genomes of any hemimetabolous insect reported to date. Journal of Medical Entomology 44: 1009-1012.

Jyoti, J. L., J. A. Quershi, J. P. Michaud, and T. J. Martin, 2006 Virulence of two Russian wheat aphid biotypes to eight wheat cultivars at two temperatures. Crop Science 46: 774-780.

Kelley, D. R., M. C. Schatz, and S. L. Salzberg, 2010 Quake: quality-aware detection and correction of sequencing errors. Genome Biology 11: 116.

Khan, W. U., F. Mohammed, F. U. Khan, F. Z. Zafar, and G. Ghuttai, 2015 Correlation studies among production traits in bread wheat under rainfed conditions. American-Eurasian Journal of Agricultural and Environmental Sciences 15: 2059-2063.

Kron, P., and B. C. Husband, 2015 Distinguishing 2N gamete nuclei from doublets in pollen using flow cytometry and pulse analysis. Cytometry Part A 87: 943-957.

Kindler, S. D., N. C. Elliott, K. L. Giles, T. A. Royer, R. Fuentes-Granados, *et al.*, 2002 Effect of Greenbugs (Homoptera: Aphididae) on yield loss of winter wheat. Journal of Economic Entomology 95: 89-95.

Langmead, B., C. Trapnell, M. Pop, and S. L. Salzberg, 2009 Ultrafast and memory-efficient alignment of short DNA sequences to the human genome. Genome Biology 10: 25.

Lapitan, N. L. V., Y. Li, and A. M. Botha, 2007 Fractional extracts of Russian wheat aphid eliciting defense responses in wheat. Journal of Economic Entomology 100: 990-999.

Lea, T., F. Vartdal, C. Davies, and J. Ugelstad, 1985 Magnetic monosized polymer particles for fast and specific fractionation of human mononuclear cells. Scandinavian Journal of Immunology 22: 207-216.

Li, H., and R. Durbin, 2009 Fast and accurate short read alignment with Burrows-Wheeler transform. Bioinformatics 25: 1754-1760.

Liu, X. M., C. M Smith, B. S. Gill, and V. Tolmay, 2001 Microsatellite markers linked to six RWA resistance genes in wheat. Theoretical and Applied Genetics 102: 504-510.

Luo, M.C., C. Thomas, F. M. You, J. Hsiao, O. Y. Shu, *et al.*, 2003 High-throughput fingerprinting of bacterial artificial chromosomes using the SNaPshot labeling kit and sizing of restriction fragments by capillary electrophoresis. Genomics 82: 378-389.

Luo, R., B. Liu, Y. Xie, Z. Li, W. Huang, *et al.*, 2012 SOAPdenovo2: an empirically improved memory-efficient short-read *de novo* assembler. GigaScience 1: 18.

Ma, L., Y. Xiao, H. Huang, Q. W. Wang, W. N. Rao, *et al.*, 2010 Direct determination of molecular haplotypes by chromosome microdissection. Nature Methods 7: 299-301.

Mandrioli, M., D. Bizarro, G. C. Manicardi, D. Gionghi, L. Bassoli, *et al.*, 1999 Cytogenetic and molecular characterisation of a highly repeated DNA sequence in the peach potato aphid *Myzus persicae*. Chromosoma 108: 436-442.

Marais, G. F. and F. Du Toit, 1993 A monosomic analysis of Russian wheat aphid resistance in the common wheat PI 292994. Plant Breeding 111: 246-248.

Marçais, G., C. and Kingsford, 2011 A fast, lock-free approach for efficient parallel counting of occurrences of k-mers. Bioinformatics 27: 764-770.

Margueron, R., and D. Reinberg, 2010 Chromatin structure and the inheritance of epigenetic information. Nature Reviews Genetics 11: 285-296.

Meksem, K., and G. Kahl, 2005 The handbook of plant genome mapping. Genetic and Physical Mapping 151-171.

Metzker, M. L., 2010 Sequencing technologies - the next generation. Nature Reviews Genetics 11: 31-46.

Meyer, J. R., 2007 A class of distinction. Department of Entomology, North Carolina State University.

Michaud, J. P., and P. E. Sloderbeck, 2005 Russian wheat aphid: an introduced pest of small grains in the high plains. Kansas State University.

Miles, P. W., 1999 Aphid saliva. Biological Reviews of the Cambridge Philosophical Society 74: 41-85.

Mirik, M., J. Ansley, J. Michels, and N. Elliott, 2009 Grain and vegetative biomass reduction by the Russian wheat aphid in winter wheat. Southwestern Entomologist 34: 131-157.

Molday, R. S., S. P. S. Yen, and A. Rembaum, 1977 Application of magnetic microspheres in labelling and separation of cells. Nature 268: 437-438.

Monajembashi, S., C. Cremer, T. Cremer, J. Wolfrum, and K. O. Greulich, 1986 Microdissection of human chromosomes by a laser microbeam. Expressive Cell Research 167: 262-265.

Monti, V., M. Mandriolo, M. Rivi, and G. C. Manicardi, 2012 The vanishing clone: karyotypic evidence for extensive intraclonal genetic variation in the peach potato aphid, *Myzus persicae* (Hemiptera: Aphididae). Biological Journal of the Linnean Society 105: 350-358.

Morrison, W. P., and F. B. Peairs, 1998 Response model concept and economic impact. *In* S. S. Quisenberry and F. B. Peairs (eds.), Response model for an introduced pest - Russian wheat aphid. Entomological Society of America, Lanham, MD.

Myers, E. W., G. G. Sutton, A. L. Delcher, I. M. Dew, D. P. Fasulo, *et al.*, 2000 A whole-genome assembly of *Drosophila*. Science 287: 2196-2204.

Nickolson, S. J., M. L. Nickerson, M. Dean, Y. Song, P. R. Hoyt, *et al.*, 2015 The genome of *Diuraphis noxia*, a global aphid pest of small grains. BMC Genomics 16: doi: 10.1186/s12864-015-1525-1.

Nkongolo, K. K., J. S. Quick, A. E. Limin, and D. B. Fowler, 1991a Sources and inheritance of resistance to Russian wheat aphid in *Triticum* species amphiploids and *Triticum tauschii*. Canadian Journal of Plant Science 71: 703-708.

Nkongolo, K. K., J. S. Quick, F. B. Peairs, and W. I. Meyer, 1991b Inheritance of resistance of PI 372129 wheat to the Russian wheat aphids. Crop Science 31: 905-907.

Novotná, J., J. Havelka, P. Starý, P. Koutecký, and M. Vítková, 2011 Karyotype analysis of the Russian wheat aphid, *Diuraphis noxia* (Kurdjumov) (Hemiptera: Aphididae) reveals a large X chromosome with rRNA and histone gene families. Genetica 139: 281-289.

Olofsson, L., A. Lundgren, and P. E. Brodelius, 2012 Trichome isolation with and without fixation using laser microdissection and pressure catapulting followed by RNA amplification: expression of genes of terpene metabolism in apical and sub-apical trichome cells of *Artemisia annua* L. Plant Science 183: 9-13.

Orlando, E., 1974 Sex determination in *Megoura viciae* Buckton (Homoptera Aphididae). Monitore Zoologico Italiano 8: 61-70.

Owen, C. S., 1983 Magnetic cell sorting. Cell separation methods and selected applications 5: 127-144.

Painter, R. H., 1958 Resistance of plants to insects. Annual Review of Entomology Journal 3: 267-290.

Pearson, W. R., and D. J. Lipman, 1988 Improved tools for biological sequence comparison. Proceedings of the National Academy of Sciences 85: 2444-2448.

Peng, J., H. Wang, S. D. Haley, F. B. Peairs, and N.L.V. Lapitan, 2007 Molecular mapping of the Russian wheat aphid resistance gene *Dn2414* in wheat. Crop Science 47: 2418-2429.

Pérez, R., F. Panzera, J. Page, J. A. Suja, and J. S. Rufas, 1997 Meiotic behaviour of holocentric chromosomes: orientation and segregation of autosomes in *Triatoma infestans* (Heteroptera). Chromosome Research 5: 47-56.

Pevzner, P. A., and H. Tang 2001 Fragment assembly with double-barreled data. Bioinformatics 17: S225-S233.

Pevzner, P. A., H. Tang, and M. S. Waterman, 2001 An Eulerian path approach to DNA fragment assembly. Proceedings of the National Academy of Sciences 98: 9748-9753.

Pike, K. S., D. Allison, L. Boydston, C. O. Qualset, H. E. Vogt, *et al.*, 1989 Suction trap reveals 60 wheat aphid species, including Russian wheat aphid. California Agriculture 43: 22-24.

Powell, G., C. R. Tosh, and J. Hardie, 2006 Host plant selection by aphids: behavioural, evolutionary, and applied perspectives. Annual Review of Entomology 51: 309-330.

Puterka, G. J., R. W. Hammon, J. D. Burd, F. B. Peairs, T. L. Randolph, *et al.*, 2012 Cyclical parthenogenetic reproduction in Russian Wheat Aphid (Hemiptera: Aphididae) in the United States: Sexual reproduction and its outcome on biotypic diversity. Journal of Economic Entomology 105: 1057-1068.

Reis-Filho, J. S., 2009 Next-generation sequencing. Breast Cancer Research 11: 1-7.

Richardson, S., and S. C. Murali, 2015 Best practices in insect genome sequencing: what works and what doesn't. Science Direct 7: 1-7.

Robinson, J., 1992 Russian wheat aphid: A growing problem for small-grain farmers. Outlook on Agriculture 21: 57-61.

Ruepp, A., A. Zollner, D. Maier, K. Albermann, J. Hani, *et al.*, 2004 The FunCat, a functional annotation scheme for systematic classification of proteins from whole genomes. Nucleic Acids Research 32: 5539-5545.

Saidi, A., and J. S. Quick, 1996 Inheritance and allelic relationships among Russian wheat aphid resistance genes in winter wheat. Crop Science 36: 256-258.

Sanger, F., S. Nicklen, A. R. and Coulson, 1977 DNA sequencing with chain-terminating inhibitors. Proceedings of the National Academy of Science, USA 74: 5463-5467.

Scalenghe, F., E. Turco, J. E. Ederström, V. Pirrotta, and M. Melli, 1981 Microdissection and cloning of DNA from a specific region of *Drosophila melanogaster* polytene chromosomes. Chromosoma 82: 205-216.

Schondelmaier, J., R. Martin, A. Jahoor, A. Houben, A. Graner, *et al.*, 1993 Microdissection and microcloning of the barley (*Hordeum vulgare* L.) chromosome 1HS. Theoretical and Applied Genetics 86: 629-636.

Schoonhoven, L. M., J. J. A. Van Loon, and M. Dicke, 2005 Insect-Plant Biology. Oxford University Press, UK.

Schubert, I., P. F. Fransz, J. Fuchs, and J. H. de Jong, 2001 Chromosome painting in plants. Methods Cell Science 23: 57-69.

Shea, G., J. Botha, and D. Hardie, 2000 Russian wheat aphid (*Diuraphis noxia*), an exotic threat to Western Australia. Grainguard™ Initiative AGWEST.

Shigenobu, S., H. Watanabe, M. Hattori, Y. Sakaki, and H. Ishikawa, 2000 Genome sequence of the endocellular bacterial symbiont of aphids *Buchnera* sp. APS. Nature 407: 81-86.

Simpson, J. T., K. Wong, S. D. Jackman, J. E. Schein, S. J. M. Jones, and I. Birol, 2009 ABySS: a parallel assembler for short read sequence data. Genome Research 19: 1117-1123.

Smith, C. M., T. Belay, C. Stauffer, P. Stary, I. Kubeckova, and S. Starkey, 2004 Identification of Russian wheat aphid (Homoptera: Apididae) populations virulent to the *Dn4* resistance gene. Journal of Economic Entomology 97: 1112-1117.

Stoetzel, M. B., 1987 Information on and identification of *Diuraphis noxia* (Homoptera: Aphididae) and other aphid species colonizing leaves of wheat and barley in the United States. Journal of Economic Entomology 80: 696-704.

Stubblefield, E., and J. Oro, 1982 The isolation of specific chicken macro-chromosomes by zonal centrifugation and flow sorting. Cytometry 5: 73-281.

Sudbery, I., J. Stalker, J. T. Simpson, T. Keane, A. G. Rust, *et al.*, 2009 Deep short-read sequencing of chromosome 17 from the mouse strains A/J and CAST/Ei identifies significant germline variation and candidate genes that regulate liver triglyceride levels. Genome Biology 10: 112.

Swanevelder, Z. H., A. K. J. Surridge, E. Venter, and A. M. Botha, 2010 Limited endosymbiont variation in *Diuraphis noxia* (Hemiptera:Aphididae) biotypes from the United States and South Africa. Journal of Economic Entomology 103: 887-897.

Tagu, D., J. P. Klingler, A. Moya, and J. C. Simon, 2008 Early progress in aphid genomics and consequences for plant-aphid interactions studies. Molecular Plant-Microbe Interactions 21: 701-708.

The International Aphid Genomics Consortium, 2010 Genome sequence of the pea aphid *Acyrthosiphon pisum*. PLoS Biology 8: e1000313.

Thole, V., A. Peraldi, B. Worland, P. Nicholson, J. H. Doonan, and P. Vain, 2012 T-DNA mutagenesis in *Brachypodium distachyon*. Journal of Experimental Botany 63: 567-576.

Tjallingii, W. F., and T. H. Esch, 1993 Fine structure of aphid stylet routes in plant tissues in correlation with EPG signals. Physiological Entomology 18: 317-328.

Tjallingi, W. F., 2006 Salivary secretions by aphids interacting with proteins of phloem wound responses. Journal of Experimental Botany 57: 739-745.

Tolmay, V. L., R. C. Lindeque, and G. J. Prinsloo, 2007 Preliminary evidence of a resistance-breaking biotype of the Russian wheat aphid, *Diuraphis noxia* (Kurdjumov) (Homoptera: Aphididae), in South Africa. African Entomoly 15: 228-230.

Treangen, T. J., and S. L. Salzberg, 2012 Repetitive DNA and next-generation sequencing: computational challenges and solutions. Nature Reviews Genetics 13: 36-46.

Ugelstad, J., A. Berge, T. Ellingsen, O. Aune, L. Kilaas, *et al.,* 1988 Monosized magnetic particles and their use in selective cell separation. Macromolecular Chemistry 17: 177-211.

Valdez, V. A., P. E Byrnea, N. L. V. Lapitan, F. B. Peairs, A. Bernardoc, *et al*., 2012 Inheritance and genetic mapping of Russian wheat aphid resistance in Iranian wheat landrace accession PI 626580. Crop Science 52: 676-682.

Van Dijk, E. L., H. Auger, Y. Jaszczyszyn, and C. Thermes, 2014 Ten years of next generation sequencing technology. Trends in Genetics 30: 418-426.

Van Emden, H. F., and R. Harrington, 2007 Aphids as crop pests doi: 10.1079/9780851998190.0000.

Vitharana, S. N., and G. S. Wilson, 2006 Fractionation of chromosome 15 with an affinity-based approach using magnetic beads. Genomics 87: 158-164.

Vitulo, N., A. Albiero, C. Forcato, D. Campagna, F. Dal Pero, et al., 2011 First survey of the wheat chromosome 5A composition through a next generation sequencing approach. PloS ONE 6: 26421.

Vláčilová, K., D. Ohri, J. Vrána, J. Číhalíková, M. Kubaláková, *et al.*, 2002 Development of flow cytogenetics and physical genome mapping in chickpea (*Cicer arietinum* L.). Chromosome Research 10: 695-706.

Von Bubnoff, A., 2008 Next-generation sequencing: The race is on. Cell 132: 721-723.

Von Dohlen, C. D., C. A. Rowe, and O. E. Heie, 2006 A test of morphological hypotheses for tribal and subtribal relationships of Aphidinae (Insecta: Hemiptera: Aphididae) using DNA sequences. Molecular Phylogenetics and Evolution 38: 316-329.

Vossen, J. H., S. Dezhsetan, D. Esselink, M. Arens, M. J. Sanz, *et al*., 2013 Novel applications of motif directed profiling to identify disease resistance genes in plants. Plant Methods 9: 37.

Vrána, J., M. Kubaláková, H. Šimková, J. Číhalíková, M. A. Lysák, *et al.*, 2000 Flow sorting of mitotic chromosomes in common wheat (*Triticum aestivum* L.). Genetics 156: 2033-2041.

Walters, M. C., F. Penn, F. Du Toit, T. C. Botha, K. Aalbersberg, *et al.*, 1980 The Russian wheat aphid. Farming in South Africa, Leaflet Series, Wheat G3: 1-6.

Warren, R. L., G. G. Sutton, S. J. Jones, and R. A. Holt, 2007 Assembling millions of short DNA sequences using SSAKE. Bioinformatics 23: 500-501.

Webster, J. A., R. L. Burton, and K. J. Starks, 1987 *Diuraphis noxia*, a new U.S. aphid pest of small grains. Journal of the Kansas Entomological Society 60: 483-484.

Wei, F. S., J. W. Zhang, S. G. Zhou, R. F. He, M. Schaeffer, *et al.*, 2009 The physical and genetic framework of the maize B73 genome. PLoS Genetics 5: e1000715.

Will, T., and A. J. E. Van Bel, 2006 Physical and chemical interactions between aphids and plants. Journal of Experimental Botany 57: 729-737.

Will, T., W. F. Tjallingii, A. Thonnessen, and A. J. E. Van Bel, 2007 Molecular sabotage of plant defence by aphid saliva. Proceedings of the National Academy of Sciences 104: 10536-10541.

Will, T., S. R. Kornermann, A. C. U. Furch, W. F. Tjallingii, and A. J. E. Van Bel, 2009 Aphid watery saliva counteracts sieve-tube occlusion: a universal phenomenon? The Journal of Experimental Biology 212: 3305-3312.

Wilson, A. C. C., P. Sunnucks, and D. F. Hales, 1997 Random loss of X chromosome at male determination in an aphid, *Sitobion* near *fragariae*, detected using an X-linked polymorphic microsatellite marker. Genetics Research 69: 233-236.

Yang, H., X. Chen, and W. H. Wong, 2011 Completely phased genome sequencing through chromosome sorting. Proceedings of the National Academy of Sciences 108: 12-17.

Zerbino, D.R., and E. Birney, 2008 Velvet: algorithms for *de novo* short read assembly using de Bruijn graphs. Genome Research 18: 821-829.

Zhang, W., J. Chen, Y. Yang, Y. Tang, J. Shang, and B. Shen, 2011 A practical comparison of *De Novo* genome assembly software tools for next-generation sequencing technologies. Plos One 6: e17915.

Zhou, R. N., and Z. M. Hu, 2007 The development of chromosome microdissection and microcloning technique and its applications in genomic research. Current Genomics 8: 67-72.

Zhou, V. W., A. Goren, and B. E. Bernstein, 2011 Charting histone modifications and the functional organization of mammalian genomes. Nature Reviews Genetics 12: 7-18.

# Chapter 3

# Research

## 3.1 Introduction

Arthropods are known as the most speciose clade of animals on earth. The Insecta class, which is the majority of arthropods, is hypothesized to hold 75% of all animals (Gaston 1991). Hemipterans contain three important families, the Phylloxeridae, the Adelgidae, and the Aphididae. The Aphididae family (order Hemiptera) represents the largest group of aphid species comprising approximately of 4,500 extant species (Miller *et al.* 1994; Davis 2012). In general, the piercing-sucking behaviour of aphids during feeding together with their ingestion of phloem sap results in extensive plant damage due to either direct feeding or indirect transmission of plant viruses (Tagu *et al.* 2008).

*Diuraphis noxia* Kurdjumov, more commonly known as the Russian wheat aphid (RWA), is one of the main insect pests that affect *Tritucum aestivum* L. (bread wheat). The RWA belongs to the family Aphididae and is characterised as an invasive pest with a major economic impact on wheat production (Haley *et al.* 2004; Burd *et al.* 2006; Jankielsohn 2011). It has the potential to cause considerable yield losses, mainly because it reproduces parthenogenically and has an exceptionally high intrinsic rate of increase (Merril *et al*. 2009). In areas where the RWA is considered to be endemic, it can also reproduce sexually. The change between sexual and parthenogenetic reproduction includes chromosome behavioural changes that take place in response to environmental stimuli, facilitated by endocrine factors. Notable differences take place, in the ways in which aphid chromosomes pair and segregate during sex determination and meiosis, even within closely related species, with consequences that can affect the inheritance of all – or parts of – the genome (Manicardi *et al*. 2015). Asexual reproduction permits for non-recombinant vertical gene transfer from mother to offspring through successive generations allowing little genetic variation in the RWA (Tagu *et al*. 2008).

Nevertheless, new RWA populations or biotypes still develop despite the lack of sexual recombination. RWA biotypes are categorised according to the varying level of damage that they inflict while feeding on wheat cultivars containing different *resistance* (*R*-) genes. This classification, based on aphid virulence, depends on the plants' response to RWA feeding being either susceptible, intermediate, or resistant (Puterka *et al.* 2012). Biotypes overcome host-plant resistance and feed on previously resistant cultivars. The constant development of virulent RWA biotypes calls for the continuous identification and introduction of new *R*-genes into susceptible wheat cultivars (Bouhssini *et al*. 2011). Fundamentally, this protects the wheat against the current RWA biotypes and prevents large scale agricultural losses (Jankielsohn 2011).

The karyotypic structure of the aphid genome has been found to vary substantially among the species. In some aphid genera the chromosome number seems to be stable, but in others it differs greatly, mainly because of successive autosomal dissociations with slight or no accompanying morphological or biological change (Manicardi *et al*. 2015).

RWA chromosomes, like the chromosomes of other aphids and some hemipteroid insects, are holocentric. Holocentric chromosomes lack localised centromeres – with centromeric activity being diffused along the length of the chromosome. As a result, during the later stages of prophase and metaphase, every condensed chromosome looks like a simple rod, or, if treated with colchicine, as a pair of chromatids aligned in parallel with a uniform gap width between them (Blackman 1987). Holocentric chromosomes present a big disadvantage for cytogenetic studies and karyotype comparisons in that they do not possess any primary and/or secondary constrictions. This means that conventionally stained preparations can only be identified on the basis of size. Thus, the only factors that can be used to detect differences in karyotype structure are the number of chromosomes or measurable structural heterozygosity (Manicardi *et al*. 2015).

Novotná *et al*. (2011) established that the karyotype of female RWA consist of 10 chromosomes (2n = 10) with four pairs of autosome chromosomes and a pair of large sex (X) chromosomes. They also noted that the male RWA only possess one sex (X) chromosome and therefore has a karyotype of 2n = 9. For that reason the RWA sex chromosome system has been identified as XX/X0, as in a number of aphid species. This system never has a Y chromosome, which is essential for parthenogenesis or asexual reproduction (Kuznetsova and Shaposhnikov 1973). Aphids are known for their large X chromosomes as reported by Novotná *et al*. (2011) for RWA. The reason for the existence of large sexual chromosomes relative to the autosomes in aphids and their origin, are still unknown (Mandrioli *et al.* 1996; Bizzarro *et al.* 2000).

In this study, the chromosomes of biotypes SAM, the most virulent RWA biotype recorded (Botha *et al.* 2013), and SA1, one of the least virulent biotypes (Jankielsohn 2011), were studied. The aim of this study was to verify the karyotype of the RWA and to characterise the sex (X) chromosomes of the RWA. To achieve these aims, female RWA were dissected in order to obtain the embryos which were used to make chromosome squashes. The squashes were used to determine the RWA karyotype. Additionally, the metaphase X chromosomes were examined separately from the autosome chromosomes by means of flow cytometry. Next generation sequencing (NGS) of the separated X chromosomes of biotype SAM was conducted and used to map against the genomes of the RWA (SAM_Contigs_Version 1.1; GCA_001465515.1; Botha *et al.* 2016 – *in press*) and *Acyrthosiphon pisum* (pea aphid) (Acyr_2.0; GCA_000142985.2; The International Aphid Genomics Consortium 2010). Orthologous regions spanning the X chromosome of the RWA was also identified through reference mapping against the well characterised X chromosome of *Drosophila melanogaster* (fruit fly) (BDGP6; Adams *et al.* 2000).

## 3.2 Materials and methods

This study made use of adult female aphids of the South African mutant RWA biotype (SAM), and its parent South African biotype 1 (SA1). The female RWA specimens were obtained from the Department of Genetics, Stellenbosch University, Cereal Genomics Laboratory. The biotypes were kept on SST 387 RWA resistant wheat cultivars in separate BugDorm® Insect cages (MegaView Science Co. Ltd, Taiwan) to prevent cross contamination with other biotypes. Aphids were kept at 20 °C ± 2 °C with continuous artificial fluorescent lighting.

### 3.2.1 Karyotyping of RWA chromosomes

In the following section the procedure for obtaining representative karyotypes for the biotypes SAM and SA1, is described.

#### 3.2.1.1 Slide preparation

Mitotic chromosomes were obtained from whole embryos dissected from adult female RWA (Figure 3.1). The chromosome spreads were prepared according to a procedure adapted from Novotná *et al.* (2011). In brief, a Hund WETZLAR Wiloskop stereo-zoom-microscope (Labotec®), was used to dissect 15 embryos into a physiological solution for *Ephistia kuehniella* (Lockwood 1961) that consisted of 0.9% (m/v) NaCl, 0.042% (m/v) KCl, 0.033% (m/v) $CaCl_2.H_2O$, 0.02% (m/v) $NaHCO_3$, and 0.25% (m/v) glucose, where after the embryos were treated with a hypotonic solution (0.075 M KCl) for 10 minutes and fixed for 15 minutes in Carnoy fixative (Traut 1976). The freshly prepared Carnoy fixative consisted of 100% ethanol, chloroform, and glacial acetic acid (1 N) in a 6:3:1 ratio. The embryonic cells were separated in 60 µl of 60% glacial acetic acid (1 N) with the assistance of a wooden micropestle and fixed on the slide using a heating plate at 45 °C.

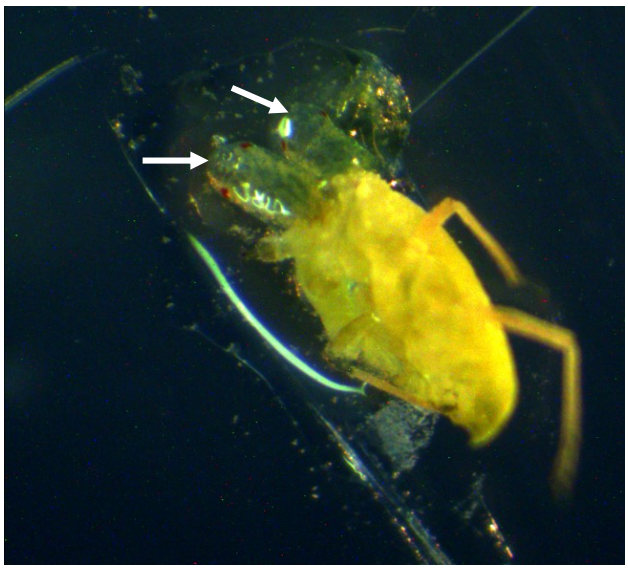

Figure 3.1: Two embryos (as indicated by arrows) dissected from an adult female RWA.

#### 3.2.1.2 Chromosome staining and visualisation

After the slides were prepared as described (Section 3.2.1.1), the samples were stained for 5-8 minutes with Hoechst 33342 (Sigma) solution (10 mg/ml) that was diluted 1:100 to a final concentration of 0.01 mg/ml. The stained slides were then briefly submerged in distilled $H_2O$ and left to dry at room temperature (RT).

The chromosomes were visualised with a Zeiss LSM780 ELYRA PS.1 (Zeiss Germany) confocal microscope. Images were edited on Zen Lite Software (Zeiss Germany) in order to visualise the karyotype and determine the size of the different chromosome pairs using a scale bar (Central Analytical Facility (CAF) fluorescent microscopy unit, Stellenbosch University, South Africa).

The different sized chromosome pairs were then subjected to two-sample *t*-tests to determine if their sizes were statistically different from one another. The *t*-tests were performed firstly between the large chromosome sizes (Group 1) and the middle autosomal chromosome sizes (Group 2); then between the middle autosomal chromosome sizes (Group 2) and the small autosomal chromosome sizes (Group 3); and lastly between the large chromosomes (Group 1) and the small autosomal chromosomes

(Group 3). Fundamentally, three *t*-tests were performed (Group 1 vs Group 2; Group 2 vs Group 3; Group 1 vs Group 3).

## 3.2.2 Flow cytometry of RWA chromosomes

In the following section a procedure is described for the isolation of the RWA sex chromosome in order to obtain DNA suitable for next generation sequencing (NGS).

### 3.2.2.1 Preparation of mitotic chromosome suspension

The RWA chromosome suspensions were obtained using an adapted procedure as described by Doležel and Bartoš (2005). Briefly, 20 female RWA were collected in a 1.5 ml Eppendorf tube. The tube containing the aphids was frozen using liquid nitrogen, where after 200 µl of ice-cold Otto buffer I (0.1 M $C_6H_8O_7$, 0.5% (v/v) Tween 20, 1% (v/v) Triton X-100) was added. The aphids were crushed in the tube using a small micropestle and incubated at RT for 5 minutes with occasional shaking. The suspension of crushed RWA was centrifuged through a 40 µm polypropylene nylon mesh cell strain filter (Fisherbrand®) at 10,000 revolutions per minute (rpm) for 30 seconds. Thereafter, staining solution containing 800 µl Otto buffer II (0.4 M $Na_2HPO_4$ $12H_2O$), 0.5 mM propidium iodide (PI), 40 µg RNase A, and 1.6 µl 2-mercaptoethanol, was added to the sample. After staining for 10 minutes at RT, the sample was vortexed and the suspension was transferred to a 5 ml round-bottom polystyrene tube (Falcon™) ready for flow sorting.

### 3.2.2.2 Flow cytometry optimization: Gating

Gating allows for the selection of single chromosomes through graphic depictions by identifying doublets, which are two chromosomes stuck together, clumps, which are more than two chromosomes stuck together, as well as debris that contaminate the series.

Doublet and clump discrimination are very important to prevent any chromosomes that are not of interest from passing through to sample collection (Kron and Husband 2015).

Gating was applied through the FACSDiva version 6.1.3 software (BD biosciences, USA) at the CAF fluorescent microscopy unit at Stellenbosch University, South Africa.

Figure 3.2 displays a gating strategy used in flow cytometry analysis known as a singlet gate scatter plot. This strategy is used to gate-out unwanted doublets and clumps. All singlets are identified according to where they cluster on the graph, which should be in a diagonal straight line. The singlets are then surrounded by a gate, allowing the flow cytometer to only sort the chromosomes included in the gating area (Figure 3.2).

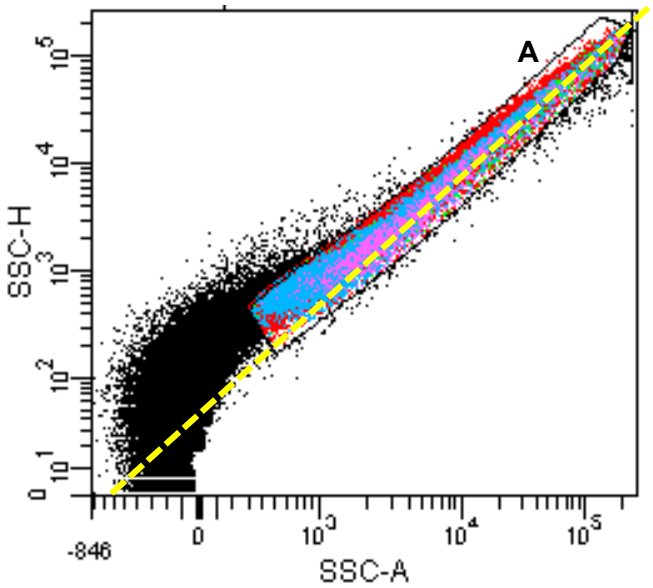


Figure 3.2: The singlet gate scatter plot was used to exclude doublets and clumps from the analysis. Gate A is an area that is straight, diagonal, 45º, and passing through zero (yellow dotted line), which includes all the single chromosomes of interest while all the particles outside the gate are excluded, as they consist of doublets, clumps, or debris.

Figure 3.3 displays a chromosome gate scatter plot that allowed for further selection of the chromosomes of interest. The graph makes use of SSC (side scatter) and fluorescence area. SSC is the light scattered at large angles and is proportional to the complexity of a particle, while fluorescence area is the amount of fluorescence a particle produces and is proportional to fluorescence intensity. In this graph the chromosomes of the same size will cluster together (Lo *et al.* 2008).

The approach in Figure 3.3 was used to distinguish between the sizes of chromosomes. Each chromosome size was assigned a colour to aid in identification. Cyan separated the

middle sized autosomal chromosomes at a fluorescence of 28,000-58,000, while blue separated the large sex chromosomes at a fluorescence of 68,000-98,000. The red and green areas in Figure 3.3 designate all the particles that are not included in this (Figure 3.3) and the previous gating strategy (Figure 3.2), respectively. Therefore, all the chromosomes that clustered in the respective colours (Figure 3.3) were sorted accordingly.

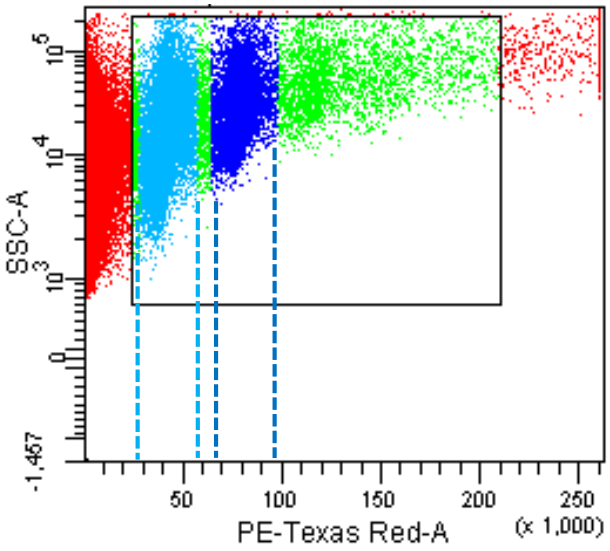


Figure 3.3: The chromosome gate scatter plot was used to identify the chromosome sizes based on fluorescence intensity. The different sized chromosomes were given a random colour to aid in identification.

### 3.2.2.3 Flow sorting

The sample containing the chromosomes as described in Section 3.2.2.1 was measured on a FACSAria flow cytometer (BD biosciences, USA) at the CAF fluorescent microscopy unit at Stellenbosch University, South Africa. Data was presented using the FACSDiva version 6.1.3 software (BD biosciences, USA). The flow cytometer charges each chromosome depending on its fluorescence intensity, which is proportional to the size of the chromosome. Propidium iodide (PI), the dye the chromosomes are stained with, is excited at 488 nm and emits at a wavelength of 617 nm. The large and middle chromosome fractions were collected separately in 5 ml polystyrene round-bottom tubes (Falcon™) containing Otto Buffer II (Section 3.2.2.1) and stored at –20 ˚C at the Department of Genetics, Stellenbosch University, Cereal Genomics Laboratory.

### 3.2.2.4 DNA purification

The different size fractionated frozen chromosomal samples (Section 3.2.2.3) were removed from the –20 ˚C freezer and thawed in a water bath at RT. After thawing, the samples were centrifuged at 12,000 rpm for 20 minutes at 8 ˚C. The supernatant was aspirated down to approximately 50 µl, where after the chromosomal pellet was resuspended. A total of 100 µg proteinase K was added to digest any contaminating proteins and the sample was incubated at 55 ˚C for 1 hour. The DNA was precipitated by adding 200 µl ice-cold 100% ethanol to the sample and incubated overnight in the –20 ˚C freezer. The sample was thawed at RT, centrifuged at 12,000 rpm for 15 minutes at 6 ˚C, and the supernatant discarded. The resulting pellet was allowed to dry for 10 minutes and resuspended in 25 µl distilled $H_2O$. DNA concentrations were quantified using the Qubit® 2.0 Fluorometer (Invitrogen) at the CAF Analytical Services Unit, Stellenbosch University, South Africa. The five samples with the highest DNA concentrations were pooled. The DNA concentration of one pair of large X chromosomes could be determined as follows:

$$\text{X chromosome pair} = \frac{\text{Total DNA (ng)}}{\text{Number of X chromosome pairs}}$$

### 3.2.2.5 Estimation of RWA genome size

Using the measured sizes of the different chromosome sets (Section 3.2.1), the number of different size chromosome pairs (Section 3.2.1), and the contribution of the X chromosome (Section 3.2.2.4), 1C of the RWA can be calculated as follows:

$$1C = [\text{X chr (pg)}] + \left[(\text{number of middle chr pairs})\left(\frac{\text{middle chr (µm)}}{\text{X chr (µm)}}\right)(\text{X chr (pg)})\right]$$

$$+ \left[(\text{number of small chr pairs})\left(\frac{\text{small chr (µm)}}{\text{X chr (µm)}}\right)(\text{X chr (pg)})\right]$$

The genome size of the RWA was calculated using the following assumption: 1 pg DNA = 0.978 x $10^9$ base pairs. Based on the consideration that AT:GC = 1:1, ignoring the

presence of modified nucleotides (Doležel *et al.* 2003; Doležel and Bartoš 2005; Doležel *et al.* 2012).

#### 3.2.2.6 Sequencing

Sodium acetate (1M) was added to the pooled sample of X chromosome DNA (Section 3.2.2.4) and the 1.5 ml Eppendorf tube was filled to 1 ml with 100% ice-cold ethanol. The samples were packaged and sent to Macrogen (Korea) for sequencing.

### 3.2.3 Next generation sequencing (NGS) and bioinformatic analysis of the RWA sex chromosome fraction

The RWA chromosome fraction obtained through flow cytometry was sequenced on an Illumina® HiSeq™ platform and aligned to the reference genomes of the RWA and pea aphid. In addition, the annotated X chromosome of the fruit fly was aligned to the RWA genome in order to annotate corresponding regions located on the sex chromosome of the RWA.

#### 3.2.3.1 Next generation sequencing

The X chromosome DNA fraction isolated through flow cytometry (Section 3.2.2.4) was sent for sequencing to Macrogen (Korea) where amplification was performed prior to sequencing using the TruSeq Nano DNA Library Preparation Kit (Illumina FC1214001). Paired-end sequencing was performed using the Illumina® HiSeq™ 2000 system. Sequence read length consisted of 101 bp and library insert sizes of 350 bp.

#### 3.2.3.2 Reference mapping of the RWA X chromosome sequence data set to that of the whole genome of the RWA and pea aphid.

Sequencing reads obtained from the Illumina® HiSeq™ 2000 platform were aligned to the reference genomes of the RWA (SAM_Contigs_Version 1.1; GCA_001465515.1; Botha *et al.* 2016 – *in press*) and the pea aphid (Acyr_2.0; GCA_000142985.2; The International

Aphid Genomics Consortium 2010) using Geneious v7.1.7 (Kearse *et al.* 2012) (Figure 3.4).

Raw sequencing reads were verified for quality using FastQC (http://www.bioinformatics.babraham.ac.uk/projects/fastqc). The first 18 bases displayed biased sequence composition at the start of the reads. These poor quality reads were filtered and trimmed by making use of FASTX-Toolkit (http://hannonlab.cshl.edu/fastx_toolkit/) to ensure that for a pair of paired-end reads each data set had 90% or more bases with a phred score greater than or equal to Q20 (Figure 3.4).

Quality trimmed reads were aligned to the RWA reference genome (SAM_Contigs_Version 1.1; GCA_001465515.1; Botha *et al.* 2016 – *in press*) as well as to that of the pea aphid (Acyr_2.0; GCA_000142985.2; The International Aphid Genomics Consortium 2010) using Burrows-Wheeler aligner (BWA) with default parameters (Li and Durbin 2010). The quality of the alignments was assessed by using Qualimap (García-Alcalde *et al.* 2012) (Figure 3.4).

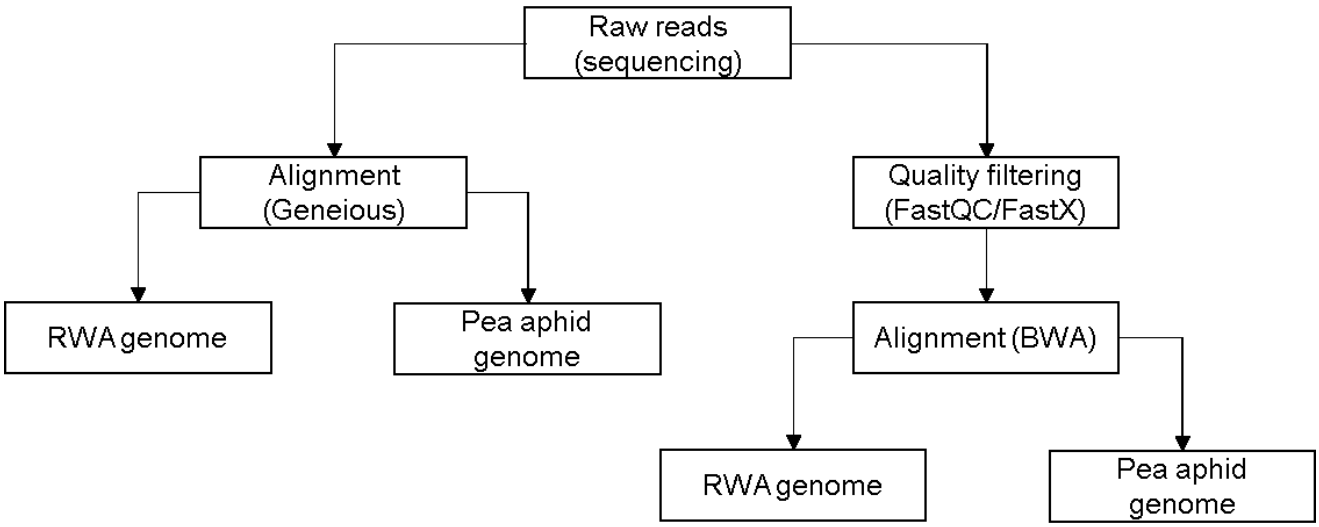


Figure 3.4: Workflow of the quality filtering and alignment of the raw reads obtained from sequencing at Macrogen (Korea) to the RWA and pea aphid genomes. Where raw read alignment was done using the Alighn to reference tool in Geneious (v7.1.7) and quality filtered reads were aligned using Burrows-Wheeler aligner (BWA). Raw reads were quality filtered using FastQC and FastX-Toolkit.

In order to determine the optimum *k-mer* size for *de novo* assembly and sequencing depth, raw sequencing reads were subjected to *k-mer* analysis by using KmerGenie (http://kmergenie.bx.psu.edu/; Chikhi and Medvedev 2014) (Figure 3.5).

The raw sequencing reads were assembled using SOAPdenovo (http://soap.genomics.org.cn/soapdenovo.html). This software package makes use of the de Bruijn graph algorithm to ultimately simplify the assembly of the contigs and scaffolds (Li and Durbin, 2010) (Figure 3.5).

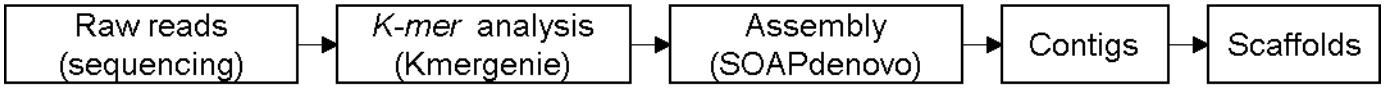


Figure 3.5: Workflow of *k-mer* analysis and SOAPdenovo of the raw reads obtained from sequencing at Macrogen (Korea) to generate contigs and scaffolds.

### 3.2.3.3 Physical mapping against the X chromosome of the fruit fly

The coding sequence (CDS) and proteins of the annotated X chromosome of the fruit fly (BDGP6; Adams *et al.* 2000) were retrieved and aligned to the CDS and proteins of the well-annotated RWA genome (SAM_Contigs_Version 1.1; GCA_001465515.1; Botha *et al.* 2016 – *in press*) using Geneious v7.1.7 (Kearse *et al.* 2012) (Figure 3.6).

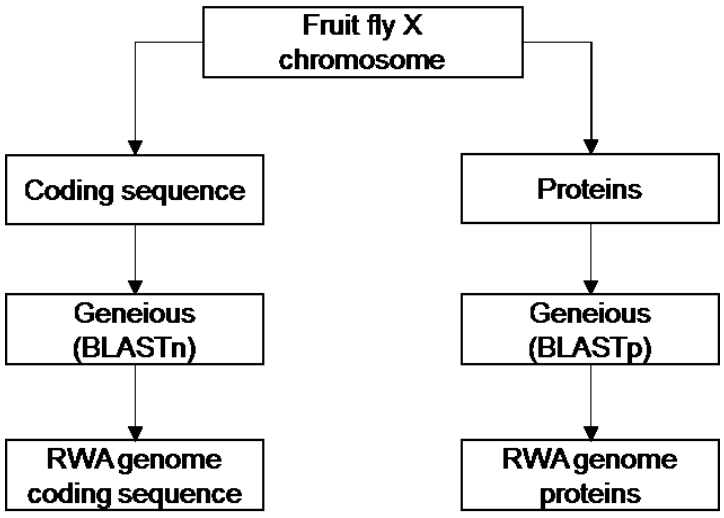


Figure 3.6: Workflow of bioinformatics analysis of the fruit fly X chromosome against the RWA genome. The coding sequences were aligned using BLASTn and the proteins were aligned using BLASTp.

The data was processed on Microsoft Excel (Microsoft Office 2010). For the CDS BLASTn the selection criteria was strict where only sequences with a 70% or more query coverage and identity were included. The protein BLASTp selection criteria included proteins with 40% or more query coverage and identity.

## 3.2.4 Fluorescent *in situ* hybridization

### 3.2.4.1 Fluorescent probes

In order to generate probes to hybridize against the RWA sex chromosome, orthologous regions were identified by aligning the X chromosome of the fruit fly to the RWA genome (as seen in Section 3.2.3.3). Primers were designed from target regions on the RWA genome that aligned to X chromosome genes of the fruit fly using Geneious v7.1.7 (Kearse *et al.* 2012). The eight primers used in the study were selected according to the percentage identical sites and the region with a BLAST hit (Table 3.1). Two probes as used by Novotná *et al*. (2011) were included as positive controls (i.e. 18S rRNA and histone H4).

In order to generate unlabelled probes, polymerase chain reactions (PCR) using the primers listed in Table 3.1 were conducted. The 20 µl PCR master mix contained 1X PCR buffer (Thermo Scientific), 2 U *Taq* polymerase (Thermo Scientific), 0.2 mM dNTP's mix (Thermo Scientific), 500 nmol of each primer, and 100 ng of template genomic RWA DNA. The PCR reaction conditions were as follows: 5 minutes at 95 °C, 35 cycles of 15 seconds at 94 °C, 15 seconds at 57 °C, 60 seconds at 72 °C, followed by a final elongation step of 10 minutes at 72 °C. PCR products were separated on a 2% agarose (SeaKem®) gel at 90 volts for 80 minutes and was visualised on a Gel Doc EZ imager (Bio-Rad) at the Department of Genetics, Stellenbosch University, South Africa. The PCR products (Table 3.1) were cleaned using a Qiagen MinElute® Reaction Cleanup Kit and labelled by PCR re-amplification with a dNTP mix containing 0.35 mM biotin-16-dUTP (Roche).

Table 3.1: Primer sequences used to generate probes for FISH. Expected product size and gene of origin in the RWA genome are given. Primer X probe 18S rRNA and X probe H4 (Novotná *et al.* 2011) were used as positive controls.

| RWA probe Name | | | Primer Sequence | Expected product size | Description | Accession number (RWA genome) |
|---|---|---|---|---|---|---|
| P1 | X probe 18S rRNA | F | 5'-CCTGAGAAACGGCTACCACATC-3' | 1,051 bp | 18S rRNA X-elimantion | 107165916 |
| | | R | 5'-GAGTCTCGTTCGTTATCGGA-3' | | | |
| P2 | X probe H4 | F | 5'-TSCGIGAYAACATYCAGGGIATCAC-3' | 210 bp | histone H4 | 107167901 |
| | | R | 5'-CKYTTIAGIGCRTAIACCACRTCCAT-3' | | | |
| P3 | X probe scaf_1481 | F | 5'-TCAGAATCCGACAACTAAACACA-3' | 1460 bp | heat shock protein cognate 3 precursor | g943.t1 |
| | | R | 5'-AGCCTCACATTGAAGTTGAGACT-3' | | | |
| P4 | X probe scaf_1801 | F | 5'-GATACGGATCCACGCGAACT-3' | 433 bp | inhibitory POU protein-like | g1176.t1 |
| | | R | 5'-ACCACACTCTGACCACGTTC-3' | | | |
| P5 | X probe scaf_1960 | F | 5'-ACGAGTTCCGATGTGCCAAT-3' | 944 bp | low-density lipoprotein | g1279.t1 |
| | | R | 5'-ACCACCTGTCCACTTTCATCC-3' | | | |
| P6 | X probe scaf_4125 | F | 5'-GGCTACTGCTGCTTCTTCCA-3' | 641 bp | actin 5C, isoform B | g2500.t1 |
| | | R | 5'-GGAATGTAGGCCTAATGCATTGG-3' | | | |
| P7 | X probe scaf_6337a | F | 5'-CTGGGGGATTCGTTGGTCAT-3' | 500 bp | actin-42A-like isoform 1 | g3570.t1 |
| | | R | 5'-TCGAGCTGAAAGGAATAGTCACT-3' | | | |
| P8 | X probe scaf_6337b | F | 5'-TCATCTATAACTGTAGTCCTGCAC-3' | 498 bp | hypothetical protein LOC100168805 | g3569.t1 |
| | | R | 5'-ATCCCCCAGCCCTGACTAAT-3' | | | |
| P9 | X probe scaf_13192 | F | 5'-AAGACTCTGGGCAACGGAAG-3' | 895 bp | actin (ACYPI006035) | g5957.t1 |
| | | R | 5'-TGCACAAACACCAAAAATATCCCA-3' | | | |
| P10 | X probe scaf_17249 | F | 5'-ATTGGTATCGATCGGTGCCG-3' | 499 bp | alpha-actinin, sarcomeric-like isoform 2 | g7053.t1 |
| | | R | 5'-CACACAACGCACTTACGCAC-3' | | | |

### 3.2.4.2 Slide preparation and treatment

Slides with mounted chromosomes were prepared as previously discussed in Section 3.2.1.1 with modifications as described by Sahara *et al.* (1999), Fuková *et al.* (2005) and Novotná *et al*. (2011). Briefly, chromosomes were dehydrated by passing them through an ethanol series (70%, 80%, and 96%, for 30 seconds each) and aged at -20 °C overnight. The chromosomes were passed through the ethanol series and air-dried at RT. In order to remove excess proteins, the chromosome slides were baked for 4 hours at 65 °C and incubated in 100 µg proteinase K (Fermentas) in 100 ml 1X Phosphate-buffered saline (PBS) (137 mM NaCl, 2.7 mM KCl, 10 mM $Na_2HPO_4$, and 1.8 mM $KH_2PO_4$; pH 7.4) for 5 minutes. The chromosomes were washed twice in 1X PBS. RNA was removed by treating the chromosomes with 20 µg RNase A (Thermo Scientific) in 100 µl 2X Saline sodium citrate (SSC) (0.3 M NaCl and 0.03 M $Na_3C_6H_5O_7$; pH 7.0) for 1 hour, followed by washing twice in 2X SSC. The chromosomes were finally incubated in 5X Denhardt's solution (Sigma) for 30 minutes. All the wash steps and incubation periods were performed at 37 °C. Denaturation of the chromosomes was performed at 68 °C for 3 minutes and 30 seconds in 70% deionized formamide (Merck) in 2X SSC. The prepared slides were subjected to a final ethanol dehydration series and air-dried at RT.

### 3.2.4.3 Probe denaturation and hybridization

Labelled probes (50 ng/µl) in Section 3.2.4.1 were mixed together with 25 µg of competitor sonicated salmon sperm DNA (Sigma), where after 20 µl of cold 100% ethanol was also added. Probes were allowed to precipitate at -80 ºC for 30 minutes and subsequently centrifuged at 13,000 rpm for 20 minutes. The supernatant was discarded and the pellet was washed with cold 70% ethanol and once more centrifuged at 13,000 rpm for 10 minutes. The supernatant was carefully discarded by pipetting and the sample was allowed to air-dry at 37 ºC. Once the sample was dry, it was dissolved in 5 µl pre-warmed deionized formamide (Merck) at 37 ºC for 30 minutes with vortexing every 10 minutes,

where after 5 µl 20% (w/v) dextran sulphate (Sigma) pre-warmed to 37 ºC was added to form the hybridization mix. Probes were denatured by heating the hybridization mix to 90 ºC for 5 minutes, where after the hybridization mix was immediately chilled on ice for 10 minutes before applying to the chromosomal slides.

The hybridization mix (10 µl) was spotted onto the prepared slide (Section 3.2.4.2) and covered with a 22x22 mm cover glass slip. The cover glass was gently pressed down to avoid any bubbles and the edges were completely sealed with PVC-U cement (Tangit). The slides were incubated overnight at 37 ºC.

#### 3.2.4.4 Probe detection and signal enhancement

The PVC-U cement (Tangit) was carefully removed from slides (Section 3.2.4.3) by using forceps and slides were submerged in 50% (v/v) formamide (Merck), allowing the cover slip to detach. The labelled chromosome slides were then subjected to wash steps as follows: three times with 2X SSC containing 50% (v/v) formamide (Merck) at 46 ºC for 5 minutes; five times with 2X SSC at 46 ºC for 2 minutes; three times with 0.1X SSC at 62 ºC for 5 minutes; and finally once with 4X SSC containing 0.1% (v/v) Tween® 20 (Merck) at RT for 5 minutes.

To enable probe detection, 450 µl of 2.5% Bovine Serum Albumin (BSA) (Sigma) dissolved in 4X SSC was dropped on each slide, covered with a 22x50 mm cover glass slip, and incubated at RT for 20 minutes. From here on incubations were performed in a dark room. Labelled chromosomes were then submerged for 1 minute in 2X SSC to remove the BSA and allow the cover glass to detach. Thereafter, 100 µl Cy3-streptavidine (Jackson Research Laboratories) was dropped onto each slide, covered with a 22x50 mm cover glass, and once again incubated at RT for 30 minutes, followed by a 1 minute submersion in 2X SSC to remove the Cy3-streptavidine and detach the cover glass. The labelled chromosomes were subjected to three washes with 4X SSC containing 0.1% (v/v) Tween® 20 at 37 ºC for 3 minutes.

To enhance the probe signals, 450 µl of 2.5% BSA dissolved in 4X SSC was dropped on each slide, covered with a 22x50 mm cover glass, and incubated at RT for 10 minutes, followed by a 1 minute submersion in 2X SSC to remove the BSA and detach the cover glass slip. Thereafter, 50 µl Biotinylated antistreptavidine (Vector) was dropped onto each slide, covered with a 22x50 mm cover glass, and incubated at 37 ºC for 20 minutes, followed by a 1 minute wash with 2X SSC to remove the antistreptavidine and cover glass. The slides were subjected to three washes with 4X SSC containing 0.1% (v/v) Tween® 20 at 37 ºC for 3 minutes. The probe detection and signal enhancement steps were repeated once more to obtain optimal signal enhancement.

#### 3.2.4.5 Slide staining and visualisation

Labelled samples were stained for 5-8 minutes with Hoechst 33342 (Sigma) solution (10 mg/ml) that was diluted 1:100 to a final concentration of 0.01 mg/ml. The stained slides were then briefly submerged in distilled $H_2O$ and left to dry at RT in the dark.

After staining, the chromosomes were visualised using a Zeiss LSM780 ELYRA PS.1 (Zeiss Germany) confocal microscope equipped with Zen Lite Software (Zeiss Germany) (CAF fluorescent microscopy unit, Stellenbosch University, South Africa).

## 3.3 Results

### 3.3.1 Karyotyping of RWA chromosomes

The karyotype was constructed to determine the number and appearance (size and shape) of chromosomes in the nucleus of a RWA cell.

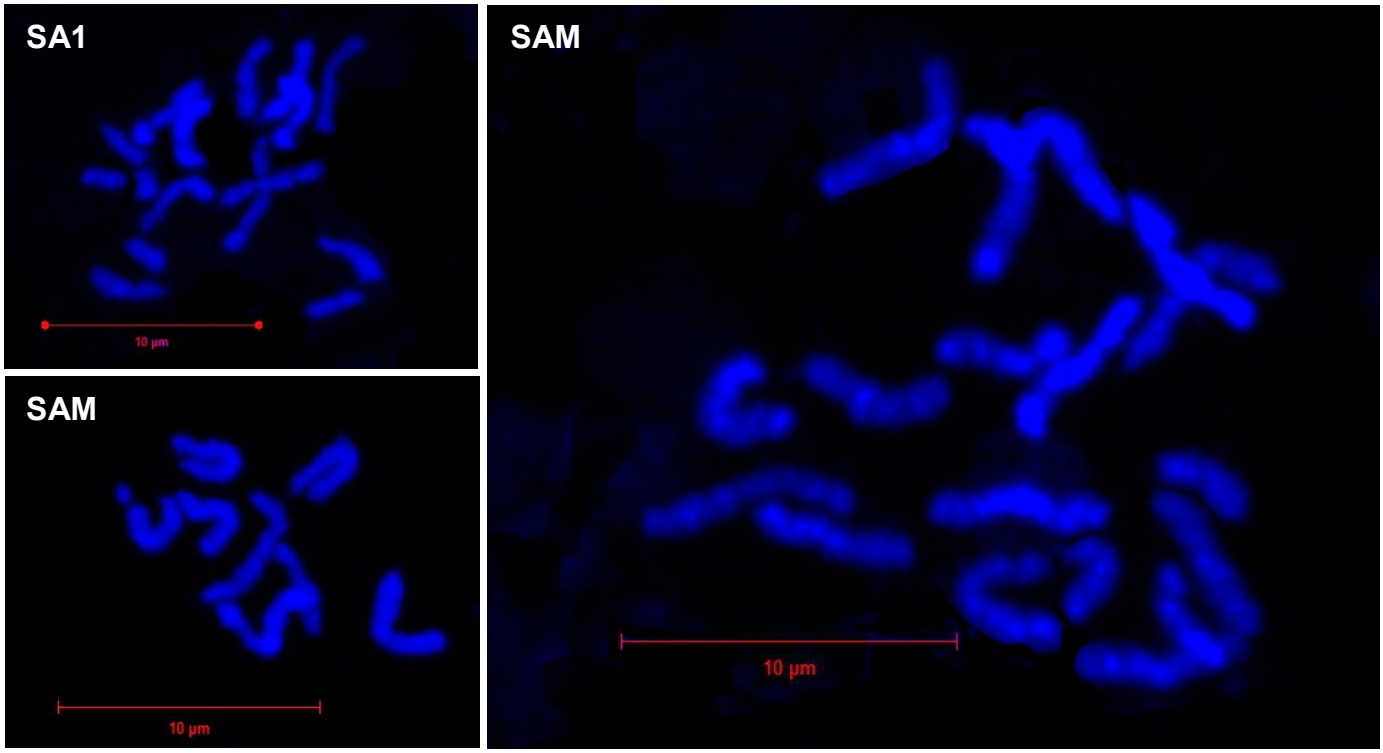


Figure 3.7: The RWA chromosomes are stained with Hoechst 33342 to enable their detection through the confocal microscope. The chromosomes of biotype SAM and SA1 are compared. A 10 µm bar is indicated in each image.

Figure 3.7 displays the chromosomes as seen on the Zeiss LSM780 ELYRA PS.1 (Zeiss Germany) confocal microscope. The Hoechst 33342 (Sigma) stain bound to the RWA DNA and stained the chromosomes fluorescent blue. The chromosomes appear to be long, slender rods of DNA which lack constriction sites or centromeres. Figure 3.7 displays different sized chromosomes that cluster together. The length of the chromosomes can be compared to the 10 µm bar present in each image. There are no observable morphological differences between the chromosomes of RWA biotype SAM and SA1.

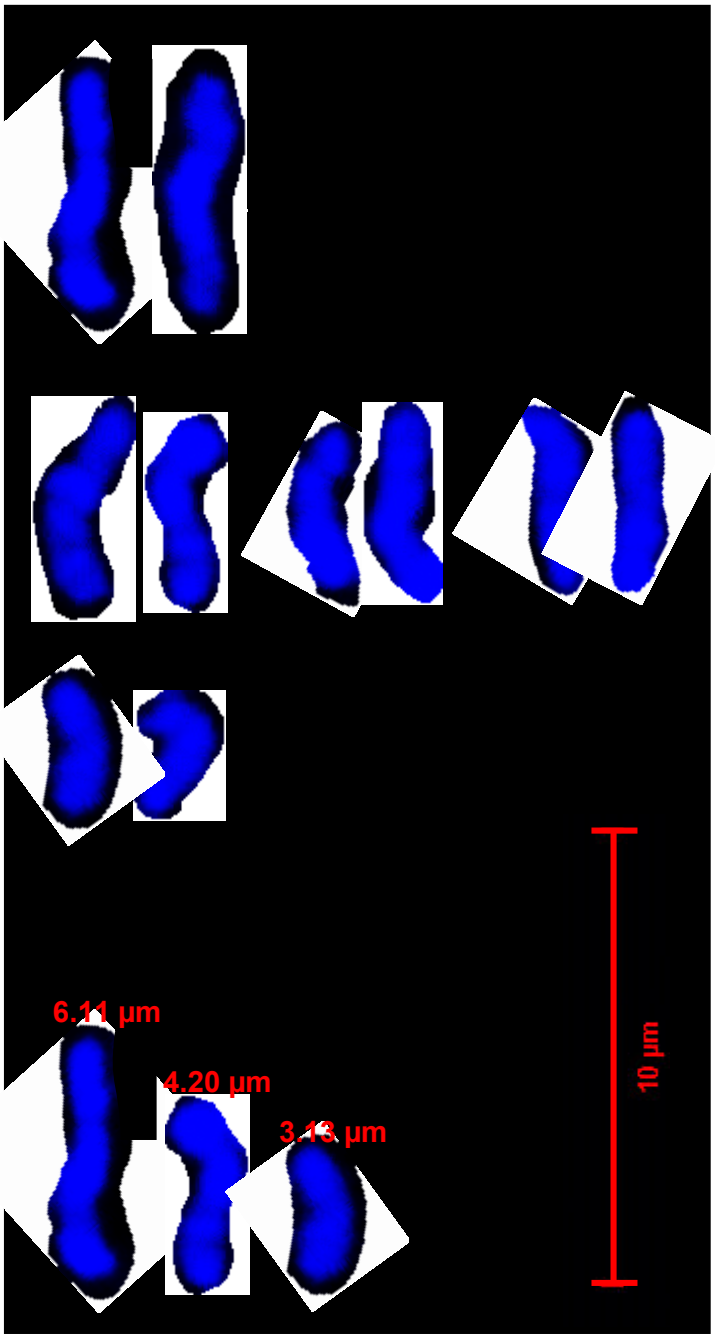


Figure 3.8: The karyotype of a female RWA showing the complete set of chromosomes of 2n=10 [2 sex chromosomes (X) and 8 autosomes (6 middle size and 2 small size chromosomes)]. Indicated is a 10 µm bar, as well as the average sizes of each of the different chromosomes, respectively.

The karyotype of the female RWA biotype SAM consists of a diploid chromosome number of 10. The chromosomes were divided into size groups according to their length. The results produced two large sex chromosomes and four autosomal chromosome pairs, of which three homologous pairs are middle sized and one homologous pair is smaller (Figure 3.8; Table 3.2). The chromosome groups varied remarkably in their length and the smallest autosome chromosome pair as well as the X chromosomes were easily

identifiable, because of their lower number. However, the remaining three middle sized autosome chromosome pairs were difficult to pair and to distinguish from one another, because of their high number and similar size (Figure 3.7; Figure 3.8).

Table 3.2: The mean lengths of the chromosomes were determined by measuring ten specimen of each size.

| | X chromosome (µm) | Middle chromosome (µm) | Small chromosome (µm) |
|---|---|---|---|
| | 6.14 | 4.32 | 3.33 |
| | 5.85 | 4.27 | 3.09 |
| | 6.23 | 3.81 | 3.25 |
| | 6.12 | 4.36 | 2.99 |
| | 6.21 | 4.35 | 3.10 |
| | 6.23 | 4.22 | 3.12 |
| | 6.26 | 4.21 | 3.12 |
| | 5.98 | 4.19 | 3.08 |
| | 6.03 | 4.08 | 3.12 |
| | 6.00 | 4.20 | 3.07 |
| **Mean** | **6.11** | **4.20** | **3.13** |
| **SD** | **0.13** | **0.15** | **0.09** |

* SD = standard deviation

From the results, the lengths of the three chromosome groups were determined by measuring ten chromosomes of each size. The data showed that the approximate length of the chromosomes were as follows: the X chromosome at 6.11 µm (SD = 0.13 µm), the middle sized chromosome at 4.20 µm (SD = 0.15 µm), and the smallest chromosome at 3.13 µm (SD = 0.09 µm) (Table 3.2; Figure 3.8; Figure 3.9). These results suggest that the X chromosome contributes approximately 28% of the total DNA based on length.

Table 3.3: *t*-Tests were performed to test if the different size chromosome groups are statistically different (Table A1, Table A2, and Table A3).

| | |
|---|---|
| ***t*-Test: X chromosome - middle chromosome** | $p = 1.89 \times 10^{-16}$ |
| ***t*-Test: middle chromosome - small chromosome** | $p = 5.42 \times 10^{-13}$ |
| ***t*-Test: X chromosome - small chromosome** | $p = 9.42 \times 10^{-22}$ |

The chromosome size groups were shown to be statistically different from one another in Table 3.3 (as calculated in Table A1, Table A2, and Table A3), with $p < 0.05$ for all the size comparisons. Figure 3.9 displays a chart that demonstrates the clear differences in

size. The X chromosome is nearly twice the size of the small chromosome and almost 1.5X the size of the middle chromosome, making it by far the largest chromosome in the karyotype of the RWA (Figure 3.9).

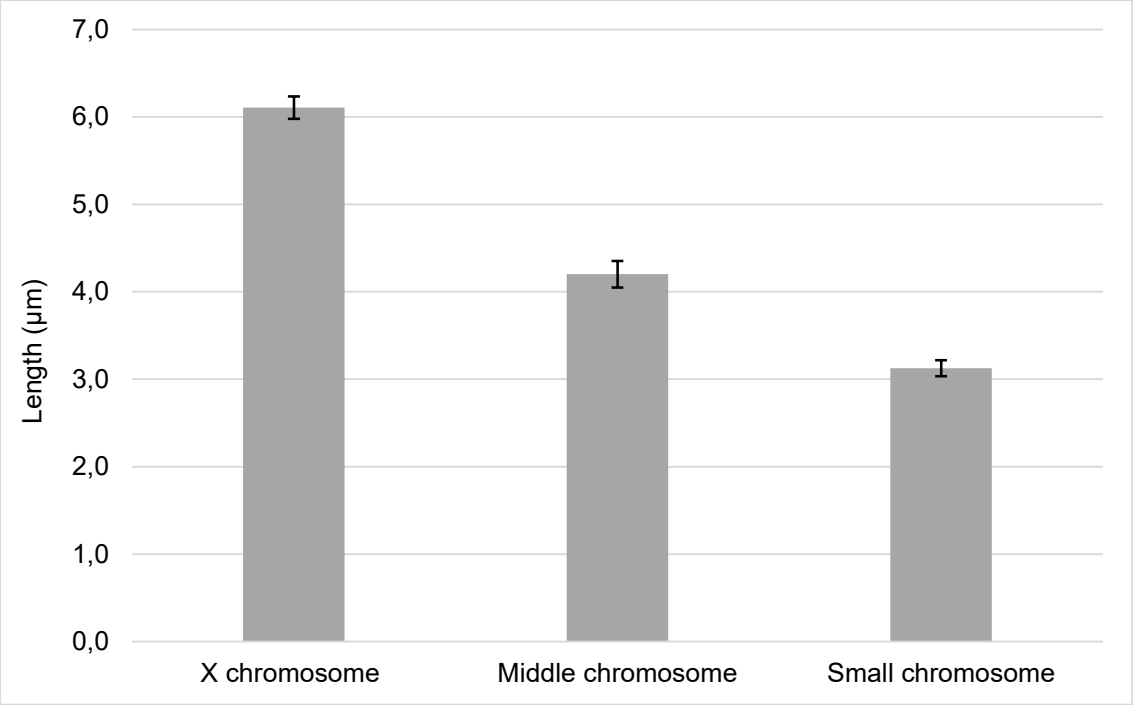


Figure 3.9: The bar chart is a visual representation of the size differences of the RWA chromosomes.

## 3.3.2 Flow cytometry separation of RWA chromosomes

Because of the size differences, flow cytometry offered an attractive protocol that could be used to isolate chromosomes from one another. In this study the method is implemented to separate the different sized chromosome groups of RWA biotype SAM. All of the flow cytometry results obtained during the study can be found in a supplemental file named **Folder A1** (see attached CD).

Figure 3.10 displays a single-parameter histogram that measures the relative fluorescence area (PE-Texas Red-A) on the x-axis versus the number of events (chromosome count) on the y-axis. The histogram in Figure 3.10 shows the total number of chromosomes that possess the physical properties – relative area and fluorescence - selected for. The peaks with the desired characteristics, in this case the middle- and large

chromosomes, were identified as the positive datasets. The left middle chromosome peak display a higher count (500), which is approximately 5X higher than that of the large chromosome, but with a lower fluorescence (31,000-61,000). The large chromosome peak on the other hand has a lower count (100), but higher fluorescence (69,000-101,000). The histogram did not display a positive peak for the small autosome chromosomes (Figure 3.10), mostly because they were too small to be distinguished from cell debris. Therefore, the small autosome chromosomes could not be separated from the other size chromosome groups through flow cytometry.

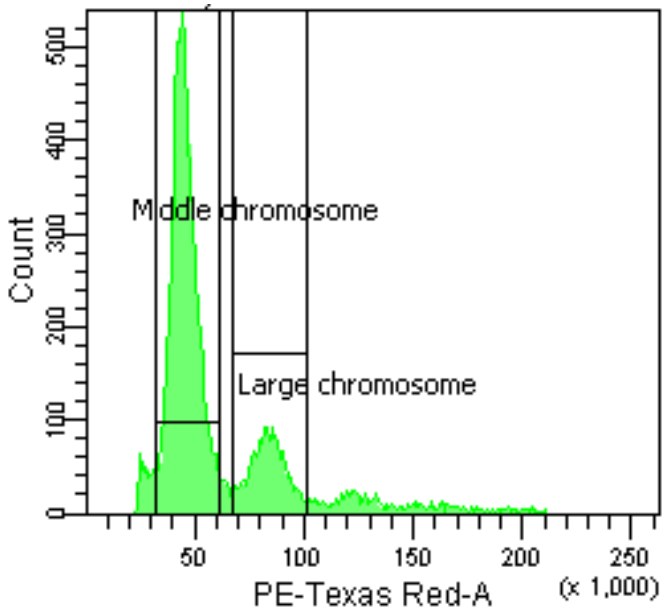


Figure 3.10: The single-parameter histogram displays positive peaks for both the middle- and large chromosomes.

Table 3.4 displays the summarized data from a flow cytometry run. The populations were determined through the gating strategies as described in Section 3.2.2.2. The data in Table 3.4 shows that each subsequent gating strategy or population (black to red to green to cyan and blue) allowed for more stringent flow sorting, only selecting the chromosomes of interest, ultimately making the run more specific. From the results it was noticed that the middle sized chromosome had the highest percentage parent (73.5%), while the large sex chromosome had a low percentage parent (15.6%) (Table 3.4). Percentage parent

refers to the percentage of gated particles. Table 3.4 also displays an average fluorescence of 40,394 for the middle chromosome and 78,095 for the large chromosome.

Table 3.4: The summarized data measured after gating allows for the calculation of the number of events passing through, percentage parent, as well as fluorescence. Each block represents the results after that gating strategy has been implemented.

Experiment Name: Trial Chromosome Sorting
Specimen Name: 22 July 2014
Tube Name: SAM after sort
Record Date: Jul 22, 2014 10:26:38 AM

| Population | #Events | %Parent | PE-Texas... Geo Mean | PE-Texa... Median |
|---|---|---|---|---|
| All Events | 289,964 | #### | #### | 1,562 |
| Singlet gate | 165,980 | 57.2 | #### | 3,004 |
| Chromosome gate | 38,018 | 22.9 | 48,929 | 41,680 |
| Middle chromosome | 27,946 | 73.5 | 40,394 | 40,177 |
| Large chromosome | 5,927 | 15.6 | 78,095 | 77,833 |

#### - not measured/not included in gating areas

### 3.3.3 Chromosomal DNA concentration

The DNA from the sorted X chromosome had to be extracted before sequencing (Table A4).

Table 3.5: The X chromosomes of the samples were pooled together and the DNA concentration was determined (Table A4).

| Biotype | Ploidy | Number of X chromosome pairs | Total DNA (ng) |
|---|---|---|---|
| SAM | 2C | 2,438,044 | 889.5 |

After flow sorting, the number of X chromosomes (2,047,296) resulted in a total amount of 889.46 ng of DNA which was sufficient for sequencing later (Table 3.5). The DNA concentration of an X chromosome pair equated to:

$$\text{X chromosome pair} = \frac{889.5}{2{,}438{,}044}$$

$$\text{X chromosome pair} = 0.36 \text{ pg}$$

This means that a single X chromosome was **0.18 pg**.

### 3.3.4 Estimation of RWA genome size

An estimate of the size of the RWA genome was calculated by using the lengths of the chromosome groups (Section 3.3.1), the number of different chromosome pairs (Section 3.3.1), the DNA concentration of a single X chromosome (Section 3.3.3), as well as the assumption that 1 pg DNA = 0.978 x $10^9$ base pairs (Doležel *et al.* 2003; Doležel and Bartoš 2005; Doležel *et al.* 2012).

1C was determined as follows:

$$1C = [0.18] + [(3)\left(\frac{4.20}{6.11}\right)(0.18)] + [(1)\left(\frac{3.13}{6.11}\right)(0.18)]$$

$$1C = 0.18 + 0.37 + 0.09$$

$$1C = \mathbf{0.64340425\ pg}$$

Thus, the estimated genome size was calculated as follows:

$$1\ pg = 0.978 \times 10^9 \text{ base pairs}$$

Therefore,

$$= 1C \times (0.978 \times 10^9)$$

$$= 0.64340425 \times (0.978 \times 10^9)$$

$$= \mathbf{629\ Mb}$$

### 3.3.5 Next generation sequencing (NGS) and bioinformatic analysis of RWA X chromosome

Using the Illumina® HiSeq™ 2000 platform offered by Macrogen, NGS produced a total of 13,818,304,294 bases from the RWA sex chromosome fraction with a read count of 136,814,894 (Table 3.6). The resulting NGS reads were of high quality as revealed by a Phred score of 96.32%. The GC content of the sequence data of the sex chromosome

was 35.44% (Table 3.6) corroborating the low GC percentage found in RWA (Botha *et al.* 2011; 2015; Nicholson *et al.* 2015).

Table 3.6: The tabulated results obtained from the NGS including the sequencing platform used, number of bases, read count, GC percentage, and Q20 percentage.

| Sequencing platform | Number of bases | Read count | GC% | Q20 (%) |
|---|---|---|---|---|
| Illumina® HiSeq™ 2000 | 13,818,304,294 | 136,814,894 | 35.44 | 96.32 |

In order to assess the quality of the obtained NGS data, a FastQC analysis was performed. The complete results obtained during the FastQC analysis are included in Folder A2 (see attached CD). The y-axis of the graphs displayed in Figure 3.11 indicates the quality scores per base of sequence. The FastQC results presented in Figure 3.11 shows that the sequences produced by Macrogen had high base quality mostly with little degradation as the run progressed at the end. Figure 3.11 (A) represents the forward sequence of the RWA X chromosome, while Figure 3.11 (B) represents the reverse sequence of the RWA X chromosome.

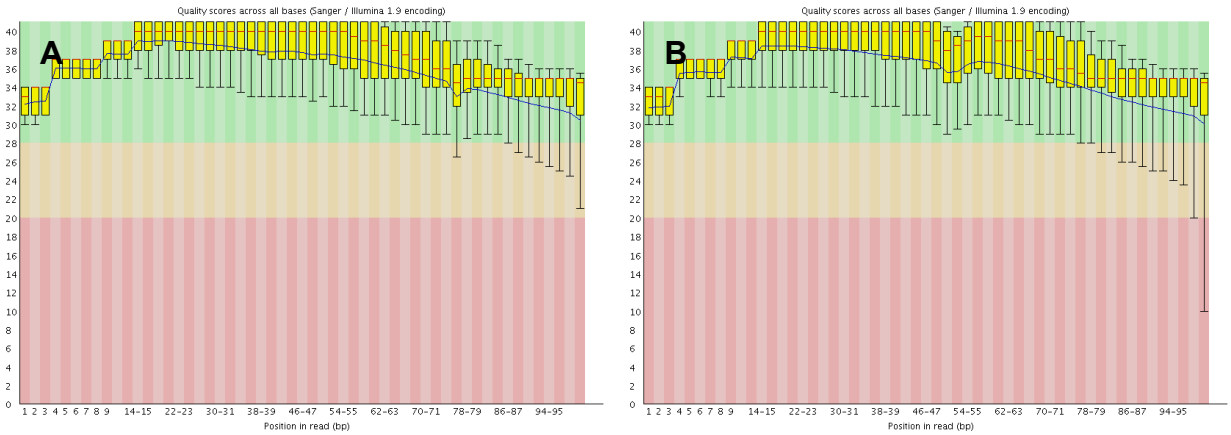


Figure 3.11: The quality of the sequence bases were assessed using FastQC. The y-axis of the graph is divided into three regions; good quality calls (green), reasonable quality calls (orange), and poor quality calls (red). Graph A represents the forward sequence, while graph B represents the reverse sequence of the RWA X chromosome.

The graphs in Figure 3.12 are very similar with both the forward sequence (A) and reverse sequence (B) displaying AT-richness. The GC% is indicated in the graphs in Figure 3.12. Figure 3.12 also displays phasing at the start of the reads.

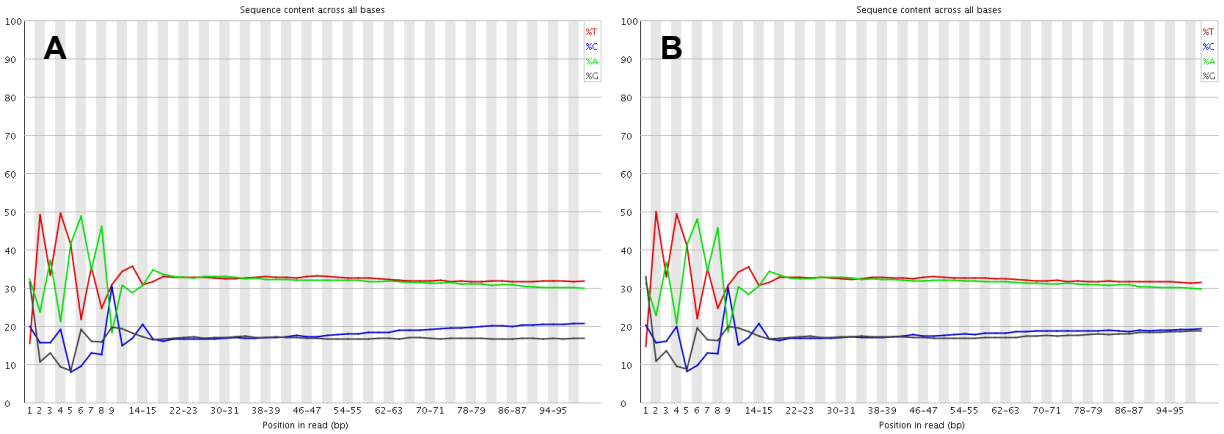


Figure 3.12: The plot indicates the percentage ATGC content per base in the sequence with the red line representing %T, blue %C, green %A, and black %G. Graph A represents the forward sequence, while graph B represents the reverse sequence of the RWA X chromosome.

contigs and scaffolds from the NGS raw reads for the X chromosome of the RWA (Folder A3 – see attached CD). The y-axis of the graphs in Figure 3.13 represents the number of *k-mers*, but it can also be interpreted as the estimated size of an assembly of this dataset. Figure 3.13 displays a plot with multiple local maxima's for *k-mer* size.

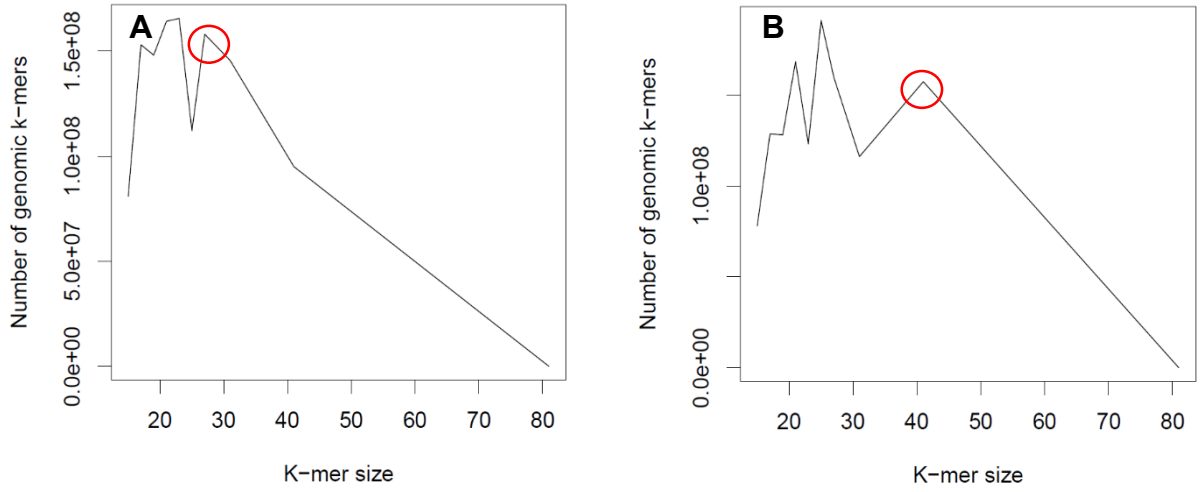


Figure 3.13: Genomic *k-mers* versus *k-mer* size. Graph A represents the forward sequence, while graph B represents the reverse sequence of the RWA X chromosome.

Figure 3.14 displays three *k-mer* histograms, where A represents the KmerGenie recommended *k-mer* size of k=27 for the forward sequence, B represents the KmerGenie recommended *k-mer* size of k=25 for the reverse sequence, and C represents the *k-mer* size k=27 for the reverse sequence that was self-selected, because the same *k*-value was needed for both the forward and reverse sequences of the RWA X chromosome to

build the contigs and scaffolds. Therefore k=27 (A and C) was selected as the best fit for the paired-end reads.

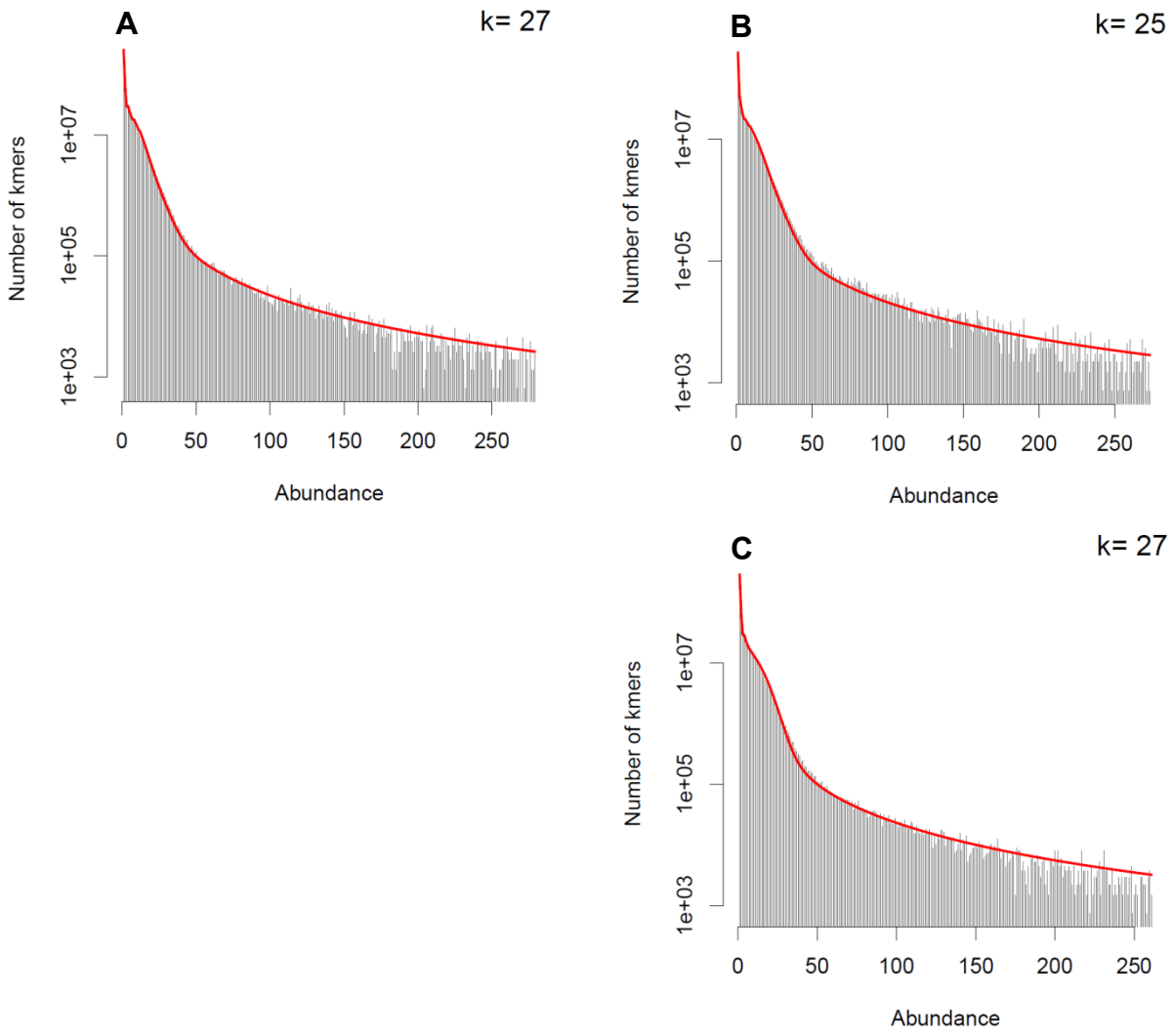


Figure 3.14: The graphs (A – C) embody *k-mer* abundance histograms. A represents the *k-mer* size that was used for the forward sequence of the RWA X chromosome, while B and C represent the *k-mer* sizes for the reverse sequence of the RWA X chromosome. A and B was recommended by KmerGenie for the forward and reverse sequences respectively, but C (self-selected) was used for the reverse sequence. Therefore, A and C was used.

(http://soap.genomics.org.cn/soapdenovo.html) produced 1,059,574 contigs for the sorted RWA X chromosome fraction, with the longest contig being 7,071 bp (N50 = 314). The GC content of the built contigs were 30.05%. A total of 671,410 bp (N50 = 1,367) scaffolds were obtained, with the longest being 46,046 bp. The GC content from the built scaffolds was 30.13% (Table 3.7; Folder A4 – see attached CD).

Table 3.7: The tabulated results produced by SOAPdenovo presenting the contig and scaffold assemblies.

| Number | Mean Size | Median Size | Longest Sequence | Shortest Sequence | GC% |
|---|---|---|---|---|---|
| **Contigs** | | | | | |
| 1,059,574 | 260 | 198 | 7,071 | 100 | 30.05% |
| **Scaffolds** | | | | | |
| 671,410 | 677 | 320 | 46,046 | 100 | 30.13% |

### 3.3.6 Mapping of the X chromosome reads to the reference RWA and pea aphid genomes

The reads from the RWA X chromosome fraction was aligned and mapped to the reference genomes of the RWA (SAM_Contigs_Version 1.1; GCA_001465515.1; Botha *et al.* 2016 – *in press*) and the pea aphid (Acyr_2.0; GCA_000142985.2; The International Aphid Genomics Consortium 2010). The Qualimap results of the RWA were compared to that of the pea aphid. Table 3.8 displays that the raw reads of the sex chromosome had a much higher mapping percentage to the RWA reference genome (82.88%) compared to that of the pea aphid (51.3%).

Table 3.8: The tabulated results produced by Qualimap analysis highlighted the differences in mapping percentage, coverage, and mapping quality between aligning the RWA and pea aphid genomes against the sorted X chromosome of the RWA.

| | Russian wheat aphid | Pea aphid |
|---|---|---|
| **Number of reads** | 139,472,676 | 137,070,267 |
| **% Mapped reads** | 82.88% | 51.30% |
| **% Unmapped reads** | 17.12% | 48.70% |
| **% Paired reads** | 82.88% | 51.30% |
| **GC%** | 35.03% | 35.15% |
| **Mean coverage (x)** | 35.66 | 6.84 |
| **Mean mapping quality** | 36.12 | 7.95 |

This also indicates that there was a much higher coverage to the RWA genome (roughly 5X higher coverage) and that the mapping quality to the RWA was also better. Table 3.8 also shows that the RWA and pea aphid have similar ACGT content, both with AT-rich reads.

A Qualimap analysis was also conducted (Folder A5 – see attached CD), which displays plots for the RWA and pea aphid, each consisting of two figures (Figure 3.15). The upper figures provide the coverage distribution (red line) and coverage deviation across the reference sequences, where coverage is presented along the y-axis and coverage deviation along the x-axis. The lower figure shows GC content, measured in percentage, across reference genome together with its average GC%.

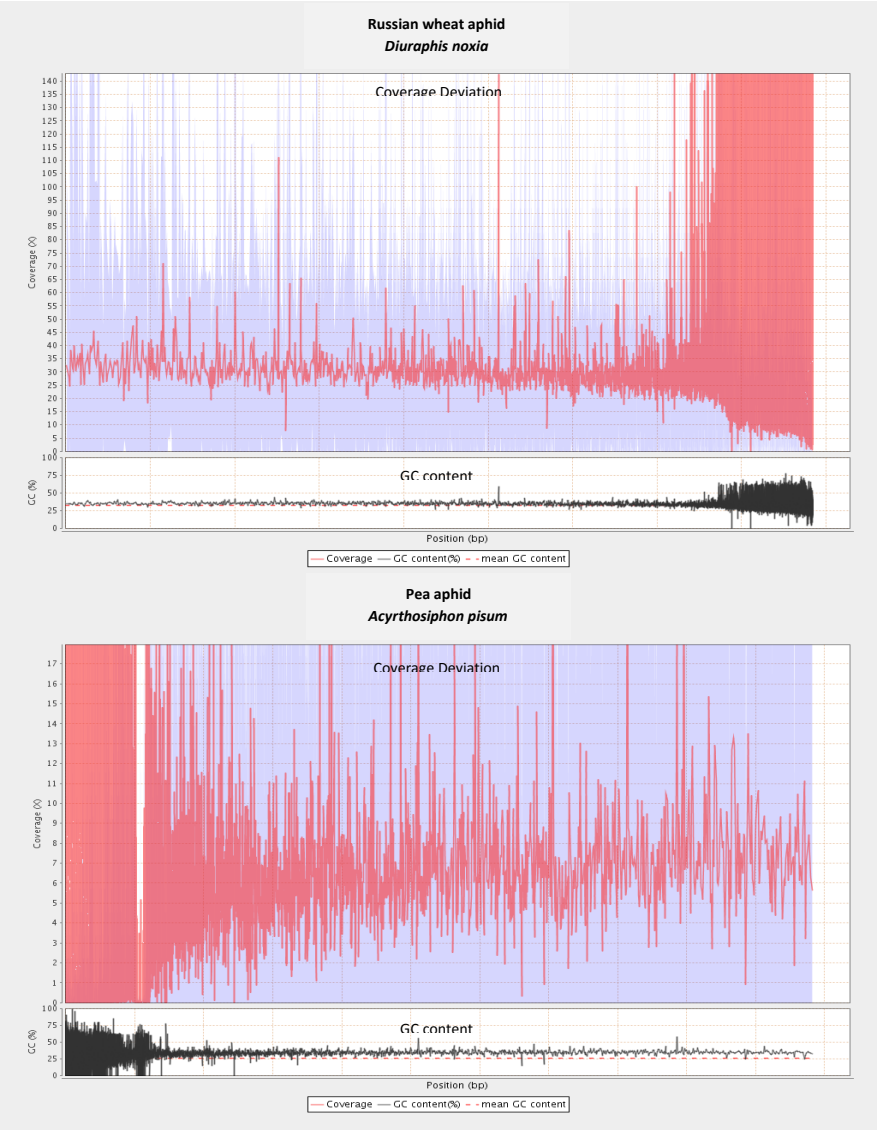


Figure 3.15: Coverage deviation and GC content of the alignment of the X chromosome reads of the RWA and the reference genomes of RWA (top) and pea aphid (bottom).

In Figure 3.15, both plots show complete coverage across the genomes of the RWA and the pea aphid. Figure 3.15 also displayed GC content (30%) that is very similar between the two aphid species as indicated by the lower figures on each plot.

Complete genome coverage was also supported by the results following the alignment done in Geneious (v7.1.7) of the raw reads from the RWA X chromosome to the reference genome of the RWA (SAM_Contigs_Version 1.1; GCA_001465515.1; Botha *et al.* 2016 – *in press*). The data is presented in Folder A6 (see attached CD).

### 3.3.7 Physical mapping of the X chromosome of the fruit fly to the available X chromosome sequences of the RWA

Table 3.9 displays a comparison between the genome and X chromosome of the fruit fly against that of the RWA genome and X chromosome. The RWA has a much larger genome size compared to the fruit fly and has five chromosome pairs, while the fruit fly has seven chromosome pairs (Lemeunier *et al.* 1986). Furthermore, the estimated RWA X chromosome size (176,040,000 bases) is so big that it is larger than the complete genome of the fruit fly of 143,725,995 bases. The fruit fly's X chromosome equates to 16.3% of its total genome, compared to the RWAs 28%. The RWA also has a much lower GC percentage across its genome and X chromosome compared to that of the fruit fly.

Table 3.9: The genome and X chromosome of the fruit fly is compared to that of the RWA by looking at size- and content differences.

| | Fruit fly | Russian wheat aphid |
|---|---|---|
| **Database version** | 84.6 | 1 |
| **Genebuild version** | dmel_r6_FB2014_05 | SAM_Contigs |
| **Estimated genome size (pg)** | 0.18 | 0.64 |
| **Assembled genome size** | 143,725,995 | 629,048,261 |
| **Genome GC%** | 42.10% | 29.50% |
| **# of contigs** | 2,442 | 186,003 |
| **Genome coding genes** | 13,918 | 35,492 |
| **# of chromosome pairs** | 7 | 5 |
| **# of chromosome fragments** | 1 | 1,466 |
| **X chromosome size** | 23,542,271 | 176,040,000 |
| **X chromosome GC%** | 42.50% | 30.40% |

The results in Table 3.10 show that when the coding sequence of the fruit fly's X chromosome was mapped against the RWA genome, that only 8.31% of the length of the RWA X chromosome was aligned. However, when the proteins of the fruit fly X chromosome was mapped against the RWA genome, the results were much better with 67.42% of the proteins of the RWA X chromosome being reported. The complete dataset obtained during the BLASTn and BLASTp analysis is presented in spreadsheet format in Folder A7 (see attached CD).

Table 3.10: The fruit fly X chromosome CDS and proteins were aligned against the RWA genome CDS and proteins in order to characterise the RWA X chromosome.

| **Fruit fly X chromosome CDS vs. RWA genome CDS (BLASTn)** | |
|---|---|
| Total length of RWA X chromosome aligned | 14,631,822 |
| % aligned | 8.31% |

| **Fruit fly X chromosome proteins vs. RWA genome proteins (BLASTp)** | |
|---|---|
| Total length of RWA X chromosome aligned | 118,687,515 |
| % aligned | 67.42% |

## 3.3.8 Fluorescent *in situ* hybridization (FISH)

### 3.3.8.1 Probe generation for the RWA sex chromosomes

The primers that were ordered for probe generation were verified as correct through gel electrophoresis to test if they amplified the correct product sizes.

All of the primers produced single bands of the correct size (Table 3.1) and no contamination was visible in the series (Figure 3.16).

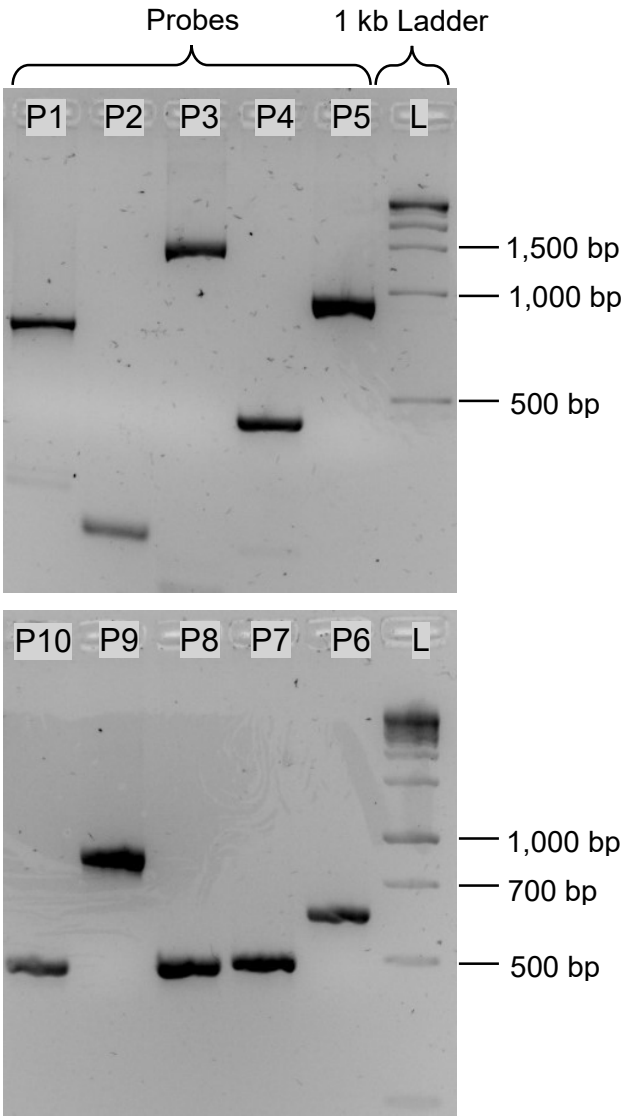


Figure 3.16: Gel electrophoresis was carried out on a 2% agarose gel at 90 volts for 80 minutes to determine if the primers amplified the correct product sizes. Probe 1 and 2 were used as positive controls. A 1 kb (Promega™) DNA ladder was used. Refer to Table 3.1 for probe names.

### 3.3.8.2 Visualisation

FISH with the control probe 1 (18S rRNA) displayed co-localization of hybridization signals (red fluoresence) at one end of the X chromosome of the RWA female (Figure 3.17 – Probe 1). Control probe 2 (histone H4) also displayed signals, but the chromosome images had a low resolution, therefore exact localization on the chromosomes could not be determined. The same occurred using the other probes – probe 3 (X probe scaf_1801), probe 5 (X probe scaf_1960), probe 6 (X probe scaf_4125), probe 7 (X probe scaf_6337a), probe 8 (X probe scaf_6337b), and probe 10 (X probe scaf_17249) – where

localization of probes did occur, but visual confirmation of the chromosomes and probe binding location was lacking (Figure A1). Probe 4 (X probe scaf_1801) and probe 9 (X probe scaf_13192) did not display any hybridization signals.

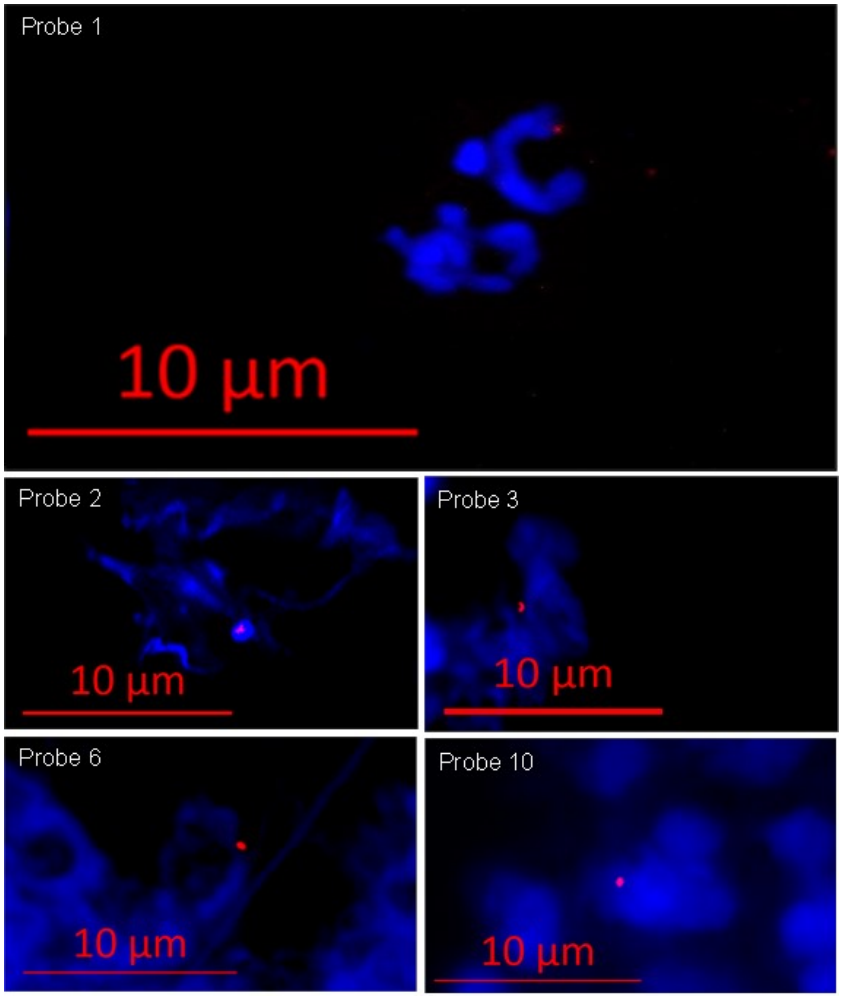


Figure 3.17: Mitotic chromosome complements of RWA after differential staining and FISH. Probe 1 and 2 was used as controls and the other probes were derived from the fruit fly X chromosome.

## 3.4 Discussion

### 3.4.1 RWA karyotype and genome size estimation

In RWA embryonic tissue, cells are constantly in the process of multiplication and differentiation. Therefore, a proportion of the cells are in late prophase or metaphase of mitosis, when the number and relative sizes of their chromosomes can be observed. RWA embryos were used in the study, because most of the cells are multiplying and differentiating constantly, meaning a large proportion of them will be in late prophase or metaphase of mitosis, when chromosomes can be best observed (Novotná *et al.* 2011).

Hoechst 33342 (Sigma) is a membrane permeant dye that binds to adenine-thymine-rich regions of DNA in the minor groove. Botha *et al.* (2012) found that the RWA has the most AT-rich insect genome sequenced, therefore enabling the Hoechst that was used to stain the RWA slide preparations to bind to the entire chromosomes as presented in Figure 3.7.

The chromosome preparations that were obtained from RWA biotype SA1 and SAM after staining did not display any variations in chromosome number, size, and shape. This might be, because SAM was developed from SA1 after laboratory induced selective pressure (Swanevelder *et al.* 2010), leading to no differences in these areas. Also, the fact that the RWA reproduces asexually contributes to the lack in chromosomal differences. During asexual reproduction the traits of only the female RWA is passed on to progeny, resulting in identical offspring with a lower genetic diversity. These factors could be the reason that the chromosomes between these two RWA biotypes are visually identical as seen in Figure 3.7.

The results of this study indicated that the X chromosome of the RWA is 1.5X the size of the middle sized chromosomes as well as twice the size of the smallest chromosomes, therefore it is easy to identify the chromosomes based on their size (Figure 3.7, Figure

3.8, Table 3.2, and Table 3.3). The X chromosome pair and small autosome chromosome pair are easily distinguished, because of their size and low numbers (Figure 3.8), however the three remaining middle autosome chromosome pairs are difficult to separate and identify, because of their similar size and the fact that RWA chromosomes lack centromeres. Apart from the lengths of the chromosomes, there are no other morphological features that would aid in the identification of different chromosomes (Figure 3.8).

The statistical investigations into X chromosome sizes of aphids are somewhat uncommon. The only data available is for a few species of the genus *Neuquenaphis* (Neuquenaphidinae), where the sizes of the X chromosomes vary from 11 to 15% of the total genome (Blackman *et al*. 2003), and for the related *Myzus persicae* species, where the size of the X chromosome almost reach 27% of the genome (Blackman and Takada 1976). In 2011, Novotná *et al.* compared female and male RWA genome sizes. They found the female genome size to be 2C = 0.86 pg, while the male genome size was 2C = 0.70 pg. The difference in DNA content between the males and females suggested that the RWA X chromosome occupies around 35% of the female haploid genome (1C = 0.43 pg), making it one of the largest sex chromosomes in the animal kingdom. The assembly of the karyotype (Figure 3.8) and statistical investigation (Table 3.2, Table3.3, and Figure 3.9) confirms that the X chromosome is by far the largest element in the karyotype of the RWA. The results in this study further suggests that the DNA content of a single X chromosome is 0.18 pg (Section 3.3.3) while the genome equates to 1C = 0.64 pg (Section 3.3.4), suggesting that the X chromosome contributed approximately 28% of the total DNA, which is slightly less than that measured by Novotná *et al.* (2011), but very close to that of the related green peach aphid, where the X chromosome reaches almost 27% of the genome size (Blackman and Takada 1976).

Arthropod genome sizes exhibit considerable diversity, with the largest reported to date being that of the grasshopper (Orthotera: *Neoconocephalus triops* L.) (1C = 7 125 (male)/7 752 (female) Mb; 7.93 pg) and the smallest being the two spotted spider mite (Trombidiformes: *Tetranychus urticae*) (1C = 90.7 Mb; 0.09 pg) (Hanraham and Johnston 2001; Johnston *et al.* 2007). In this study, the genome of the female RWA is estimated to be 629 Mb (Section 3.3.4), which is more than the 421 Mb that Novotná *et al.* (2011) predicted using flow cytometry. The genome of the model aphid, pea aphid, is 517 Mb, roughly 17.8% smaller than the RWA genome size predicted in this study.

### 3.4.2 Flow cytometry and next generation sequencing

Ultimately, the flow cytometry that was used to isolate the X chromosomes of the RWA also proved to be a method to identify the X chromosome based on its relative size and fluorescence. Figure 3.10 presented that the X chromosomes had a higher fluorescence than the middle chromosomes, because of its bigger surface area. A larger surface area allows for more fluorescent dye, in this case propidium iodide (PI), to bind to double stranded DNA by intercalating between base pairs. The results of the histogram in Figure 3.10 compares with the karyotype of the RWA. The karyotype of the female RWA consists of 10 chromosomes – two large sex (X) chromosomes, six middle autosome chromosomes, and a single set of small autosome chromosomes (Figure 3.8). The histogram in Figure 3.10 supports this data by the two distinct peaks. The large chromosomes have a larger area than the autosome chromosomes resulting in a higher fluorescence peak. However, the fact that the RWA possesses more middle chromosomes in their karyotype resulted in the peak with the higher count particles passing through the instrument (Figure 3.10). The small chromosomes did not generate a peak, because of its small size and low fluorescence, causing the instrument to classify the small autosomes as debris and sorting it under the negative dataset with the undesired characteristics (waste). Table 3.4 also linked in with the karyotype when the

percentage parent was studied. In this case, the large chromosomes had a lower percentage parent (15.6%) compared to the middle chromosomes (73.5%), because of their frequency - two out of ten chromosomes are large. Furthermore, Table 3.4 also shows that the X chromosome is almost 1.5X times the size when the fluorescence intensity was calculated correlating with Figure 3.9.

The samples collected during flow cytometry for DNA extraction were chosen based on the trails (Folder A1) that presented the best peaks and physical properties selected for as seen in Figure 3.10. The samples all contained a large amount of chromosomes and had sufficient DNA concentrations and the samples were pooled together.

The NGS results produced by Macrogen were subjected to further analysis. It is stipulated that in a random library there should be little to no difference between the different bases of a sequence run (i.e. A, T, G, and C). In other words, the lines in the plot presented in Figure 3.12 were expected to run parallel with one another as close as possible. However, the results in Figure 3.12 is explained in a study conducted by Botha *et al.* (2012), and a more recent study by Nicholson *et al.* (2015) where they showed that the RWA has the most AT-rich insect genome sequenced to date. Briefly, Botha *et al.* (2012) reported it to be comparable to the GC content described in *A. pisum* (pea aphid) (29.6%) (The International Aphid Genomics Consortium 2010) and *A. mellifera* (honeybee) (33%) (The Honeybee Genome Sequencing Consortium 2006). The high AT-rich genomes of the RWA and the pea aphid contradict the hypothesized positive correlation between insect genome size and AT content. This AT-richness of the RWA genome has also recently been reported by Nicholson *et al.* (2015) and according to them the RWA genome is composed of 29.1% GC and 70.9% AT which is the lowest GC% of any currently-assembled insect genome including the pea aphid. The data (Figure 3.12, Table 3.6, Table 3.7, and Table 3.8) in this study correspond with these findings. The high AT-richness within aphid genomes may be evidence of relaxed GC biases and previous

mutational hotspots (Rocha *et al.* 2010) which may be indicative of RWA genome plasticity.

### 3.4.3 Bioinformatic analysis and reference mapping

Libraries produced by amplification such as in this case through using the Truseq Nano DNA Sample Prep Kit (Illumina) inherit an intrinsic bias in the position at which reads start (Figure 3.12). This bias does not concern an absolute sequence, but instead provides enrichment of a number of different *k-mers* at the 5' end of the reads. According to Chikhi and Medvedev (2014), in cases like these, the statistical model in KmerGenie does not always correctly fit the input data for some values of *k*. KmerGenie software suggests that the plot in Figure 3.13 should ideally be concave with a smooth curve and a clear global maximum (Chikhi and Medvedev 2014). However, Figure 3.13 does not display a smooth curve, but rather a plot with multiple local maxima's for *k-mer* size. Therefore, the best *k-mer* value that KmerGenie predicted may be suboptimal. Subsequently, KmerGenie recommends that in later analysis (e.g. *de novo* assembly), a larger *k* than the one predicted by the software should also be attempted. In principal, when the number of predicted genomic *k-mers* remains high during a large range of *k's*, the largest *k* value in this range is likely to be a better choice (as indicated by the red circles in Figure 3.13), resulting in the selected k=27 rather than k=25 (Figure 3.14).

The mapping (Table 3.8) and coverage (Figure 3.15) results of the RWA and pea aphid were compared, because the pea aphid is closely related to the RWA and well characterised. Figure 3.15 displays coverage - if one genomic region has a coverage of 10X, it means that, on average, 10 different reads are mapped to each nucleotide of the region. The data presented an expected outcome with higher mapping percentage, coverage, and quality to the RWA. These results are due to the fact that the X chromosome is isolated from the RWA. Because of the close relation between these two

species, mapping and coverage against the pea aphid also produced high quality results as well as conformation that the RWA and pea aphid have nearly similar AT content. However from the results in Figure 3.15 it can be concluded that mapping coverage stretches the whole genome of the RWA and pea aphid, suggesting that the RWA X chromosome fraction sent for sequencing was contaminated with other autosome chromosomes, resulting in whole genome coverage. Therefore, the process of flow cytometry is not considered specific enough as it does not allow sorting of only the chromosome of interest, in this case the X chromosome.

### 3.4.4 Physical mapping of the X chromosome

The fruit fly is a well-known model organism, because of its abundance, simplicity to breed and that they are low cost subjects. What is more important is that mapping populations exist to enable for physical mapping. The fruit fly X chromosome is well characterised and studied with its coding genes, non-coding genes, and pseudogenes identified. Mapping the X chromosome of the fruit fly to the RWA genome allowed for some characterisation of the RWA X chromosome. The X chromosome of the fruit fly aided in the alignment of 67.42% of the proteins of the RWA X chromosome by using the proteins of the fruit fly and determining on which contigs of the RWA these proteins were mapped. This information will aid in the identification of these proteins and what their functions are.

As an additional means of X chromosome characterisation, fluorescent *in situ* hybridization (FISH) was conducted to identify regions of interest on the sex chromosome. The probes were chosen based on mapping the X chromosome of the fruit fly against the RWA genome to identify possible orthologous regions. The gene descriptions are presented in Table 3.1. After the product sizes of the probes were confirmed the hybridization was conducted to obtain the images in Figure 3.17. Probe 1 (18S rRNA) and 2 (histone H4) were used as controls in the study.

In aphids, nucleolus organiser regions (NORs), i.e., clusters of genes for 18S rRNA (Probe 1), have been examined not only as chromosomal markers, but also for their possible role in X-chromosome elimination in oocytes destined to develop as males. During this process one of the X chromosomes is eliminated to generate eggs with two autosomal sets and a single X chromosome (Orlando 1974; Blackman and Hales 1986). It has been shown that the prometaphase X chromosomes are connected by a narrow protein-DNA bridge carrying the NOR (Mandrioli *et al.* 1999). From the results in Figure 3.17, it can be observed that probe 1 localized a terminal cluster of rRNA on the X chromosome in female RWA. This confirmed that the RWA X chromosome bears the NOR. Novotná *et al.* (2011) confirmed that the H4 probe also localizes a single cluster of histone genes at the end of the X chromosome. In Figure 3.17 it can be seen that probe 2 (H4) localization definitely occurs, however in these cases the localization area cannot be confirmed. The same results can be observed in the other probes (3, 5, 6, 7, 8, and 10) where localization takes place, but resolution in the images were insufficient to allow for separation of single chromosomes on a spread. Despite this limitation, it was nonetheless confirmed that these genes are also present in the RWA X chromosome data set.

# 3.5 Appendix

Table A1: *t*-Test with two samples assuming equal variances (X chromosome vs. Middle chromosome).

| | X chromosome | Middle chromosome |
|---|---|---|
| **Mean** | 6.11 | 4.20 |
| **Variance** | 0.02 | 0.03 |
| **Observations** | 10 | 10 |
| **Pooled variance** | | 0.02 |
| **Df** | | 18 |
| **t stat** | | 28.58 |
| **P(T<=t) one-tail** | | $9.45 \times 10^{-17}$ |
| **t critical one-tail** | | 1.73 |
| **P(T<=t) two-tail** | | $1.89 \times 10^{-16}$ |
| **t critical two-tail** | | 2.10 |

Table A2: *t*-Test with two samples assuming equal variances (Middle chromosome vs. Small chromosome).

| | Middle chromosome | Small chromosome |
|---|---|---|
| **Mean** | 4.20 | 3.13 |
| **Variance** | 0.03 | 0.01 |
| **Observations** | 10 | 10 |
| **Pooled variance** | | 0.02 |
| **Df** | | 18 |
| **t stat** | | 18.09 |
| **P(T<=t) one-tail** | | $2.71 \times 10^{-13}$ |
| **t critical one-tail** | | 1.73 |
| **P(T<=t) two-tail** | | $5.42 \times 10^{-13}$ |
| **t critical two-tail** | | 2.10 |

Table A3: *t*-Test with two samples assuming equal variances (X chromosome vs. Small chromosome).

| | X chromosome | Small chromosome |
|---|---|---|
| **Mean** | 6.11 | 3.13 |
| **Variance** | 0.02 | 0.01 |
| **Observations** | 10 | 10 |
| **Pooled variance** | | 0.01 |
| **Df** | | 18 |
| **t stat** | | 56.75 |
| **P(T<=t) one-tail** | | $4.71 \times 10^{-22}$ |
| **t critical one-tail** | | 1.73 |
| **P(T<=t) two-tail** | | $9.42 \times 10^{-22}$ |
| **t critical two-tail** | | 2.10 |

Table A4: The DNA concentration of an X chromosome pair was determined as follows, where the total DNA concentration of the flow cytometry trails were divided by the number of X chromosome pairs sorted.

| Biotype | Sample # | # of chromosome pairs | [DNA] (ng/ul) | Total DNA (ng) | Total DNA (pg) | Total DNA (pg)/# of chromosome pairs |
|---|---|---|---|---|---|---|
| SAM | Sample #5 | 251782 | 0.95 | 20.90 | 20900 | 0.08 |
| SAM | Sample #6 | 138966 | 0.38 | 8.36 | 8360 | 0.06 |
| SAM | Sample #10 | 425200 | 6.10 | 134.20 | 134200 | 0.32 |
| SAM | Sample #11 | 459050 | 9.10 | 200.20 | 200200 | 0.44 |
| SAM | Sample #12 | 416004 | 8.90 | 195.80 | 195800 | 0.47 |
| SAM | Sample #13 | 631000 | 7.80 | 171.60 | 171600 | 0.27 |
| SAM | Sample #14 | 116042 | 7.20 | 158.40 | 158400 | 1.37 |
| SAM | **Total** | 2438044 | 40.43 | 889.46 | 889460 | **0.36** |
| SAM | **Average** | 348292 | 5.78 | 127.07 | 127065.71 | **0.36** |

Flow cytometry data and trails included in the study can be found in a supplemental file named **Folder A1** (see attached CD).

FastQC results achieved from assessing the quality of the data obtained from the NGS analysis can be found in a supplemental file named **Folder A2** (see attached CD).

KmerGenie estimated the best *k-mer* length for genome de novo assembly to build contigs and scaffolds from the NGS raw reads for the X chromosome of the RWA and can be found in a supplemental file named **Folder A3** (see attached CD).

The tabulated results produced by SOAPdenovo presenting the contig and scaffold assemblies can be found in a supplemental file named **Folder A4** (see attached CD).

Qualimap results obtained from mapping the flow sorted RWA X chromosome against the RWA genome and pea aphid genome can be found in a supplemental file named **Folder A5** (see attached CD).

Physical mapping of the flow sorted X chromosome against the RWA genome can be found in a supplemental file named **Folder A6**. All of the data is presented in a spread sheet format obtained from Geneious (v7.1.7) (see attached CD).

Physical mapping of the fruit fly X chromosome against the RWA genome can be found in a supplemental file named **Folder A7**. All of the data is presented in a spread sheet format (see attached CD).

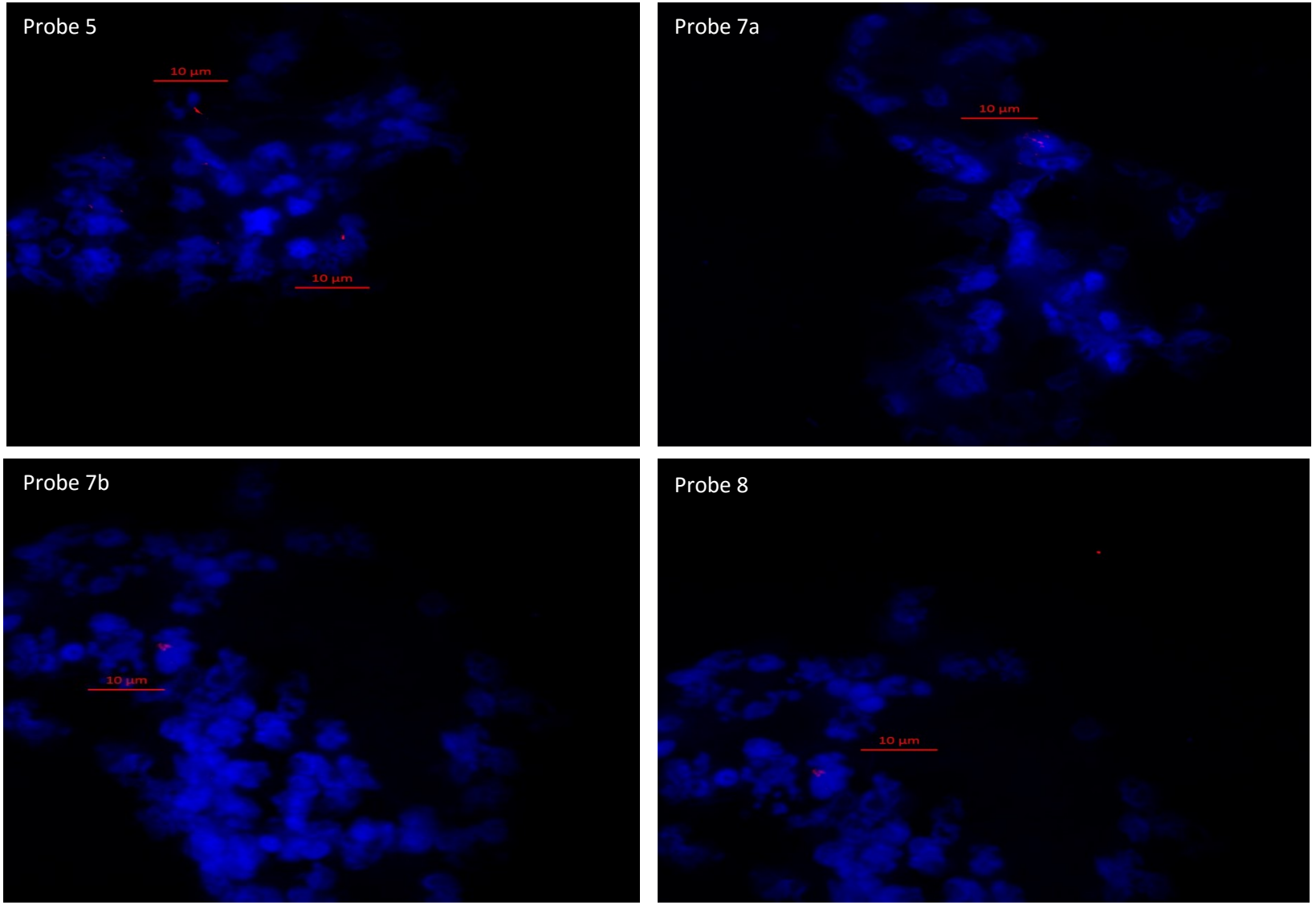


Figure A1: Mitotic chromosome complements of RWA after differential staining and FISH. Probe 1 and 2 was used as controls and the other probes were derived from the fruit fly X chromosome.

## 3.6 List of references

Adams, M. D., S. E. Celniker, R. A. Holt, C. A. Evans, J. D. Cocayne, *et al.,* 2000 The genome sequence of *Drosophila melanogaster.* Science 287: 2185-2195.

Bizzaro, D., M. Mandrioli, M. Zanotti, M. Giusti, and G. C. Manicardi, 2000 Chromosome analysis and molecular characterisation of highly repeated DNAs in the aphid *Acyrthosiphon pisum* (Aphididae, Hemiptera). Genetica 108: 197-202.

Blackman, R. L., and H. Takada, 1976 Naturally occurring chromosomal translocation in *Myzus persicae* (Sulzer). Journal of Entomology 50: 147-156.

Blackman, R.L., and D. F. Hales, 1986 Behavior of the X-chromosomes during growth and maturation of parthenogenetic eggs of *Amphorophora tuberculata* (Homoptera, Aphididae), in relation to sex determination. Chromosoma 94: 59-64.

Blackman, R. L., 1987 Reproduction, cytogenetics and development. *In:* A. K. Minsk and P. Harrewijn (eds), Aphids: their biology, natural enemies and control 2A: 163-195.

Blackman, R. L., P. A. Brown, C. C. Ramfrez, and H. M. Niemeyer, 2003 Karyotype variation in the South American aphid genus *Neuquenaphis* (Hemiptera, Aphididae, Neuquenaphidinae). Hereditas 138: 6-10.

Botha, A. M., L. van Eck, C. S. Jackson, N. F. V. Burger, and T. Schultz, 2011 Phloem feeding insect stress and photosynthetic gene expression. Applied Photosynthesis. Online at http://www.intechopen.com/books/applied-photosynthesis/phloem-feeding-insect-stress-and-photosynthetic-gene-expression.

Botha, A. M., 2013 A co-evolutionary conundrum: The arms race between *Diuraphis noxia* (Kurdmojov) a specialist pest and its host *Triticum aestivum* (L.). Arthropod Plant Interactions 7: 359-372.

Botha, A. M., N. F. V. Burger, W. Cloete, L. van Eck, K. Breeds, *et al.*, 2016 Draft genome of female *Diuraphis noxia* (Hemiptera: Aphididae) reveals high levels of genetic diversity despite parthenogenecity and hypomethylation as a mean to enhance genomic plasticity. Genome Biology – *in press.*

Bouhsinni, M. E., F. C. Ogbonnaya, M. M. Mosaad, K. Street, A. Amri, *et al.*, 2011 Progress in host plant resistance in wheat to Russian wheat aphid (Hemiptera : Aphididae) in North Africa and West Asia. Australian Journal of Crop Science 5: 1108-1113.

Burd, J. D., D. R. Porter, G. J. Puterka, S. D. Haley, and F. B. Peairs, 2006 Biotypic variation among North American Russian wheat aphid (Homoptera: Aphididae) populations. Journal of Economical Entomology 99: 1862-1866.

Chikhi, R. and P. Medvedev, 2014 Informed and automated *k-mer* size selection for genome assembly. Bioinformatics 30: 31-37.

Davis, G. K., 2012 Cyclical parthenogenesis and viviparity in aphids as evolutionary novelties. Journal of Experimental Zoology 318: 448-459.

Doležel, J., J. Bartoš, H. Voglmayr, and J. Greilhuber, 2003 Nuclear DNA content and genome size of trout and human. Cytometry 51:127-128.

Doležel, J., and J. Bartoš, 2005 Plant DNA flow cytometry and estimation of nuclear genome size. Annals of Botany 95: 99-110.

Doležel, J., J. Vrána, J. Šafář, J. Bartoš, M. Kubaláková, *et al.*, 2012 Chromosomes in the flow to simplify genome analysis. Functional and Integrative Genomics 12: 397-416.

Fuková, I., P. Nguyen, and F. Marec, 2005 Codling moth cytogenetics: karyotype, chromosomal location of rDNA, and molecular differentiation of sex chromosomes. Genome 48: 1083-1092.

García-Alcalde, F., K. Okonechnikov, J. Carbonell, L. M. Cruz, S. Götz, *et al.,* 2012 Qualimap: evaluating next generation sequencing alignment data. Bioinformatics 28: 2678-2679.

Gaston, K. G., 1991 The magnitude of global insect species richness. Conserved Biology 5: 283-296.

Haley, S. D., F. B. Peairs, C. B. Walker, J. B. Rudolph, and T. L. Randolph, 2004 Occurrence of a new Russian wheat aphid biotype in Colorado. Crop Science 44: 1589-1592.

Hanrahan, S. J., and J. S. Johnston, 2001 New genome size estimates of 134 species of arthropods. Chromosome Research 19: 809-823.

Jankielsohn, A., 2011 Distribution and diversity of Russian wheat aphid (Hemiptera: Aphididae) biotypes in South Africa and Lesotho. Entomological Society of America 11: 1736-1741.

Johnston, J. S., K. S. Yoon, J. P. Strycharz, B. R. Pittendrigh, and J. M. Clark, 2007 Body lice and head lice (Anoplura: Pediculidae) have the smallest genomes of any hemimetabolous imsect reported to date. Journal of Medical Entomology 44: 1009-1012.

Kearse, M., R. Moir, A. Wilson, S. Stones-Havis, M. Cheung, *et al.,* 2012 Geneious basic: an integrated and extendable desktop software platform for the organization and analysis of sequence data. Bioinformatics 28: 1647-1649.

Kron, P., and B. C. Husband, 2015 Distinguishing 2N gamete nuclei from doublets in pollen using flow cytometry and pulse analysis. Cytometry Part A 87: 943-957.

Kuznetsova, V. G., and G. C. Shaposhnikov, 1973 Chromosome numbers of aphids (Homoptera, Aphidinea) of the world auna. Entomologicheskoe Obozrenie 52: 116-135.

Lemeunier, F., J. R. David, and L. Tsacas, 1986 The *melanogaster* species group. In: Ashburner M., H. I. Carson, and J. K. Thompson, eds. The Genetics and Biology of *Drosophila*. London: Academic Press 3: 147-188.

Li, H., and R. Durbin, 2010 Fast and accurate long-read alignment with Burrows- Wheeler transform. Bioinformatics 26: 589-595.

Lockwood, A. P. M., 1961 ‘‘Ringer’’ solutions and some notes on the physiological basis of their ionic composition. Comparative Biochemistry and Physiology 2: 241-289.

Lo, K., R. R. Brinkman, and R. Gottardo, 2008 Automated gating of flow cytometry data via robust model-based clustering. Journal of the International Society for Advancement of Cytometry 73: 321-332.

Mandrioli, M., D. Bizarro, G. C. Manicardi, D. Gionghi, L. Bassoli, *et al.*, 1996 Cytogenetic and molecular characterisation of a highly repeated DNA sequence in the peach potato aphid *Myzus persicae*. Chromosoma 108: 436-442.

Mandrioli, M., D. Bizzaro, M. Giusti, G. C. Manicardi, and U. Bianchi 1999 The role of rDNA genes in X chromosome association in the aphid *Acyrthosiphon pisum*. Genome 42: 381-386.

Manicardi, G. C., M. Mandrioli, and R. L. Blackman, 2015 The cytogenetic architecture of the aphid genome. Biological Reviews 90: 112–125.

Merrill, S. C., T. O. Holtzer, and F. B. Peairs, 2009 *Diuraphis noxia* reproduction and development with a comparison of intrinsic rates of increase to other important small grain aphids: a meta-analysis. Environmental Entomology 38: 1061-1068.

Miller, H., D. R. Porter, J. D. Burd, D. W. Mornhinweg, and R. L. Burton, 1994 Physiological effects of Russian wheat aphid (Homoptera: Aphididae) on resistant and susceptible barley. Journal of Economic Entomology 87: 493-499.

Nicholson, S. J., M. L. Nickerson, M. Dean, Y. Song, P. R. Hoyt, *et al.,* 2015 The genome of *Diuraphis noxia*, a global aphid pest of small grains. BMC Genomics 16: 429.

Novotná, J., J. Havelka, P. Starý, P. Koutecký, and M. Vítková, 2011 Karyotype analysis of the Russian wheat aphid, *Diuraphis noxia* (Kurdjumov) (Hemiptera: Aphididae) reveals a large X chromosome with rRNA and histone gene families. Genetica 139: 281-289.

Orlando, E., 1974 Sex determination in *Megoura viciae* Buckton (Homoptera Aphididae). Monitore Zoologico Italiano 8: 61-70.

Puterka, G. J., R. W. Hammon, J. D. Burd, F. B. Peairs, T. L. Randolph, *et al.*, 2012 Cyclical parthenogenetic reproduction in Russian Wheat Aphid (Hemiptera: Aphididae) in the United States: Sexual reproduction and its outcome on biotypic diversity. Journal of Economic Entomology, 105: 1057-1068.

Rocha, E. P. C., and E. J. Feil, 2010 Mutational patterns cannot explain genome composition: Are there any neutral sites in the genomes of bacteria? PLoS Genetics doi: 10.1371/journal.pgen.1001104.

Sahara, K., F. Marec, and W. Traut, 1999 TTAGG telomeric repeats in chromosomes of some insects and other arthropods. Chromosomes Research 7: 449-460.

Swanevelder, Z. H., A. K. J. Surridge, E. Venter, and A. M. Botha, 2010 Limited endosymbiont variation in *Diuraphis noxia* (Hemiptera:Aphididae) biotypes from the United States and South Africa. Journal of Economic Entomology 103: 887-897.

Tagu, D., J. P. Klingler, A. Moya, and J. C. Simon, 2008 Early progress in aphid genomics and consequences for plant-aphid interactions studies. Molecular Plant Microbes 21: 701-708.

The Honeybee Genome Sequencing Consortium, 2006 Insights into social insects from the genome of the honeybee *Apis mellifera*. Nature 443: 931-949.

The International Aphid Genomics Consortium, 2010 Genome sequence of the pea aphid *Acyrthosiphon pisum*. PLoS Biology 8: e1000313.

Thomas, T., J. Gilbert, and F. Meyer, 2012 Metagenomics – a guide from sampling to data analysis. Microbial Informatics and Experimentation 2: 3.

Traut, W. 1976 Pachytene mapping in female silkworm, *Bombyx mori* L. (Lepidoptera). Chromosoma 58: 275-284.

# Chapter 4

# Summary

## 4.1 Summary

Aphids are recognized as global agricultural pests that cause significant economic losses worldwide with devastating effects on crop production. *Diuraphis noxia* Kurdjumov, more commonly known as the Russian wheat aphid (RWA), is a widely distributed pest of, especially wheat, *Triticum austivum* L., (Stoetzel 1987) mostly because of the development of new RWA biotypes that are virulent to different deployed resistant wheat cultivars. RWA biotypes have raised major concerns regarding durability of future RWA resistance sources (Haley *et al.* 2004).

Over the past 100 years aphids have been extensively studied as a popular model group among cytogeneticists and thus far approximately a 1000 species have been karyotyped, of which numerous show big differences in chromosome number and morphology (Kuznetsova and Shaposhnikov 1973; Blackman 1980). The chromosomes of aphids have been shown to be holocentric, meaning that they lack centromeres and display kinetic activity along the length of the chromosome (Blackman 1987). This makes chromosomes of similar size and shape almost identical, making it impossible to differentiate from one another. However, since then modern technology has afforded scientists an opportunity to isolate specific DNA sequences in aphids. Molecular techniques along with fluorescent *in situ* hybridization (FISH) have allowed the localization of rRNA, satellites, and telomeric $(TTAGG)_n$ repeats (Spence *et al.* 1998; Bizarro *et al.* 2000). Furthermore, advances in science has also contributed to answering the research questions presented in this study.

In order to address the first research question relating to the composition of the karyotype of the RWA and identifying the large X chromosome from the other autosome chromosomes, the embryos of female RWA were dissected to isolate differentiating cells that are mostly in metaphase when chromosomes can be best observed. The karyotype

was constructed from these samples and it was shown that the female RWA does, in fact, possess a diploid (2n) chromosome number of 10, corroborating with results demonstrated by Novotná *et al.* (2011). The X chromosomes were shown to be the largest chromosomes in the karyotype and could easily be distinguished from the other chromosomes.

The successful differentiation of the RWA X chromosome led to the next research question, which was the physical contribution of the X chromosome to the genome of the RWA. To address this, an attempt was made to isolate the RWA X chromosome using flow cytometry. The RWA chromosomes were sorted from one another based on their size, however the small autosome chromosomes could not be separated from the debris, because of their small size and low fluorescence. The flow cytometry results displayed successful separation of the large X chromosomes and middle autosome chromosomes. Using the size differences and the measured lengths of the chromosome pairs, the size of the X chromosomes were calculated to be 0.18 pg (equating to 176.9 Mb).

The next question then was to conduct physical mapping on the sorted chromosomes. To accomplish this, the DNA from the isolated X chromosomes was sequenced. Bioinformatic analysis confirmed that the RWA genome is AT-rich. Physical mapping of the proteins of the RWA against the proteins of the fruit fly X chromosome aided in further characterisation of the RWA X chromosome, resulting in the alignment of 67.42% of the length of the RWA X chromosome. Fluorescent *in situ* hybridization also confirmed orthologous regions of the fruit fly X chromosome to be present in the RWA karyotype, which ultimately suggested that these PCGs are present in the RWA X chromosome data set.

In conclusion, it is clear from the karyotype results obtained in this study that the RWA X chromosome is really large compared to the other autosome chromosomes and that

further investigation of the RWA X chromosome through flow cytometry, sequencing, and FISH, allowed for the determination of important characteristics like genome size, X chromosome protein content, and possible X chromosome genes. The results in the study also suggested that the X chromosome occupies more than a quarter of the RWA genome, suggesting that more investigation studies into X chromosome genetic variability would be beneficial and might even help with future resistance programmes.

## 4.2 List of references

Bizzaro, D., M. Mandrioli, M. Zanotti, M. Giusti, and G. C. Manicardi, 2000 Chromosome analysis and molecular characterisation of highly repeated DNAs in the aphid *Acyrthosiphon pisum* (Aphididae, Hemiptera). Genetica 108: 197-202.

Blackman, R. L., 1980 Chromosome numbers in the Aphididae and their taxonomic significance. Systematic Entomology 5: 7-25.

Blackman, R. L., 1987 Reproduction, cytogenetics and development. *In:* A. K. Minsk and P. Harrewijn (eds), Aphids: their biology, natural enemies and control 2: 163-195.

Haley, S. D., F. B. Peairs, C. B. Walker, J. B. Rudolph, and T. L. Randolph, 2004 Occurrence of a new Russian wheat aphid biotype in Colorado. Crop Science 44: 1589-1592.

Kuznetsova, V. G., and G. C. Shaposhnikov, 1973 Chromosome numbers of aphids (Homoptera, Aphidinea) of the world auna. Entomologicheskoe Obozrenie 52: 116-135.

Novotná, J., J. Havelka, P. Starý, P. Koutecký, and M. Vítková, 2011 Karyotype analysis of the Russian wheat aphid, *Diuraphis noxia* (Kurdjumov) (Hemiptera: Aphididae) reveals a large X chromosome with rRNA and histone gene families. Genetica 139: 281-289.

Spence, J. M., R. L. Blackman, J. M. Testa, and P. D. Ready, 1998 A 169 base pair tandem repeat DNA marker for subtelomeric heterochromatin and chromosomal rearrangements in aphids of the *Myzus persicae* group. Chromosome Research 6: 167-175.

Stoetzel, M. B., 1987 Information on and identification of *Diuraphis noxia* (Homoptera: Aphididae) and other aphid species colonizing leaves of wheat and barley in the United States. Journal of Economic Entomology 80: 696-704.